Regulation of iron-sulfur cluster assembly in a facultative phototrophic Alpha-proteobacterium

Inaugural-Dissertation
zur Erlangung
des
Doktorgrades der Naturwissenschaften
(Dr. rer. nat.)

vorgelegt von

M. Sc.- Biol. Xin Nie
aus
Sichuan, V. R. China

angefertigt am Institut für Mikrobiologie und Molekularbiologie
Fachbereich Biologie und Chemie
Justus-Liebig-Universität Gießen

Giessen, December 2019

The thesis was performed in the Institut of Microbiologie und Molecularbiologie (Fachbereiches 08) Justus-Liebig-Universität Gießen from February 2016 to December 2019 under the guide from Prof. Dr. Gabriele Klug.

1. **Supervisor:** **Prof. Dr. Gabriele Klug**
   Institut für Mikrobiologie und Molekularbiologie
   Justus-Liebig-Universität Gießen
2. **Supervisor:** **Apl. Prof. Dr. Elena Evguenieva-Hackenberg**
   Institut für Mikrobiologie und Molekularbiologie
   Justus-Liebig-Universität Gießen

Contents

Abbreviations

aa	amino acid
ADP	adenosinediphosphate
Ap	ampicillin
APS	ammoniumpersulfate
ATP	adenosinetriphosphateμ
BChl	bacteriochlorophyll
Bp	base pair(s)
BSA	bovine serum albumin
Cpm	counts per minute
℃	centigrade
Da	Dalton
dATP	deoxyriboadenosine triphosphate
dCTP	deoxyribocytosine triphosphate
DMSO	dimethyl sulfoxide
DNA	deoxynucleic acid
DNase	deoxyribonuclase
dNTP	deoxyribonucleotide
DTT	1, 4-dithiothreitol
E. coil	*Escherichia coil*
EDTA	ethylene diamine tetraacetic acid
e.g	*exempli gratia* (for example)
et al.	*et alii* (and others)
etc.	*et cetera* (and other things)
EtOH	ethanol
g	gram
Gm	gentamycin
H	hour (h)
His	histidine
IPTG	isopropyl-β-Dthiogalactopyranoside
kDa	kilodalton
Kb	kilo base pairs
Km	kanamycin
LHI	light-harvesting complex I
LHII	light-harvesting complex II
M	molar (mol/l)
min	minute(s)
ml	milliliter
mmol	millimole
mM	millimolar
mRNA	messenger RNA
Ci	microcurie
μg	microgram
μl	microliter
μm	micrometer
μM	micromolar
nm	nano meter
nt	nucleotide
OD	optical density
PAGE	polyacrylamide gel electrophoresis
PBS	phosphate-buddered saline
PCR	polymerase chain reaction
PMSF	phenylmethylsulfonyl fluorid
PNK	polynucleotide kinase triphosphate
PS	Photosynthesis
R. sphaeroides	*Rhodobacter sphaeroides*
RNA	ribonucleic acid
RNase	ribonuclease
ROS	reactive oxygen species
rpm	revolution per minute
SDS	sodium dodecyl sulfate
sec	second(s)
Tc	tetracycline
TCA	trichloroacetic acid
Tris	Trishydroxymethylaminomethane
Tp	trimethoprim
UV	ultraviolet
V	volt

Publications

The following publications are based on this work.

1. **Xin Nie**, Bernhard Remes, Gabriele Klug*. Multiple sense and anti-sense promoters contribute to the regulated expression of the *isc-suf* operon for iron sulfur cluster assembly in *Rhodobacter. Microoganisms*, **2019**, 7 (12), 671. doi: 10.3390/ microorganisms7120671.

2. **Xin Nie,** Gabriele Klug*. Interplay between formation of photosynthetic complexes and regulation of genes for iron-sulfur cluster assembly in *Rhodobacter sphaeroides*. Completion, manuscript in preparation.

1. Introduction

1.1 Iron-sulphur proteins

1.1.1 Formation of iron-sulphur proteins

Iron is a first row transition metal in the periodic table and is also an abundant metal that is the fourth most plentiful element in the Earth's crust. Iron is essential for all organisms. Normally, iron mainly exists in one of two redox states that are inter-convertible: the reduced Fe^{2+} ferrous form and the oxidized Fe^{3+} ferric form. The ferrous form Fe^{2+} shows much better solubility than the ferric form Fe^{3+}. For this reason, iron is considered as the ideal choice during the evolution of early life. Iron and sulphur are present in the reduced Fe^{2+} state and in the oxidized S^{2-} state to form different types of Fe-S cluster: the rhombic (2Fe-2S) and cubane (4Fe-4S) cluster (Beinert *et al.*, 1997) (Fig. 1.1).

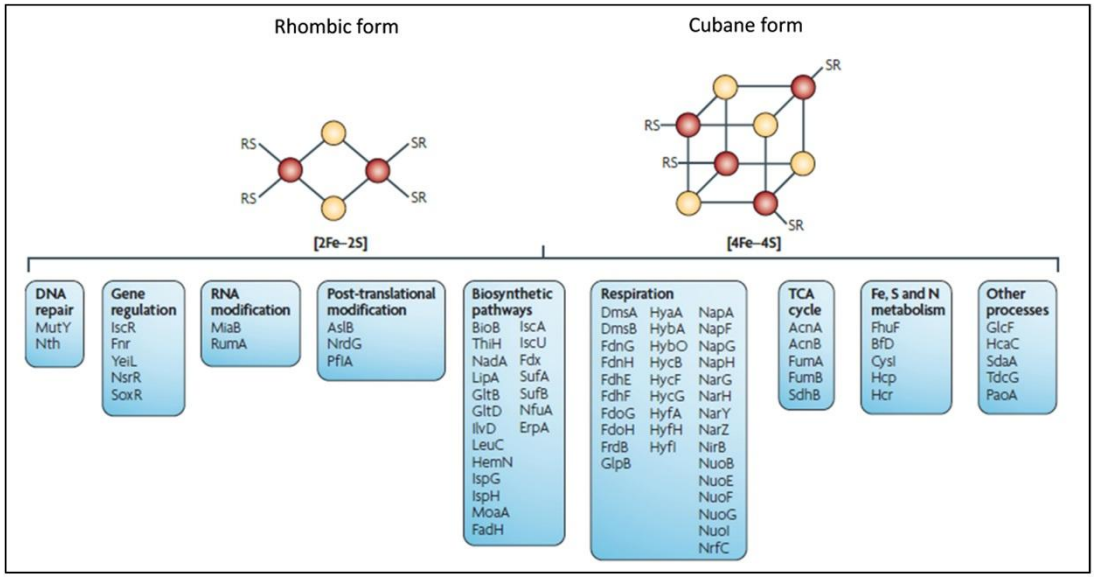

Fig. 1.1. Fe-S cluster: structure (rhombic and cubane form of Fe-S cluster) and function in the Fe-S proteins. The iron atoms (red) are bound to the inorganic sulphur atoms (yellow) from cysteine residues in the peptide backbone (SR). Some functions of the Fe-S proteins in *E coli* are listed in the figure. TCA, tricarboxylic acid cycle. Modified from (Py and Barras, 2010).

The Fe-S cluster represents one of nature's simplest, multifunctional, and earliest catalyst and electron carrier (Beinert *et al.*, 1997) and plays an important role in many major biological processes. The most important of them is that iron functions with different inorganic atoms that are inserted to proteins, for example as Fe-S cluster,

Fe-N (heme) and so on. (2Fe-2S) or (4Fe-4S) cluster usually is inserted into the peptide backbone (SR) through coordination of two or four iron ions and two or four cysteine ligands (Fig. 1.1) or alternative ligands such as histidine, aspartate and arginine (Lill, 2009) and function as a catalyst or electron carrier. Proteins containing Fe-S cluster are commonly called Fe-S proteins and participate in many metabolic processes (Fig. 1.1), e.g. as electron carriers in redox reactions, in redox sensing, oxidative stress defense, biosynthesis of metal-containing cofactors, DNA replication and repair, regulation of gene expression, tRNA modification (Py and Barras, 2010; Johnson *et al.*, 2005), ATP biosynthesis (Liu *et al.*, 2018) and photosynthesis (Frazzon and Dean, 2001).

Although Fe-S cluster can be easily synthesized by chemical methods from $Fe^{2+/3+}$ and S^{2-} releasing agents (Malkin and Rabinowitz, 1966), it is sure that Fe-S cluster assembly is a much more difficult biological cellular processes. Indeed, it is known that the process of maturation of Fe-S cluster *in vivo* requires a set of iron-sulfur (Fe-S) cluster (Isc) biosynthesis genes or proteins that use Fe^{2+} and L-cysteine as substrates (Zheng *et al.*, 1998). In the past, the mechanisms how Fe-S cluster are built and inserted into proteins were intensely investigated in several model organisms (Fidai *et al.*, 2016; Dos Santos, 2017; Zheng and Dos Santos, 2018). Fe-S protein biogenesis mainly has two important steps: the first step is the assembly of the Fe-S cluster on the scaffold that is the sulphur from the cysteine desulphurase and the iron from a donor protein, and the second step is the delivery of the Fe-S cluster that is from the scaffold and the insertion of Fe-S cluster to the target protein (Roche *et al.*, 2013) (Fig. 1.2).

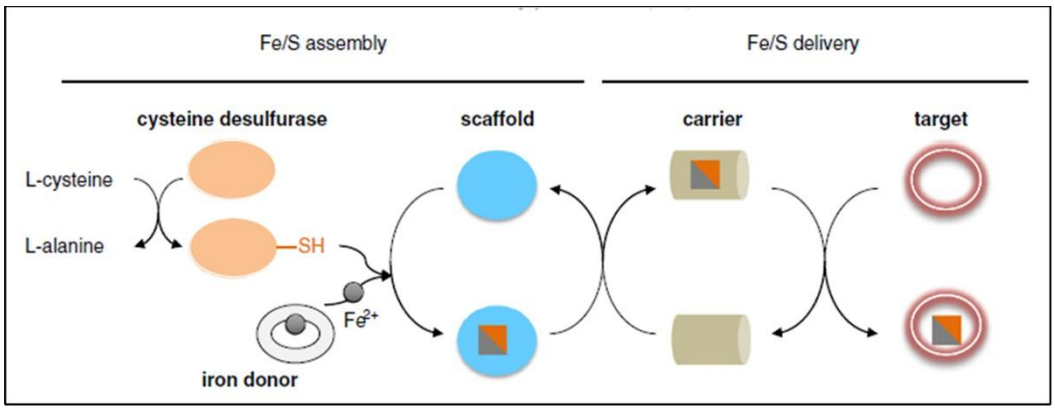

Fig. 1.2. The main steps of Fe-S cluster biogenesis pathway. The Fe-S cluster assembles on a scaffold

protein, which receives sulfur from a cysteine desulfurase and iron from an iron donor. Then, the pre-formed Fe-S cluster is transferred to a carrier protein, which delivers it to the final target proteins.

1.1.2 Function of iron-sulphur proteins

Redox sensing is a main function of Fe-S cluster. A well-studied redox sensor is that the transcription factor FNR (**f**umarate **n**itrate **r**eduction) in the model organism *E. coli*, known for involvement in switching from aerobic to anaerobic respiration. Under anaerobic conditions, FNR binds a $(4Fe\text{-}4S)^{2+}$ cluster and acts in its transcriptionally active dimer form. When O_2 is present, the cluster is converted to its $(2Fe\text{-}2S)^{2+}$ form, leading to dissociation of the protein into inactive monomers and thus loss of the DNA-binding ability (Crack *et al.*, 2014). Under strictly anaerobic conditions, FeoC (ferrous iron transport protein C) can bind a redox-active $(4Fe\text{-}4S)^{2+}$ cluster that is oxygen-sensitive and rapidly decays to a $(2Fe\text{-}2S)^{2+}$ cluster, similar to the Fe-S cluster in the FNR transcriptional regulator (Smith *et al.*, 2019). The NADH oxidation-site is connected with the quinone-reduction site by a chain of seven Fe-S clusters (Gnandt *et al.*, 2016). The majority of anaerobic organisms have more Fe-S proteins than aerobic organisms with a similar genome size (Andreini *et al.*, 2017). Though they share some common features, it was clearly demonstrated that different species have their own systems for the maturation of Fe-S cluster and the insertion of Fe-S cluster into proteins. The first gene of Fe-S cluster assembly was identified in the *nif* operon of *Azotobacter vinelandii* and was related to nitrogenase maturation (Jacobson *et al.*, 1989), but the Isc (**i**ron **s**ulphur **c**luster) and Suf system were identified as the main system for the regulation of Fe-S assembly in most bacteria.

Though components of the Isc and Suf system were also found in most bacteria, the regulation of genes for Fe-S cluster assembly was mostly investigated in the model organism *E. coli* and few other members of the gamma-proteobacteria. In *E. coli*, Fe-S cluster assembly is mainly catalyzed by the Isc system under non-stress conditions, while the Suf system functions primarily under oxidative stress and/or iron starvation (Fig. 1.3) (Outten *et al.*, 2004; Lee *et al.*, 2004; Giel *et al.*, 2006; Yeo *et al.*, 2006; Lee *et al.*, 2008). In *E. coli*, these proteins for Fe-S cluster assembly are mainly encoded by the *isc* operon and *suf* operon. The *isc* operon encodes the regulator IscR, a cysteine desulfurase

(IscS), a scaffold protein (IscU), an A-type carrier protein (IscA), a DnaJ-like co-chaperon (HscB), a DnaK-like chaperone (HscA) and a ferredoxin (fdx) (Roche *et al.*, 2013) (Fig. 1.3). IscU is crucial for functional interaction with IscS and sulfur transfer between the two proteins (Tanaka *et al.*, 2019). Another operon for Fe-S cluster assembly is *suf* that was also discovered in *E. coli* (Takahashi and Tokumoto, 2002). The *suf* operon encodes an A-type protein (SufA), a heterodimeric cysteine desulfurase (SufS and SufE) and a pseudo-ABC transporter (SufB, SufC, and SufD) that could act as a scaffold.

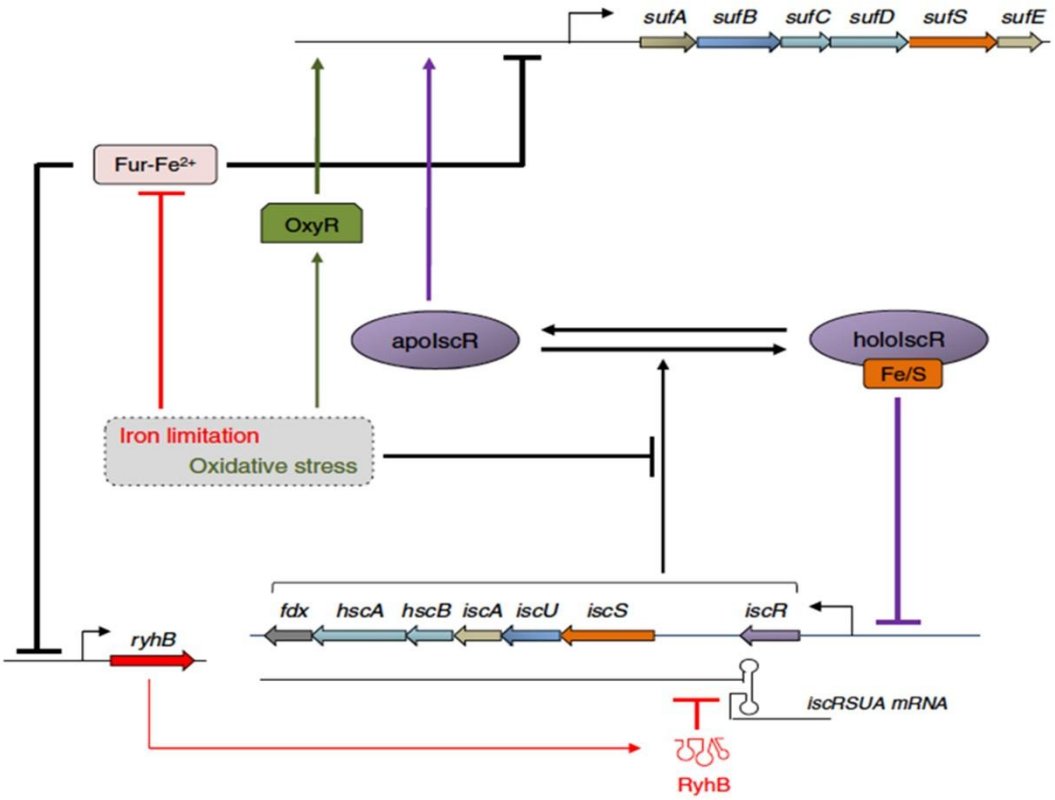

Fig.1.3. A model of the genetic regulation of Fe-S homeostasis in *E. coli*. The *suf* (top) and *isc* (bottom) operons are depicted. The *isc* operon expression is shown to be under the influence of IscR and of the small non coding RNA, RyhB. The *suf* operon expression is shown to be under the control of Fur, OxyR and IscR regulators (Roche *et al.*, 2013).

The IscR transcriptional regulator is encoded by the first gene of the *iscRSUA-hscBA-fdx* operon in *E. coli* and can coordinate a (2Fe-2S) cluster. IscR occurs in two types: Holo-IscR (containing the Fe-S cluster) and Apo-IscR (lack of Fe-S cluster). Under normal condition, maturation of the IscR regulator is dependent on the Isc system. (Schwartz *et al.*, 2001; Giel *et al.*, 2013). Holo-IscR represses its own

expression to give rise to an auto-regulatory circuit that senses the Fe-S state of the cell. IscR also contributes to regulation of the *suf* operon in *E. coli* (Yeo *et al.*, 2006; Giel *et al.*, 2006) (Fig. 1.3). Apo-IscR activates *suf* operon expression (Nesbit *et al.*, 2009). Induction of the *isc* and *suf* operons by Apo-IscR occurs under iron-limiting conditions and under oxidative stress (Outten *et al.*, 2004; Yeo *et al.*, 2006; Lee *et al.*, 2008). A main regulator of Fe-S assembly in *E. coli* is IscR, but also other regulatory proteins as Fur (ferric uptake regulator), OxyR and RyhB are involved. The expression of the *isc- suf* operon is regulated by the small RNA (sRNA) RyhB that has a role in the control of bacterial sensitivity to gentamicin during iron starvation (Chareyre *et al.*, 2019). sRNA RhyB base pairs with the Shine-Dalgarno (SD) sequence of *iscR* mRNA resulting in the degradation of the 3´part of the *isc* operon mRNA and the stabilization of the 5´part including the *isc* coding region (Desnoyers *et al.*, 2009). The sRNA RhyB is also under negative control of Fur (Masse *et al.*, 2005). The iron-sensing regulator Fur binds to the *suf* promoter as Fur-Fe^{2+} and represses the *suf* genes (Lee *et al.*, 2008). The *ryhB* gene is not expressed in this condition. The *suf* operon is activated in two ways in iron limitation: (i) Fur repression is released, and (ii) the *ryhB* gene is expressed. OxyR is a known sensor for oxidative stress in *E. coli* and many other bacteria and acts as an activator of the *suf* operon (Lee *et al.*, 2004). In oxidative stress conditions and iron limitation, OxyR activates the expression of the *suf* operon, meanwhile the IscSUA system is thought to be non-functional and Apo-IscR formation is favoured. Moreover, oxidative agents might directly damage the Fe-S cluster bound to IscR. As over-expression of the Suf system was reported to enable IscR maturation, the Isc system will be completely shut down under stress conditions (Roche *et al.*, 2013) (Fig. 1.3).

Both Isc and Suf systems share some similarity with other bacterial systems, but numbers and types of *isc-suf* operons and their compositions are different among different bacterial species, e.g., the function of their respective L-cysteine desulfurase IscS or SufS is specific for each cellular pathway (Buhning *et al.*, 2017). However, the Isc system is widely conserved from prokaryotes to higher eukaryotes. The regulation of Fe-S assembly in alpha-proteobacteria *Rhodobacter sphaeroides* (*R. sphaeroides*) is

rarely known. In *R. sphaeroides*, the genes related to Fe-S cluster assembly are located in a single *isc-suf* operon (Fig. 1.4). The IscR regulator that can coordinate an Fe-S cluster is encoded by the first gene of the operon. The operon also encodes two cystein desulfurases (IscS and SufS), the membrane component of an iron-regulated ABC transporter (SufB), a hypothetical protein (RSP_0439), the ATPase subunit of an ATP transporter (SufC), an Fe-S cluster assembly protein (SufD), and two proteins of the Yip1 family (RSP_0433 and RSP_0432) (Fig. 1.4). In this operon, there are five promoters, three sense promoters and two anti-sense promoters. Two sense promoters (P1 and P2) are in upstream of *iscR* and another sense promoter (P3) that initiates the transcripts of the *suf* genes is within *iscS*. Furthermore, two anti-sense promoters might lead to transcripts that were partially anti-sense to *isc-suf* transcripts. P4 leads to a transcript mostly anti-sense to the *iscR* mRNA. P5 represents the promoter for transcription of RSP_0444. The interactions of the promoters of *isc-suf* operon and the regulation of photosynthetic complexes and regulators that related to Fe-S cluster synthesis have been investigated in this work by the use of different combined constructs.

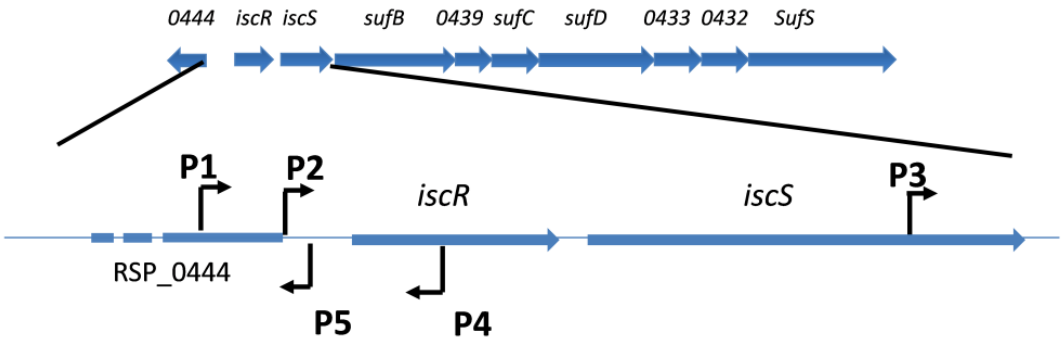

Fig. 1.4. Schematic overview of the *isc-suf* operon of *R. sphaeroides*. P1-P5 indicate the 5 promotors for the TSS identified by dRNAseq. Arrows represent the direction of the transcription.

1.2 Reaction Oxygen Species (ROS)

Iron availability and its biological functional changed once oxygenic photosynthesis appeared and released molecular oxygen into the atmosphere from 2.2 to 2.7 billion years ago. Nowadays, O_2 is the third most abundant element on earth (Morgan and Anders, 1980). Since cyanobacteria or plants can use sun light and produce ATP to

split H_2O and release O_2, the concentration of O_2 in the atmosphere increased (Lane, 2002). O_2 is an excellent electron acceptor in the aerobic respiration and in the important metabolic pathways. More and more organisms, except for some anaerobic species, evolved to use O_2 for ATP production by use of electron transport chains that transport electrons to O_2 (Halliwell and Gutteridge, 2007). O_2 is also called molecular oxygen or triplet oxygen ($^3\Delta g$-), and two unpaired electrons are present in the $\pi 2p$ orbital in this ground state. There are two completely different types of O_2 reactions to generate different reactive oxygen species. Type I is from the transfer of electrons, Type II is from the transfer of the energy (Fig. 1.5).

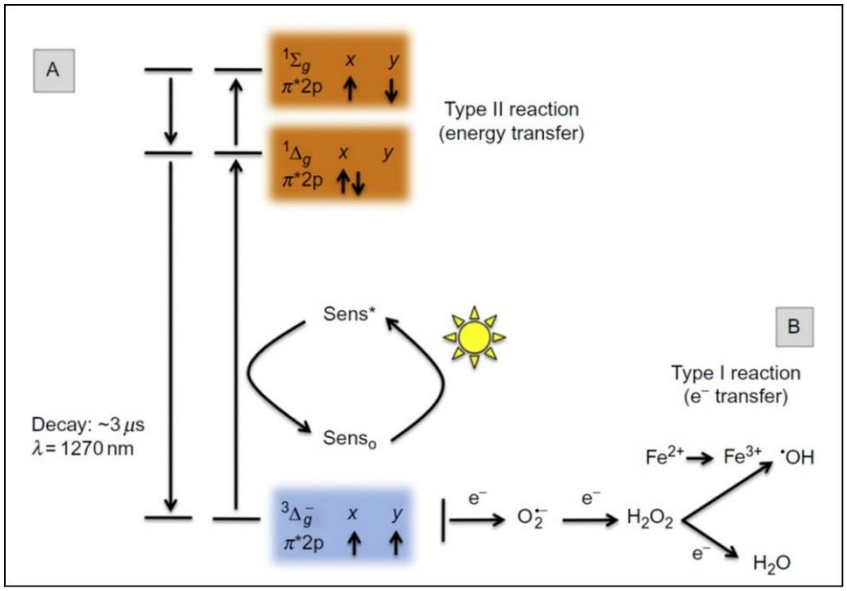

Fig. 1.5. Schematic overview of reactive oxygen species formation. (A) Sensitized formation of singlet oxygen. A photosensitizer ($Sens_0$) is excited by absorption of light ($Sens^*$) and subsequently may transfer energy to triplet-ground state-oxygen ($^3\Delta g$-). This type II reaction generates singlet oxygen, by spin conversion of one electron in the orbital. (B) Electron transfers (e^-) to triplet oxygen generate superoxide ($O_2^{\bullet-}$), hydrogen peroxide (H_2O_2) and water or hydroxyl radicals (•OH) are formed by the Fenton reaction in the presence of divalent metal ions, normally as Fe^{2+} (Glaeser *et al.*, 2011).

1.2.1 ROS from electron transfer

Molecular oxygen can accept electrons from any suitable donor by redox enzymes (Imlay, 2003). Single electrons from redox reactions in the respiratory chain can lead to reduction of molecular O_2. The sequential reception of electrons leads to the sequential reduction of O_2, and furthermore leads to the formation of a lot of different kinds of reactive oxygen species (ROS) including the superoxide anion ($O_2^{\bullet-}$), peroxide ($O_2\bullet^{-2}$), the hydroxyl radical (•OH) and the hydroxyl ion (OH^-) (Fig. 1.6) (Seaver and Imlay,

2004).

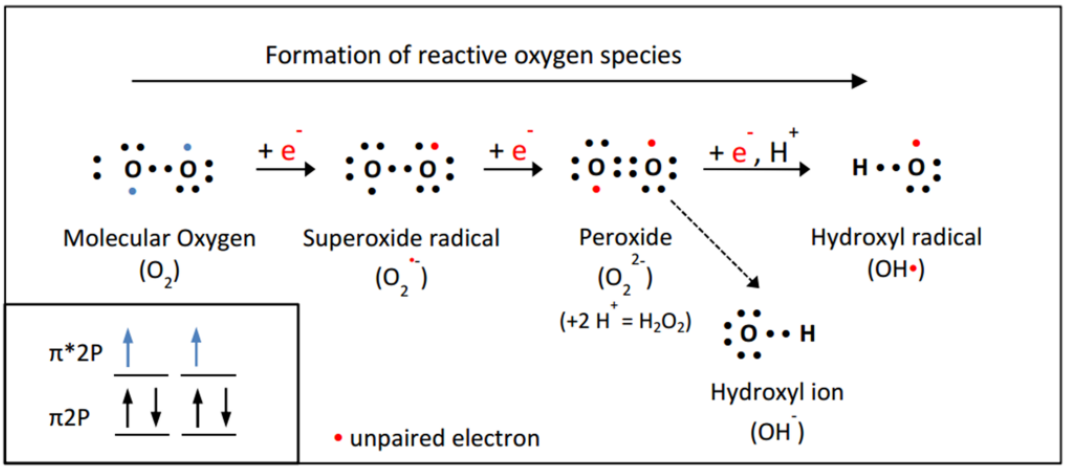

Fig. 1.6. Formation of ROS by sequential reduction of O_2 through the addition of electrons. In the ground state molecular O_2 appears with two unpaired electrons in the orbital. The reduction of O_2 leads to the formation of a lot of ROS including superoxide anion($O_2^{\bullet-}$), peroxide ($O_2^{\bullet-2}$) hydroxyl radical (•OH) and hydroxyl ion (OH^-) (Katrin Müller, 2016).

Another source for ROS formation from electron transfer can be found in iron metabolism. Though almost all organisms need a basic iron level, an excess of iron can trigger ROS formation in the Fenton reaction (Fenton, 1894). The Fenton reaction is driven by H_2O_2 and $O_2^{\bullet-}$ during aerobic respiration (Lemire *et al.*, 2013). In the Fenton reaction, reduced iron (Fe^{2+}) can be oxidised by H_2O_2 to ferric iron (Fe^{3+}), producing a hydroxyl radical (•OH) and a hydroxide ion (OH^-). In the next step $O_2^{\bullet-}$ can reduce ferric iron (Fe^{3+}) to ferrous iron (Fe^{2+}) and O_2. In addition, H_2O_2 and $O_2^{\bullet-}$ can interact to generate •OH in the Haber Weiss reaction (Fig. 1.7) (Kehrer, 2000). These reactions can happen again and again to produce further ROS. The Fenton reaction is not only limited to iron but also can be triggered by other metal ions such as copper and nickel (Lloyd *et al.*, 1997).

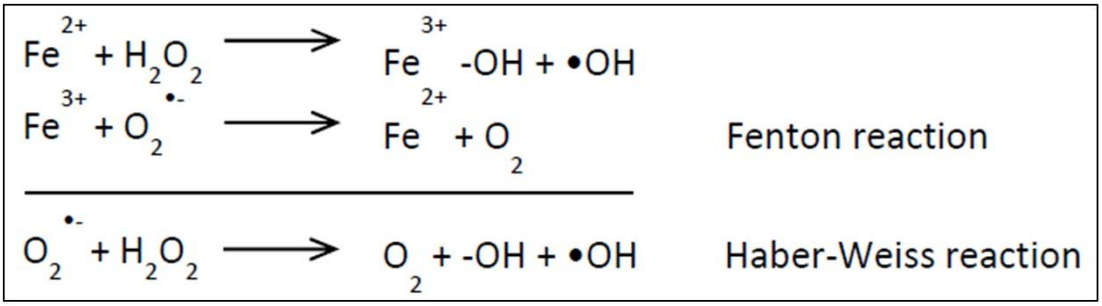

Fig. 1.7. Fenton and Haber-Weiss reaction.

1.2.2 ROS from energy transfer

Another main and special reactive oxygen species (ROS) is singlet oxygen ($^1O_2$) generated in many biological systems. Singlet oxygen can freely diffuse through biological membranes. But the formation of singlet oxygen is different from the above described ROS, since it depends on energy rather than electron transfer. The type II photosensitization results in energy transfer to ground state molecular oxygen and thereby a spin conversion of an electron. During the process of this reaction, the excited sensitizer transfers its excess energy to ground state molecular O_2, producing excited state $^1O_2$, and regenerating the ground state sensitizer (Fig. 1.5) (Chiu *et al.*, 2010). The $^1O_2$ can be mainly generated by two different routes in the cell, photo-excitation reactions (light reactions, dependence on the light) and chemiexcitation reactions (dark reactions, independence on the light) (Fig. 1.8) (Devasagayam and Kamat, 2002). In the cell, the generation of singlet oxygen is mainly dependent on light (Fig. 1.8 a,b). Photosensitized generation of singlet oxygen by the photosynthetic apparatus is also the main natural source of singlet oxygen in anoxygenic photosynthetic microorganisms, for example *R. sphaeroides and R. capsulatus*. Examples that are known naturally occurring photosensitizers are porphyrins, bilirubin, and bacteriochlorophyll (Roeder *et al.*, 1990).

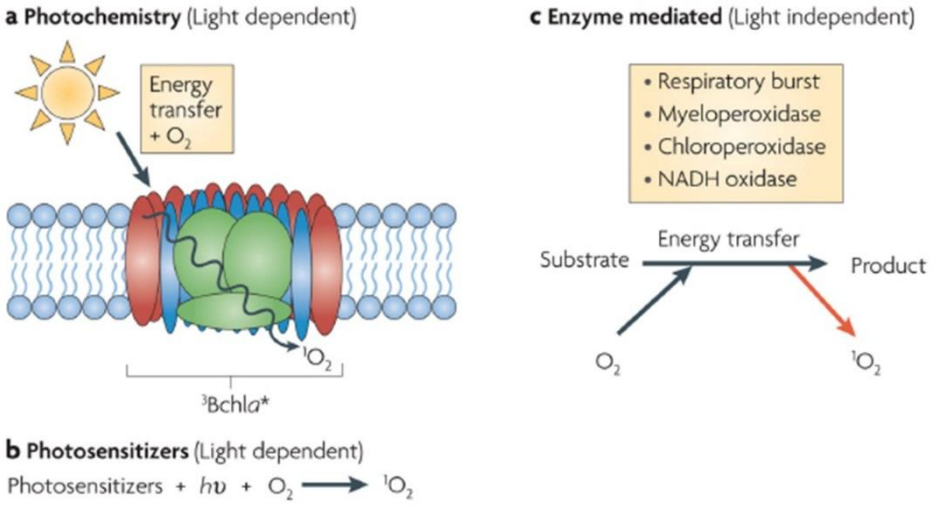

Fig. 1.8. Source of singlet oxygen in the cell (Ziegelhoffer and Donohue, 2009). a, b: the generation of

singlet oxygen is dependent on light. c: the generation of singlet oxygen is mediated on enzyme and independent on light.

In the photosynthetic bacterium *R. sphaeroides*, bacteriochlorophyll in the photosynthetic apparatus is usually used as photosensitizer to generate singlet oxygen in the presence of light and oxygen. When oxygen and light are simultaneously present, the bacteriochlorophyll absorbs energy from light resulting in the transfer of energy to oxygen to generate the singlet oxygen, which is called a kind of photooxidative stress (Fig 1.8). In non-photosynthetic bacteria, there are also several endogenous photosensitizes, such as porphyrins, rhodopsins or flavins (Ryter and Tyrrell, 1998). They are also able to generate singlet oxygen whenever light and oxygen are present (Redmond and Gamlin, 1999). However, the generation of singlet oxygen can also be independent of the light. The damage of ROS to Fe-S cluster and the regulation of the *isc-suf* operon to Fe-S cluster have been investigated by the change of growth conditions and the addition of hydrogen peroxide (H_2O_2) and tertiary butyl alcohol (tBOOH) as oxidative stress agents. In the cell, many pathways can generate singlet oxygen without light (Fig 1.8c). However, other pigments carotenoids, can directly quench singlet oxygen.

1.3 Iron homoeostasis

Iron has many essential biological functions, besides its beneficial functions, excess iron as a source of ROS formation in the Fenton reaction also has a threat to the cell and ROS is a major source of the damage of Fe-S cluster. In addition, the oxidised, insoluble, ferric form (Fe^{3+}) is poorly available for cells. Therefore, the regulatory mechanisms of the organisms for iron homoeostasis should be intensively investigated. Oxygen and different kinds of reactive oxygen species (ROS) can damage DNA, lipids, proteins and membranes, and reduced oxygen is more reactive than molecular oxygen, thus ROS are toxic to the cell. The damage to the cell that can be caused by oxidative stress shows quite some diversity. The process how Fe-S cluster transfers the redox signal to their protein partner is dependent on a change of coordination number or ligand specificity upon reduction or oxidation. Superoxide can oxidize Fe-S cluster and

then iron is released into the cytosol and reacts with hydrogen peroxide, generating the hydroxyl radical which reacts with DNA (Keyer and Imlay, 1996). $O_2^{\bullet-}$ anions are electrostatically attracted to the catalytic iron atoms in Fe-S cluster present in many proteins (Woodmansee and Imlay, 2003). After binding, the $O_2^{\bullet-}$ oxidised cluster gets unstable and decays, losing the catalytic iron atom and thereby the protein's function or enzymatic activity (Flint *et al.*, 1993). H_2O_2 directly oxidizes cysteinyl residues and creates sulphenic acid adducts that can either form disulphide crosslinks with other cysteines or be oxidised further to sulphinic acid moieties to affect the structure of proteins (Imlay, 2003). The highly reactive •OH is considered as the main contributing reactive oxygen species in endogenous oxidation and damage of cellular DNA (Cadet *et al.*, 1999).

To achieve balanced iron homoeostasis, organisms need to develop some regulatory mechanisms that scavenge excessed iron, storage efficient iron, and reduce iron containing proteins under iron-limiting conditions, as well as express the iron homeostatic machinery according to the iron availability (Andrews *et al.*, 2003). The mechanisms sensing the redox state, altering the environment, and detoxifying ROS play crucial roles in cell survival and are regulated by many genes and some transcription factors that are involved in Fe-S assembly. In an overarching manner, the regulation of the iron metabolism genes controls the iron homoeostasis assured by iron uptake, storage, and consumption. Bacteria can conduct the iron-uptake via siderophores, chelating and thereby solubilising the iron prior to transport, metal-type ABC transporters (Koster, 2001), and the ferrous iron transporting Feo system first discovered in *E. coli* (Kammler *et al.*, 1993).

1.4 Phylogenetics and physiology of *R. sphaeroides*

The bacterium *R. sphaeroides* represents an extensively studied model organism regarding bacterial photosynthesis. It is a rod-shaped, gram-negative, facultative photoheterotroph belonging to the α-subdivision of the proteobacteria with a length of 0.2-0.5 μm that carries one lateral flagellum (Imhoff, 2001). It is a non-sulphur purple bacterium living in mud, and aquatic environment in nature (Woese *et al.*, 1984). The *R.*

sphaeroides genome mapping was performed in 1989. It has two circular chromosomes, chromosome I (CI, ~3.0 Mbp) and chromosome II (CII, ~0.9 Mbp), and five circular plasmids with an overall size of ~4.6 Mbp (Suwanto and Kaplan, 1989; Choudhary *et al.*, 2004) and GC content is 65-69% (Suwanto and Kaplan, 1989). *R. sphaeroides* acts as a model organism for many studies regarding anoxygenic photosynthesis (especially regarding the process and gene expression of photosynthesis) and the adaption to changing environmental conditions by its metabolic versatility (Wei *et al.*, 2017). It is able to produce ATP under different growth conditions, including anoxygenic photosynthesis in the presence of light under anaerobic conditions, fermentation, aerobic respiration and anaerobic respiration with dimethyl sulfoxide (DMSO) as an electron acceptor.

In low oxygen condition, *R. sphaeroides* can perform aerobic respiration to produce ATP and forms high amounts of photosynthetic complexes and genes for pigment synthesis, pigment binding proteins and for the Cytbc1 complex are strongly induced. In high oxygen conditions, it can also grow by aerobic respiration, but the presence of photosynthetic complexes leads to formation of ROS, which destroy Fe-S cluster. The released iron leads to further ROS formation in the Fenton reaction. Meanwhile, the photosynthetic complexes and genes for pigment synthesis, pigment binding proteins and for the Cytbc1 complex are strongly inhibited. Besides aerobic respiration, *Rhodobacter* can also perform anaerobic respiration for energy acquisition by the use of dimethyl sulfoxide (DMSO) as an electron acceptor and carbon sources, and anoxygenic photosynthesis in the presence of light. The latter is the most special feature for *R. sphaeroides.* A photon from the light is absorbed and transferred to the quinone pool in the photosynthetic apparatus to complete the oxidation of the quinol and cyclic electron transfer for energy acquisition. But the aerobic respiration is the most preferred pathway to produce energy and can be performed whenever the concentration of the oxygen is low or high (Tabita *et al.*, 1990). Therefore, *R. sphaeroides* can be found in the running and standing water. In the different conditions, oxygen and light that is potentially harmful to cell are the major regulatory factors. The expression patterns of genes and the formation of photosynthetic complexes occur large

changes in adaptation to the changing conditions (Schindel and Bauer, 2016; Remes *et al.*, 2017) (Fig. 1.9).

Moreover, *R. sphaeroides* can also fix N_2 and CO_2 (Joshi and Tabita, 1996), and produce some important by-products, e.g. tetrapyrroles, polyhydroxyalkanoates, chlorophylls, heme, and vitamin B_{12} (Neidle and Kaplan, 1993; Matsumoto *et al.*, 2019).

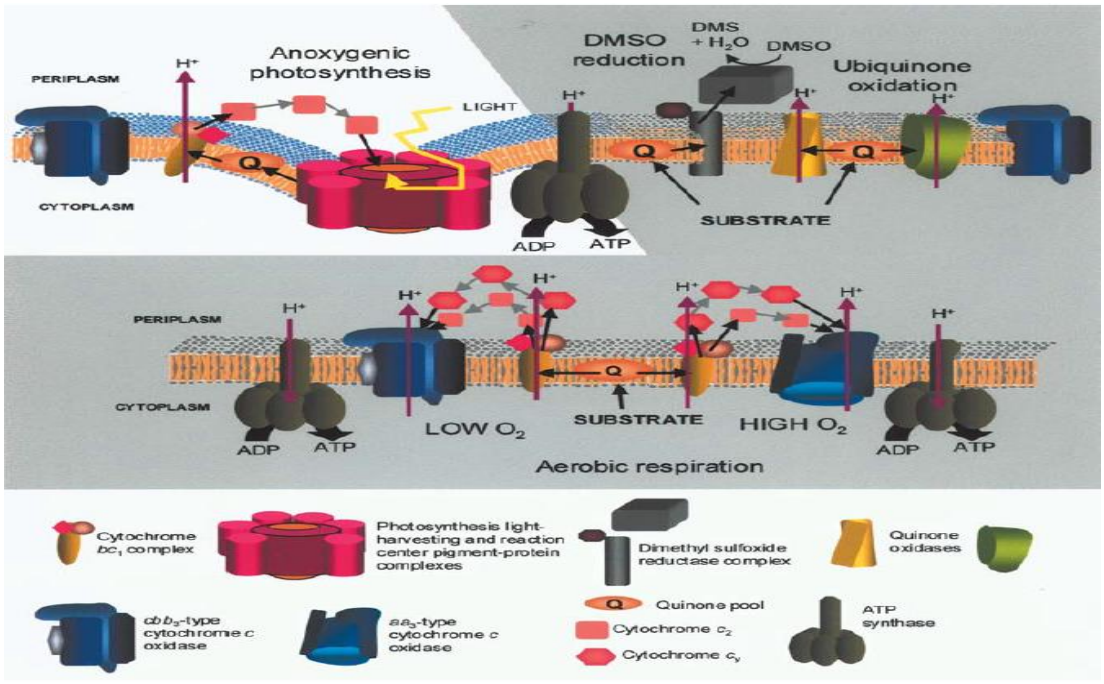

Fig. 1.9. Growth pathway of *R. sphaeroides* under aerobic, microaerobic, anaerobic conditions.

1.5 The photosynthesis (genes and complexes) in *R. sphaeroides*

The metabolic pathways of the light energy can be separated into phototrophy and photosynthesis. Phototrophy is the conversion from light energy to chemical energy for the production of ATP, while photosynthesis is the reduction of carbon dioxide (CO_2) into chemical energy for growth by using light energy (Bryant and Frigaard, 2006). In the photosynthesis, light energy can be used in the oxygenic photosynthesis (such as eukaryotic organisms and cyanobacteria) and anoxygenic photosynthesis (such as purple bacteria, green sulphur, and non-sulphur bacteria, as well as heliobacteria and the acidobacteria) (Macalady *et al.*, 2013). In the oxygenic photosynthesis, the light energy transfers electrons from water (H_2O) to carbon dioxide (CO_2) to produce

carbohydrates. In this transfer, the CO_2 receives electrons and is reduced into carbohydrates, meanwhile the water loses electrons and is oxidized into O_2. The anoxygenic photosynthesis uses of an alternative electron donor, such as H_2, H_2S, or other certain organic compounds instead of H_2O, and therefore no O_2 is produced, for example, *R. sphaeroides.*

1.5.1 The photosynthetic apparatus in *R. sphaeroides*

1.5.1.1 The structure of the photosynthetic apparatus in *R. sphaeroides*

The photosynthetic apparatus of *R. sphaeroides* is located within the invaginated inner membranes. It consists of one photochemical RC, a cytochrome and two light-harvesting complexes (LHI and LHII) (Fig. 1.10). In *R. sphaeroides*, the amount of LHI and LHII is determined by light and oxygen (Drews, 1995). Only under phototrophic condition, light intensity has a strong effect on the amount of LHII. Three multimeric trans-membrane protein complexes are formed: the RC, the cytochrome (cyt) bc1 complex and the antenna or light-harvesting complexes (LHC) (Drews, 1985; Vermeglio and Joliot, 1999) (Fig. 1.11). The pigments bacteriochlorophyll (BChl), carotenoids (Crts) and other cofactors can non-covalently bind with the proteins of the RC and LH to form complexes (Drews, 1985). The synthesis of bacteriochlorophyll starts from protoporphyrin IX and requires Fe-S cluster for catalysis (Zappa *et al.*, 2010). Insertion of iron into protoporphyrin IX completes the synthesis of heme (Yin *et al.*, 2013), while the synthesis of BChl requires with the insertion of magnesium and further enzymatic modifications (Zappa *et al.*, 2010). In addition to the BChls, there is another photopigment-carotenoids. They have two major functions in photosynthesis, accessory light harvesting and photoprotection. First, Crts improve energy collection because they can absorb light at shorter wavelengths than the BChls, and then transfer energy to BChl. Second, they protect photosynthetic cells because they can quench high energy states of BChl (Frank, 1995) and the toxic singlet oxygen (Di Mascio *et al.*, 1989) (Yu *et al.*, 2018). The maximum absorbance of the green BChl related with the LH I is 875 nm and related with the LH II complex occur at 800 and 850 nm, whereas the absorbance of the yellow carotenoids is in the range of 450 to 550 nm.

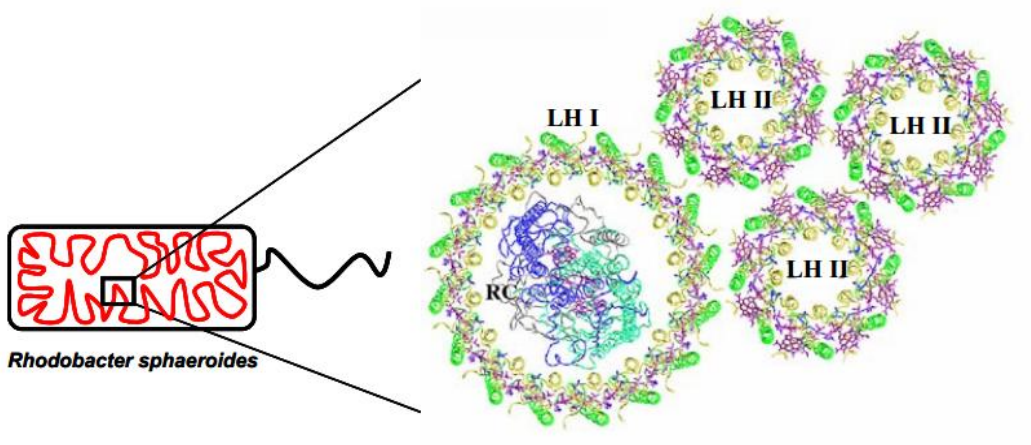

Fig. 1.10. Photosynthetic apparatus located in the vesicular intracytoplasmic membranes. LH, light-harvesting complex; RC, reaction center (Han, 2006).

1.5.1.2 The function of the photosynthetic apparatus in *R. sphaeroides*

In *R. sphaeroides*, the anoxygenic photosynthesis takes place in the photosynthetic apparatus (Fig. 1.11). When the BChl related with the LHII absorb a photon, the excitation is transferred to the BChl bound to LHI, subsequently reaches the RC (where initial charge separation happens) in less than 100 picoseconds (ps). In the RC, the excited primary donor, which is a bacteriochlorophyll dimer, accepts an electron from LHI, and then the electron is transferred to a molecule of bacteriopheophytin in 2-3 ps, subsequently reaches the primary quinone (Q_A) and the secondary quinone (Q_B) in ~200 ps. The fast electron transfers nearly ensure that every photon is absorbed and one electron is transferred in the RC. Q_B picks up two protons from the cytoplasm and then is released from the RC into the quinone pool where Q_B undergoes a second reduction step and picks up two protons from the cytoplasm again. The electron transfer is cyclic and completed by the oxidation of the quinol and soluble cyt c_2. During this cycle process, the (Fe_2S_2) cluster of the Rieske protein, which is bound in the binding with cyt bc_1 complex catalyzes the reaction, and the final release of four protons into the periplasm (Fig. 1.11). Thus, the cyclic electron transfer of redox reactions couples with the transfer of the protons from the cytoplasm to the periplasm and creates a proton gradient that drives the production of ATP (Vermeglio and Joliot, 1999).

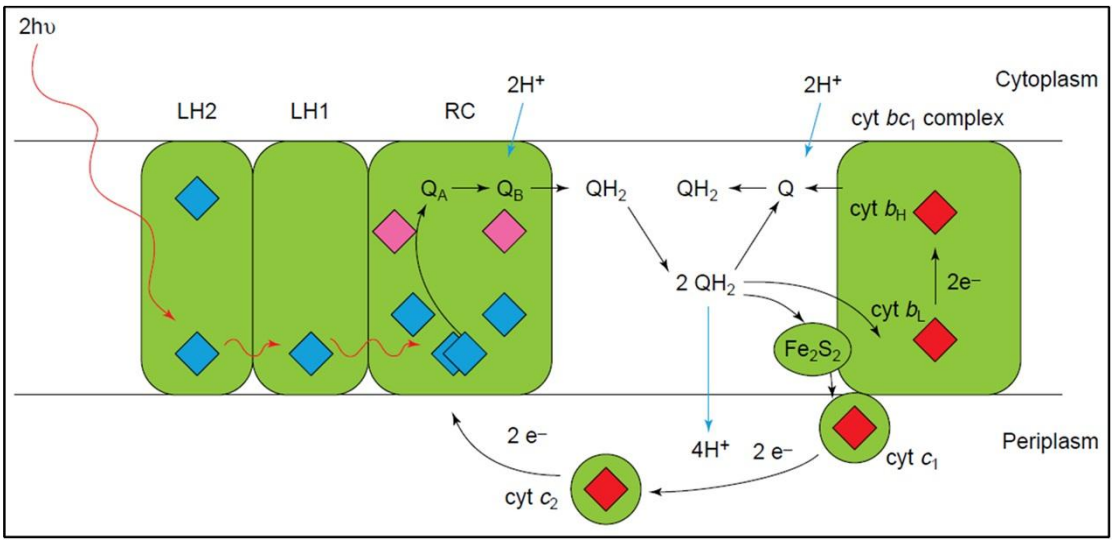

Fig. 1.11. Schematic representation of the photosynthetic cyclic electron-transfer chain in *R. sphaeroides* (Vermeglio and Joliot, 1999). Bacteriochlorophyll molecules are represented by blue diamonds and bacteriopheophytin molecules by pink diamonds. Hemes are denoted by red diamonds. The red arrows represent excitation transfer and the black and blue arrows correspond to electron and proton transfer, respectively.

The important enzymes of bacteriochlorophyll synthesis contain Fe-S cluster (Sirijovski *et al.*, 2007; Selvi and Sharma, 2008), and the cytochrome bc1 complex also requires Fe-S cluster (Purvis *et al.*, 1990; Borek *et al.*, 2018). There may be a regulatory system between the expression and assembly of Fe-S cluster (*isc-suf* operon) and the photosynthetic apparatus (complexes).

1.5.2 Regulation of the formation of photosynthetic complexes in *R. sphaeroides*

The genes encoding proteins of photosynthetic complexes and enzymes for pigment synthesis in *R. sphaeroides* mostly are located in the photosynthetic gene cluster, and the details are shown in the Fig 1.12. The 45 kb DNA region of the *R. sphaeroides* genome clusters most of the photosynthesis genes together. The photosynthetic gene cluster contains the genes for the carotenoid synthesis (*crt*), bacteriochlorophyll synthesis (*bch*) and the genes for photosynthetic proteins of LHI (*pufBA*), and RCs (*pufLM*, *puhA* (H-subunit)), as well as genes for some regulators PpsR (photopigment suppression), PpaA (photopigment and *puc* activation) and TspO (tryptophan-rich sensory protein) (Comayras *et al.*, 2005; Choudhary and Kaplan, 2000) (Fig. 1.12). The two *puc* operons encode the photosynthetic proteins of LHII. The

expression of the part of photosynthetsis genes and some pigments have been investigated in this work by the use of different photosynthetic mutants.

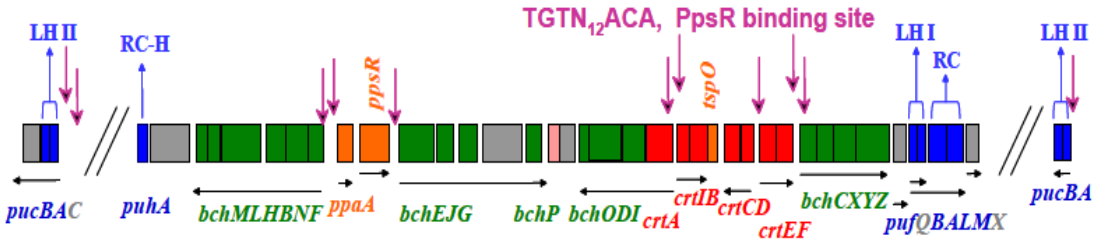

Fig. 1.12. Scheme of the photosynthetic gene cluster and *puc* operons arrangement in *R. sphaeroides*. Putative transcripts are shown as black horizontal arrows, PpsR-binding sites are shown as purple vertical arrows and components of the photosynthetic apparatus are shown as blue vertical arrows. Colors: green, bacteriochlorophyll biosynthesis genes (*bch*); red, carotenoid biosynthesis genes (*crt)*; blue, genes encoding structural polypeptides of photosynthetic apparatus; gray, genes encoding assembly factors or proteins of unknown function; orange, genes encoding regulatory factors; pink, genes encoding enzymes common to bacteriochlorophyll and ubiquinone biosynthesis. RC-H, H-subunit of RC (Han, 2006).

In *R. sphaeroides*, the expression of photosynthesis genes and the synthesis of photosynthetic complexes and pigments are regulated by two major signals: oxygen and light. A large number of regulatory proteins is involved in the regulation, such as the two-component PrrB/PrrA activation system, AppA/PpsR (antirepressor/repressor) system, FnrL, Spb, TrxA, IHF, PpaA, TspO. In high oxygen condition, *R. sphaeroides* performs aerobic respiration and can not form photosynthetic complexes, since PpsR represses the expression of photosynthesis genes. However, most of the purple non-sulphur photosynthetic bacteria are facultative anaerobic (McEwan, 1994). In low oxygen condition, the photosynthesis genes are triggered to form photosynthetic complexes in *R. sphaeroides* (Gregor and Klug, 1999). *R. sphaeroides* can also produce ATP by anaerobic respiration and anoxygenic photosynthesis. In the absence of oxygen and light, it is called anaerobic dark condition which increases the expression of photosynthesis genes. In this case, *R. sphaeroides* can also produce ATP by the use of DMSO as an electron acceptor and form a large amount of photosynthetic complexes. In the absence of oxygen and the presence of light, anoxygenic photosynthesis can take place and the expression of photosynthesis genes is increased. *R. sphaeroides* can produce ATP by the single photosystem with cyclic electron transport (Fig. 1.11). In

this kind of the growth conditions, the amount of photosynthetic complexes depends on the light intensity. Blue light represses the expression of the photosynthesis genes under intermediate oxygen tension (Shimada *et al.*, 1992; Braatsch *et al.*, 2002).

R. sphaeroides has two c type cytochromes (Cyt c): Cyt cy and Cyt.c2. Cyt cy can not join in photosynthetic electron transfer, just can join in respiratory electron transfer. However, Cytc2 can not only transfer electrons from the Cyt bc1 complex to a terminal cbb3/aa3 oxidase in respiratory electron transfer, but also can transfer electrons from the cyt bc1 complex to the photooxidized RC complex for photosynthetic electron transfer (Fig. 1.13) (Oh and Kaplan, 2000; Vermeglio and Joliot, 1999).

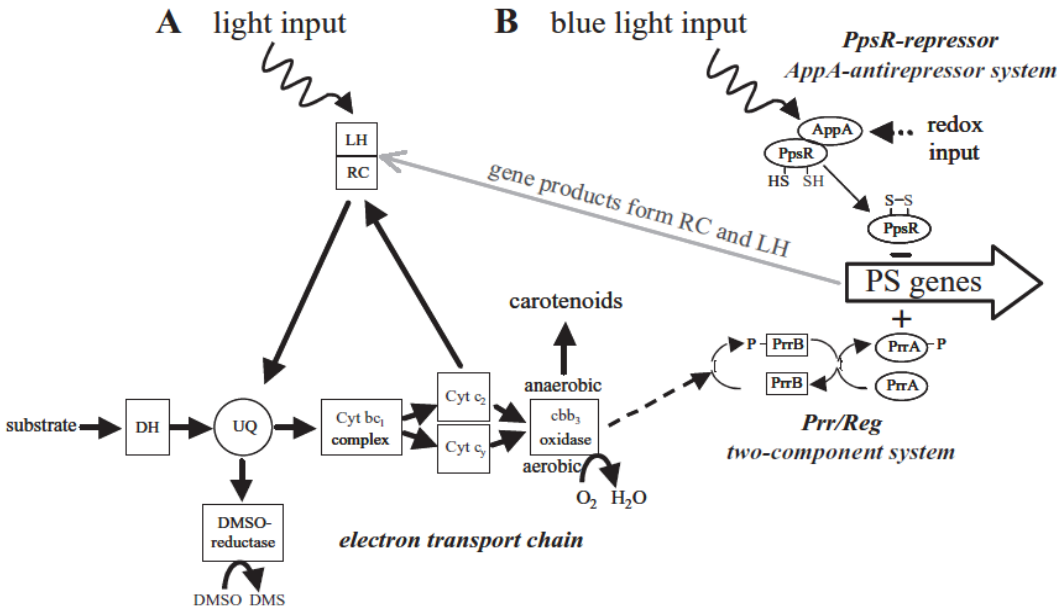

Fig. 1.13. Model for different mechanisms of light sensing and signal transduction in *Rhodobacter* (Happ *et al.*, 2005). Thick arrows indicate electron transport, thin arrows indicate signal transmission. Cyt *aa*3 was omitted from the figure as it is not expressed under anaerobic conditions. A. Regulation mediated by electron flow. B. AppA-PpsR regulatory system. Cyt, cytochrome; DH, dehydrogenase; DMS, dimethyl sulphide; DMSO, dimethyl sulphoxide; LH, light harvesting complexes; RC, reaction centre; UQ, ubiquinone; +/–, activation/repression of gene expression.

In the anaerobic condition, the electron flow of reductant through the cbb3-oxidase is used in the biosynthesis of carotenoids at the last step (Oh and Kaplan, 1999). The absorption of blue light by the BLUF-type photoreceptor AppA of *R. sphaeroides* regulates the expression of the photosynthesis genes, which is independent on the photosynthetic electron transport by release of a stable AppA-PpsR complexes

that represses DNA-binding of the PpsR repressor (Zeilstra-Ryalls and Kaplan, 2004). Strains lacking cytc2 can not perform photosynthetic electron transport. Photosynthetic electron transport effects on the expression of the *isc-suf* operon have been investigated in this work by the mutant.

1.5.3 Regulation by the photosynthetic regulators (AppA/PpsR) in *R. sphaeroides*

The *ppsR* gene is located in the upstream of many *bch* and *crt* genes in the photosynthesis gene cluster (Fig. 1.12). PpsR has a HTH (**h**elix-**t**urn-**h**elix) motif in the C-terminal region, which plays a key role in DNA-binding as a tetramer (Gomelsky *et al.*, 2000; Masuda and Bauer, 2002). The conserved binding motif TGT-N_{12}-ACA is located downstream of, or overlapping with, putative σ70-type promoters of photosynthesis genes (Choudhary and Kaplan, 2000) (Fig. 1.12). PpsR represses the transcription of photosynthesis genes, such as the *puf* and *puc* operon, genes for the synthesis of BChl (*bch*) and carotenoid (*crt*) as well as other tetrapyrrole synthesis genes in high oxygen tension (Penfold and Pemberton, 1994). The sRNA PcrX regulates the expression of photosynthesis genes by RNase E-mediated cleavage (Eisenhardt *et al.*, 2018).

The flavoprotein AppA (**a**ctivation of **p**hotopigment and **p**uc expression) antagonizes the repressor activity of PpsR and activates the expression of the genes for pigment synthesis and *puc* operon. The protein can not only perceive redox signals, but also can transfer light signals. The flavoprotein AppA has two main domains that locate in the N-terminal regeion and C-terminal. The N-terminal BLUF domain of AppA was identified as a type of blue light phototreceptor for sensing light (Gomelsky and Klug, 2002; Han *et al.*, 2004; Han *et al.*, 2007). AppA regulates photosynthesis gene expression in response to blue light and redox signals (Gomelsky and Kaplan, 1997; Braatsch *et al.*, 2002; Masuda and Bauer, 2002). The transfer of the light signal from BLUF domain and the concentration of the oxygen can influence the affinity between AppA and PpsR and consequently regulate DNA-binding activity of PpsR (Gomelsky and Klug, 2002; Han *et al.*, 2004). The C-terminal domain of AppA harbours a

cysteine-rich cluster (Cys-X5-Cys-Cys-X4-Cys-X6-Cys-Cys) that could sense the redox signal through a dithiol-disulfide switch. The C-terminal domain of AppA is also linked to a heme-binding domain and is the main redox sensor. The heme cofactor affects the interaction of the C-terminal part of AppA to PpsR but also its interaction to the N-terminal light sensing AppA-BLUF domain (Han *et al.*, 2007).

The model of function of AppA protein binding with PpsR is shown in Fig. 1.14. In high oxygen tension, the AppA can not release the repression of photosynthesis genes by PpsR in spite of light (Masuda and Bauer, 2002; Nishino *et al.*, 2018). In the absence of light and in low oxygen tension, the AppA protein adopts an active state and can bind with PpsR to form stable AppA-PpsR complexes that allow the expression of the photosynthesis genes (Metz *et al.*, 2012; Pandey *et al.*, 2017). This transition apparently does not involve the FAD cofactor of AppA. AppA in this state antagonizes PpsR and PpsR mediated repression of the *puf* and *puc* operons is released. When blue light is present, it excites FAD, stimulating the reversion of AppA from the active state to the inactive state, thus leading to a tighter repression of the *puf* and *puc* operons. If oxygen tension is very low, blue light repression is still present through the AppA/PpsR system (Braatsch *et al.*, 2002).

A recent study reavealed that PpsR can bind with the vitamin B_{12}-dependent photoreceptor AerR to alter PpsR's function (Yamamoto *et al.*, 2018). In other bacteria, the AppA/PpsR system has been investigated and was confirmed by two mathematical models (Pandey *et al.*, 2017; Arisaka *et al.*, 2018; Nishino *et al.*, 2018).

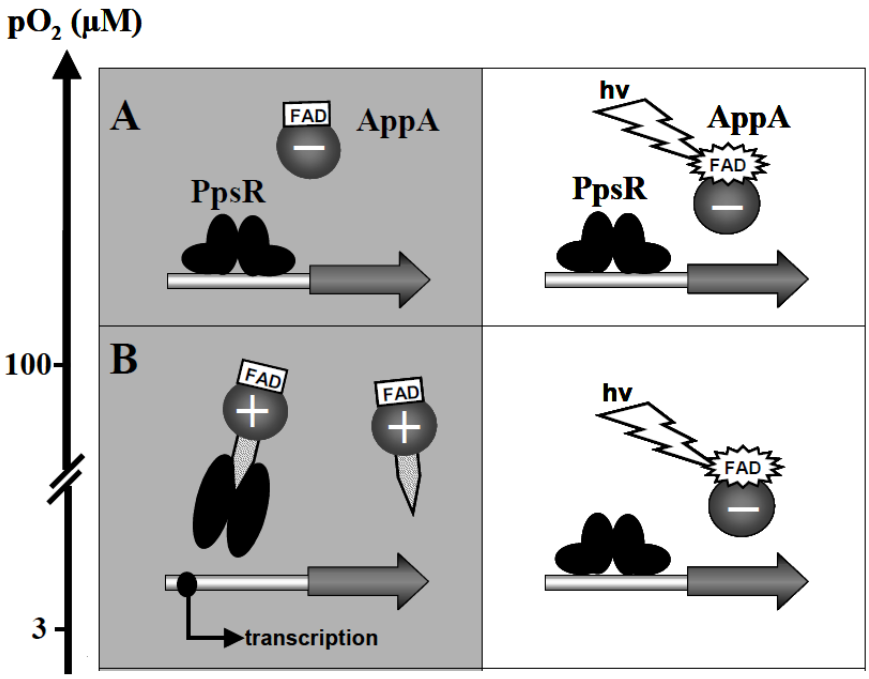

Fig. 1.14. Model for function of AppA as an integrator of redox and light signals (Han, 2006). The oxygen and light dependent effect of AppA on *puc* expression is mediated by the transcriptional repressor PpsR (Gomelsky and Kaplan, 1998; Masuda and Bauer, 2002). **(A)** in high oxygen, AppA is in an inactive conformation (−) independently of light. **(B)** in low oxygen, the AppA protein undergoes a transition to an active conformation (+) and forms a stable AppA-PpsR complex that allows gene expression. Blue light-excited AppA (−) is incapable of inhibiting PpsR activity. The maintenance of the light dependent repression (Shimada *et al.*, 1992) is mediated by the FAD cofactor of the AppA protein (Braatsch *et al.*, 2002; Braatsch and Klug, 2004).

1.5.4 Regulation of photosynthesis genes expression by other factors

Besides the factors mentioned above, many additional factors have been observed to affect the expression of photosynthesis genes. In *R. sphaeroides*, PpaA activates the expression of photopigments and *puc* operon in high oxygen tension, but the expression of the *ppaA* gene is repressed by the repressor PpsR (Fig. 1.15) (Gomelsky *et al.*, 2003). This regulation also prevents harmful ROS from cell. CryB belongs to a cryptochrome family and also can regulate light-dependent the expression of photosynthesis genes by directly binding to AppA (Geisselbrecht *et al.*, 2012). The sRNA PcrZ, whose transcription is regulated by PrrA and FnrL can repress photosynthesis genes and the *appA* gene, leading to a stronger repression of photosynthesis genes by PpsR (Mank *et al.*, 2012). In low oxygen, PrrA and FnrL protein can activate the transcription of the photosynthesis genes. The PrrAB two component system can regulate different

metabolic pathways, such as CO_2 fixation, N_2 fixation, H_2 uptake and oxidation (Eraso and Kaplan, 2009; Zeilstra-Ryalls and Kaplan, 1995).

In general, the expression of the photosynthesis genes is regulated by oxygen, light and many different regulators in the different signal transduction pathways that form a complicated regulatory network in *R. sphaeroides* (Fig. 1.15). Some of the regulators are specific for the expression of the photosynthesis genes, but some other regulators affect more extensive targets. Photosynthesis genes are not all regulated by the same regulatory pathways, even these may overlap.

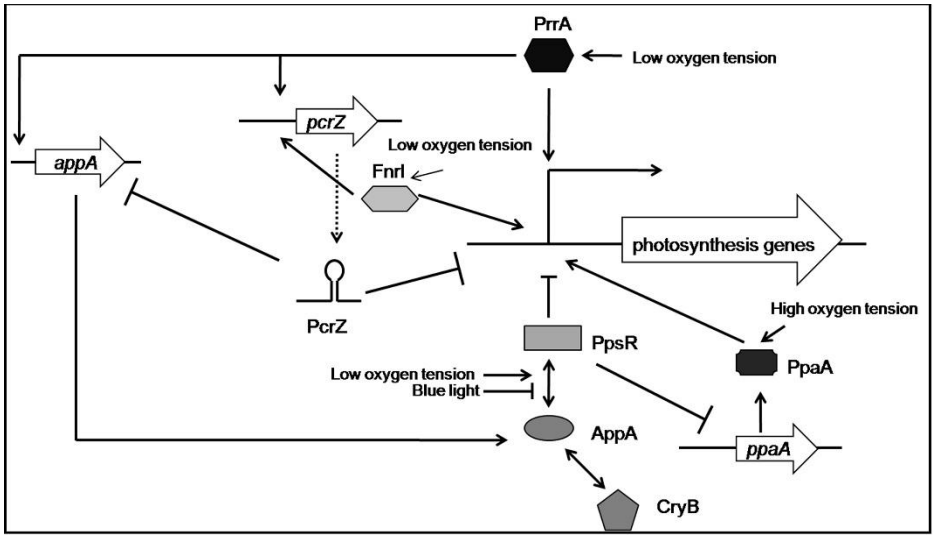

Fig. 1.15. Regulation of photosynthesis genes by light and oxygen tension in *R. sphaeroides.* Genes are depicted as white arrows, while proteins are shown as symbols containing the respective protein name. Upon a drop of oxygen tension the transcriptional regulators FnrL and PrrA, as well as the anti-repression of PpsR via AppA and PpaA activate the expression of the photosynthesis genes. PpaA activates the expression of photosznthesis genes in high oxygen tension. At the same time PcrZ expression is triggered PrrA- and FnrL-dependent, leading to repression of photosynthesis genes and seemingly also AppA expression. CryB also can regulate the expression of photosynthesis genes by directly binding to AppA (Peng, 2016).

1.6 Iron and oxidative stress-dependent regulators in *R. sphaeroides*

The microarray and real time RT PCR analyses from previous studies of the Klug group revealed that the expression of the *isc-suf* operon is regulated by the different growth conditions and by the iron-dependent regulators Fur/Mur, Irr, IscR protein as well as by redox-dependent regulator OxyR protein (Peuser *et al.*, 2011; Peuser *et al.*,

2012; Remes *et al.*, 2014; Remes *et al.*, 2015).

1.6.1 Regulation of oxidative stress-dependent regulators OxyR

The OxyR protein belongs to the LysR family of bacterial regulators and was first known in *Salmonella enterica serovar Typhimurium* and *E.coli* by mutations that are more resistant to hydrogen peroxide (Zheng and Storz, 2000; Christman *et al.*, 1985). OxyR has a helix-turn-helix (HTH) DNA-binding site in the N-terminal domain and forms a tetramer in solution (Storz *et al.*, 1990). The reaction between OxyR and hydrogen peroxide is highly specific (Zheng and Storz, 2000).

The mass spectrometry measurements and thiol-disulfide quantitation assays on the purified protein OxyR showed that C199 and C208 are in disulfide bond form in the oxidized OxyR, and in dithiol form in the reduced OxyR. OxyR activation and deactivation is a consequence of the C199–C208 disulfide bond formation and reduction (Fig. 1.16). Since the oxidized OxyR has a disulfide bond between cysteine residues C199 and C208, the oxidized OxyR binds to DNA differently than the reduced protein (Zheng and Storz, 2000). The reduced OxyR is oxidized by H_2O_2. Oxidized OxyR is in turn reduced by GSH (glutathione)/glutaredoxin1 (Fig. 1.16) (Zheng and Storz, 2000).

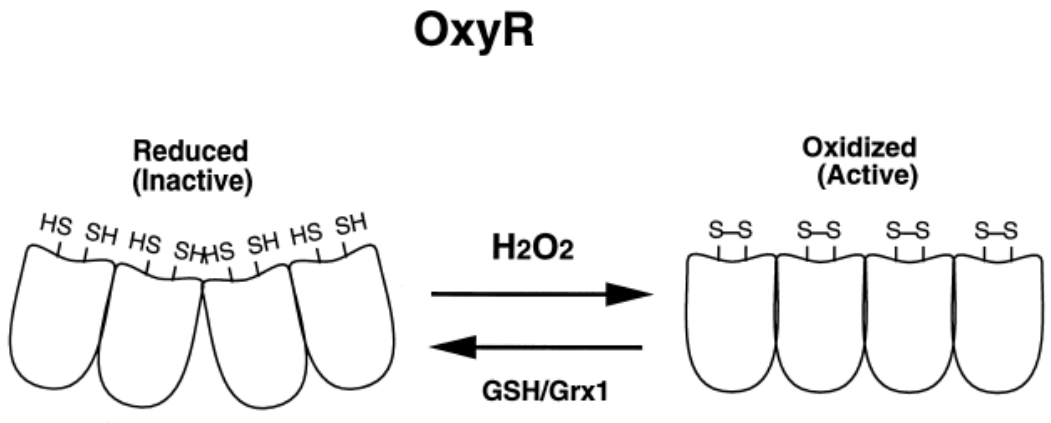

Fig. 1.16. Model for OxyR activation and inactivation (Zheng and Storz, 2000).

OxyR regulates the expression of many genes related to the defence against peroxides and Fe-S cluster assembly by contacting the alpha subunit of DNA polymerase in response to H_2O_2 (Kehres *et al.*, 2002; Outten *et al.*, 2004), but the

manner of the regulation is different (Sund *et al.*, 2008; Wan *et al.*, 2018). In the most of the cases, OxyR activates the expression of these genes in the presence of H_2O_2 by the binding of oxidized OxyR to the upstream region, such as the genes that are related to Fe-S cluster assembly, whereas under no-stress conditions reduced OxyR binds to the DNA but has no regulatory effect on the expression of these genes.

In *R. sphaeroides*, OxyR also has the same function and activates genes for iron metabolism in response to H_2O_2 (Zeller *et al.*, 2007). In iron limitation under anaerobic conditions, the change of one third of the iron-regulated genes was independent of oxygen availability. Activation of these genes including the *isc-suf* operon was dependent on OxyR in iron limitation under the aerobic conditions. The OxyR mutant had an increased ROS production and impaired growth in iron limitation (Remes *et al.*, 2017). The finding identified that the genes related iron did not directly respond to iron-limitation but their expression is rather activated by increased ROS levels in *R. sphaeroides*. The OxyR regulator provides a link between the responses to oxidative stress and iron.

1.6.2 Regulation of iron-dependent regulators IscR

IscR is a member of the Rrf2 super family of transcriptional regulators and contains a helix-turn-helix (HTH) DNA-binding site. Most of the members from the Rrf2 family have conserved Cys residues that can ligate the Fe–S cluster to become Fe–S protein. In many living organisms, IscR plays two main roles as a sensor of cellular Fe–S level and a global transcriptional regulator for Fe–S biogenesis (Giel *et al.*, 2006; Lee *et al.*, 2008; Giel *et al.*, 2013). But most functions of IscR have been intensely investigated in γ-proteobacteria, such as *E. coli*. The first gene of the *isc* operon encodes the IscR transcriptional regulator in *E. coli*. IscR regulates the expression of at least 40 genes including the *isc-suf* operon that encodes the Fe–S cluster biogenesis genes (*suf* genes) and genes for other Fe-S proteins (Schwartz *et al.*, 2001; Giel *et al.*, 2006). IscR is indeed a Fe–S protein and represses its own gene. However, IscR also regulates some other genes that encode Fe–S proteins and non-Fe–S proteins. Therefore, IscR is as global regulator in gene transcription (Giel *et*

al., 2006; Loiseau *et al.*, 2007; Angelini *et al.*, 2008; Wu and Outten, 2009; Carey *et al.*, 2018; Jousset *et al.*, 2018).

Normally, most of the Fe–S proteins have four Cys to ligate Fe–S cluster, while the IscR protein that contains a (2Fe-2S) cluster only have three Cys and one His to ligate Fe–S cluster in *E. coli* (Fleischhacker *et al.*, 2012). The three Cys residues of Fe–S proteins are essential for the formation of the holo-IscR (Yeo *et al.*, 2006; Nesbit *et al.*, 2009), which may decrease the affinity for Fe–S cluster and is therefore only able to bind the Fe–S cluster when other proteins do not require them (Schwartz *et al.*, 2001). Interestingly, IscR is also a Fe–S protein and a main iron-dependent regulator in *R. sphaeroides*, but the IscR protein only has a single-Cys residue to ligate Fe–S cluster. This difference of the structure of IscR raised the question how *R. sphaeroides* IscR ligates an Fe–S cluster and regulates the assembly of the Fe–S cluster (Remes *et al.*, 2014). In the different growth conditions, especially in the oxidative stress conditions, the Fe–S of IscR is likely one of the first cluster destroyed or rebuilt due to the instability of the ligation. IscR regulated genes are involved in Fe-S cluster biosynthesis, iron homeostasis, resistance to oxidants, and pathogenicity in many bacterial (Vergnes *et al.*, 2017; Andre *et al.*, 2017; Romsang *et al.*, 2018; Saninjuk *et al.*, 2019). IscR can also regulate heme uptake (Schwiesow *et al.*, 2018).

The similarity of the protein sequences between *E. coli* and *R. sphaeroides* is only 44%. The low similarity is from C-terminal region that can bind with the Fe-S cluster in *E. coli*. However, the determination of the content and spectrum of Fe-S cluster of IscR protein hints to the presence of an (2Fe-2S) center and indeed binds each other. IscR from *R. sphaeroides* may have different modes in the regulation of the coordination of the Fe-S cluster (Remes *et al.*, 2015). In *R. sphaeroides* IscR is encoded by the first gene *iscR* of *isc-suf* operon and was not only identified to bind with the *iscR* gene (Remes *et al.*, 2015), but also can bind to a sequence motif, a named "Iron-Rhodo-Box" in the front of some genes of iron metabolism (Rodionov *et al.*, 2006). The analyses of the transcriptome by microarray analyses and RT-PCR indicated the expression of a total of 110 genes or operons are directly or indirectly

dependent on the IscR, such as the *suf* operon, RSP_6006-1546-1548 (encoding HemP, bacterioferritin, ferredoxin, putative iron-regulated protein), RSP_2913 (for subunit of ABC Fe siderophore transporter), RSP_1545-1543 (thiol oxidoreductase with cytochrome c heme-binding sites), RSP_0920-0922 (ExbB, ExbD, TonB for ferric siderophore acquisition), RSP_4274-4275 (FecR and FecI), and the RSP_3413-3417 operon (ABC Fe-siderophore transport and *TonB* dependent ferrichrome-iron receptor). The repression and specific binding of the IscR with the promoters of *iscR* and *hemP* were confirmed *in vitro* (Remes *et al.*, 2015).

The role of *R. sphaeroides* IscR is as a transcriptional repressor for genes involved in iron metabolism by direct binding to the promoter region of genes preceded by a specific DNA-binding motif (Iron-Rhodo-box), and a sensor of the Fe–S cluster status of the cell to coordinate an iron sulfur center and provide the probability that in this ligation of the Fe-S cluster despite the marked differences in sequence from *E. coli*. A mutant of lacking IscR has a more impaired in the iron limitation than the wild-type and has a significantly increased ROS levels in the normal condition or in the iron limitation condition. dRNAseq (differential RNA seq) analyses for *R. sphaeroides* shown the operon including *iscR* has five promoters and is co-transcribed with the subsequent *suf* operon (Remes *et al.*, 2015). IscR may also sense oxidative stress through destabilization of the Fe-S cluster (Roche *et al.*, 2013). The details of the regulation of the multi-promoters will be analysed under the different conditions in this study.

1.6.3 Regulation of iron-dependent regulators Fur/Mur

The Fur protein (ferric uptake regulator) of *E. coli* plays a role as transcriptional repressor of iron-regulated promoters (siderophore genes and operons) due to its iron-dependent DNA binding activity in *E. coli* and in many other bacteria (Bagg and Neilands, 1987; Hantke, 2001; Choi and Ryu, 2019). Fur contributed to increased expression of iron transporter-coding genes under low-iron conditions (Choi and Ryu, 2019). Fur also plays an important role in defending against oxidative stress and iron starvation (Aranzaes *et al.*, 2007; Sevilla *et al.*, 2019; Wang *et al.*, 2019;

Pinochet-Barros and Helmann, 2018).

The Fur protein contains the N-terminal domain, which contains a HTH motif with an unusual turn and has the ability to bind DNA, and the C-terminal domain that contains two metal-binding sites and is related to dimerization (Stojiljkovic and Hantke, 1995). The Fur protein always appears to be a dimer in solution no matter of the presence or absence of Fe^{2+} (Coy and Neilands, 1991; Michaud-Soret *et al.*, 1997). Recent work reported that Fur proteins are highly stable as iron metallated tetramers in solution (Perard *et al.*, 2018; Nader *et al.*, 2019). In the *E. coli* Fur protein, one metal-binding site is occupied by Zn^{2+} (Jacquamet *et al.*, 1998; Althaus *et al.*, 1999). The binding ability of the active Fe^{2+} in the C-terminal domain is weak and may be occupied *in vitro* by Mn^{2+}, Co^{2+} or some other first-row divalent transition metal cations (Adrait *et al.*, 1999). A 19-base-pair sequence (5'GATAATGATAATCATTATC3'), which is named Fur box, is the functional target of the Fur protein and together with the Fur dimer to represents a classical bacterial Fur-DNA interaction repressors model, where a protein dimer recognizes a palindromic DNA sequence (Escolar *et al.*, 1999).

In normal condition, Fur can ligate the divalent Fe^{2+} and bind the target DNA sequences (Fur boxes or iron boxes, Fig. 1.17), subsequently repress the transcription of the iron-regulated genes. However, when iron is scarce, the balance is broken to release Fe^{2+} and the RNA polymerase replaces the repressors and binds the promoter region to promote the expression of genes for the biosynthesis of siderophores and other iron-related functions (Fig. 1.18) (Klebba *et al.*, 1982; Griggs *et al.*, 1987). In some cases, Fur indirectly regulates the metabolism of iron by regulating three types of activators: two-component signal transduction systems, AraC-like regulators of the synthesis of siderophores and their uptake systems, and extracytoplasmic function (ECF) sigma factors (Braun *et al.*, 1998).

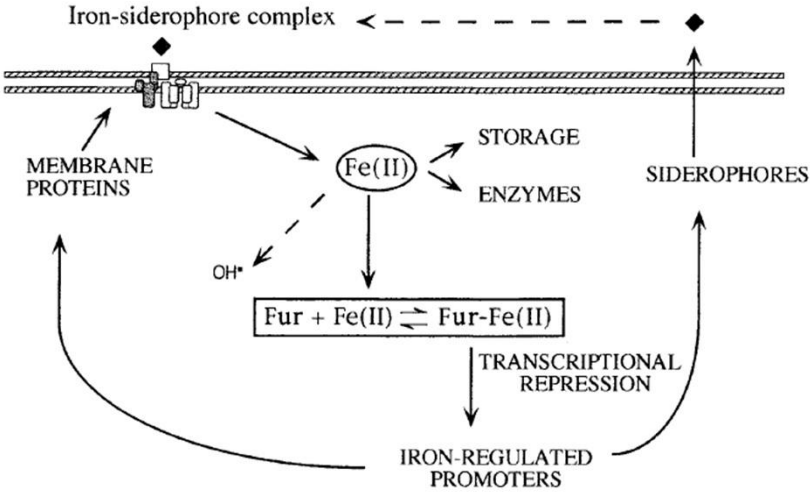

Fig. 1.17. The regulation of the iron transport in *E. coli*. It is based on the existence of two configurations of the Fur protein in an equilibrium which is displaced by Fe^{2+} towards the form competent for binding DNA and thus for repression of transcription. The lack of iron results in the derepression of an entire collection of genes for the biosynthesis and transport of siderophores and hence the activity of one or more high-affinity iron uptake systems. These scavenge the Fe^{3+} present in the medium and drive ferrisiderophore complexes through an elaborate transport scheme which includes not only specific outer membrane receptors but also periplasmic and inner membrane proteins. The metal is then reduced intracellularly to Fe^{2+}. Transport of this chemical element in aerobically grown cells is subjected to a very fine tuning, since iron overload promotes generation of the highly reactive forms of oxygen (Escolar *et al.*, 1999).

Fur is a global regulator for the iron metabolism and the homologues of the *fur* gene have been described in many Gram-negative and in Gram-positive bacteria. Another Fur-like protein related to the regulation of Mn^{2+} transport was detected in alpha-proteobacteria and was called Mur (manganese uptake regulator) (Wexler *et al.*, 2003; Chao *et al.*, 2004). The incorporation of Mn-oxides by ancient anoxygenic phototrophs was a step in the evolution of oxygenic photosynthesis (Espiritu *et al.*, 2019). RSP_2494 (named Fur/Mur) in *R. sphaeroides* was classified as Mur (Rodionov *et al.*, 2006). A study of the *fur*/*mur* deletion strain showed that it was more impaired in growth than the wild type in iron limitation condition and more genes related to the iron metabolism had a significant response to iron limitation. While the expression of the genes involved in the ribosomal proteins and photosynthesis is similar in both strains (Peuser *et al.*, 2011). A binding site for the Fur/Mur was predicted in the upstream region of the *sitABCD* operon, encoding the subunits of an ABC Mn^{2+}/Fe^{2+} transport system (Giel *et al.*, 2006). The Fur/Mur protein can indeed bind with the upstream

region of *sitA* in *vitro* and the *fur*/*mur* of *R. sphaeroides* deletion strain has a 37 times higher level of *sitA* than the wild type in the iron limitation condition, which is consistent to a repressor function of Fur/Mur in the presence of iron. Fur/Mur in *R. sphaeroides* also has a significant influence of iron-dependent regulation (Peuser *et al.*, 2011). The expression of the *E. coli* Fur regulon is also impacted by O_2 tension (Beauchene *et al.*, 2017).

1.6.4 Regulation of iron-dependent regulators Irr

The Irr protein belongs to a distinct sub-branch of the Fur super-family and is only found in the members of the *Rhizobiales* and *Rhodobacterales*. In *Rhizobiales* most iron-dependent genes are regulated by Irr (Sangwan *et al.*, 2008; Small *et al.*, 2009; Costa *et al.*, 2017). Normally, Irr can bind to a conserved sequence, which is called Irr box or ICE motifs (iron control elements) in the promoters regions of its target genes. In high iron condition, Irr is degraded in *Bradyrhizobium japonicum* but not in *Rhizobium leguminosarum*, which is mediated by its interaction with heme, whose concentration increases with the iron availability (Hamza *et al.*, 1998; Singleton *et al.*, 2010). Reactive oxygen species (ROS) also promote the heme-dependent degradation of Irr (Yang *et al.*, 2006; Kobayashi *et al.*, 2016). Heme-bound Irr activates O_2 to form highly reactive oxygen species (ROS) with the “active site conversion” from heme iron to non-heme iron to degrade itself (Kitatsuji *et al.*, 2016). Since Irr is a Fe-heme ((Fe-N) protein, it can directly ligate with the cofactor heme but the ligation is more efficient if the synthesis of the heme synthezised by the enzyme ferrochelatase (Qi and O'Brian, 2002).

RSP_3179 encodes a homolog of the Irr protein of *Rhizobia* in *R. sphaeroides*. The analyses of the transcriptome revealed that Irr regulates some genes related to the iron metabolism and some genes related to stress responses, citric acid cycle, oxidative phosphorylation, transport, and photosynthesis (Peuser *et al.*, 2012). Lower expression levels of most genes in normal condition in the absence of Irr suggest an activating function of Irr. Irr was not required for an activation of genes for iron metabolism in response to iron limitation. The induction of these genes under iron limitation was even

stronger in the absence of Irr. A irr deletion strain can grow better than the *fur/mur* mutant in normal condition but grows worse than wild type in iron limitation. However, the mutant had significantly increased resistance to oxidative stress (H_2O_2 and singlet oxygen). Thus, Irr has no major function in iron homeostasis in *R. sphaeroides*. Irr can directly bind to the *mbfA* gene (membrane bound ferritin) and *ccpA* (cytochrome c peroxidase), which were predicted (Rodionov *et al.*, 2006) and confirmed experimentally (Peuser *et al.*, 2012). The *mbfA* gene encodes MbfA protein that is homologous with rubrerythrin, a non-heme iron protein providing oxidative stress protection by the reduction of intracellular H_2O_2. The *ccpA* gene encodes an iron- heme protein that reduces peroxides (Sztukowska *et al.*, 2002). Therefore, Irr plays a role in the regulation of the genes related to oxidative stress defense, which prevents the formation of high levels of ROS by reducing the strong activation of genes for iron metabolism in response to iron limitation (Peuser *et al.*, 2012).

1.6.5 Regulation of iron-dependent regulators RirA

In *Rhizobia*, the iron regulator RirA (*Rhizobial* iron regulator A) with 4Fe-4S belongs to the Rrf2 family of putative transcriptional regulators (Pellicer Martinez *et al.*, 2017; Pellicer Martinez *et al.*, 2019) and iron-sensing regulators (Dokpikul *et al.*, 2016). The *rirA* mutation activated the expression of at least eight operons that were related to the synthesis or uptake of siderophores, or of other iron sources (Sasaki *et al.*, 2016; Amarelle *et al.*, 2019). RirA not only regulated iron metabolism, but also influenced the systhesis of heme in *Sinorhizobium meliloti* (Amarelle *et al.*, 2016). RirA was required for oxidative stress resistance in *Sinorhizobium* (Crespo-Rivas *et al.*, 2019).

The transcription of the *rirA* gene itself increased about two fold in iron repletion compared to iron depletion. The growth rates of the *rirA* deletion strains were reduced in both conditions, iron repletion and iron depletion, but did not appear to affect the fixation of N_2 *Rhizobium leguminosarum* (Todd *et al.*, 2002). No RirA homologs were predicted for *R. sphaeroides* (Giel *et al.*, 2006), however a recent publication suggests the presence of two RirA homologs (RSP_2888 and RSP_3341) (Imam *et al.*, 2015). RSP_2888 and RSP_3341 are RirA-like proteins with cysteine residues and maybe

ligate with Fe-S cluster and sense oxygen in the C-terminal domain. A recent study reveals that RSP_2888 and RSP_3341 encode RirA homologs and play a role of the regulation of iron metabolism and photosynthesis gene expression in *R. sphaeroides* (Imam *et al.*, 2015). A total of 69 genes were differentially expressed by comparing RNA levels and ChIP-seq analysis between wild type and ΔRSP_3341 cells including some iron-dependent genes, which were directly and indirectly repressed by RSP_3341 in *R. sphaeroides*. Another RirA-like protein in *R. sphaeroides*, RSP_2888 (MppG), was predicted to contribute the regulation of photosynthesis and was also involved in the regulation of iron containing proteins such as AppA and the synthesis of bacteriochlorophyll (Imam *et al.* 2015). Thus, the balance of the iron pool and the transcriptional regulation of iron-dependent genes in the cell has a complex regulatory network in *R. sphaeroides*.

1.7 Objective

Fe-S proteins appear in all organisms and have many essential functions, but oxidative stress can destroy Fe-S cluster. Organisms need to develop systems to regulate Fe-S cluster assembly. But current research on the regulated expression of the genes for Fe-S cluster assembly are mostly limited to the gamma-proteobacterium *E. coli*. The phototrophic bacterium *R. sphaeroides* is an alpha-proteobacterium and the organization of genes for Fe-S assembly differs from *E. coli*. There is a high demand for Fe-S cluster, since proteins required for formation of photosynthetic complexes and for photosynthetic electron transport contain Fe-S cluster. In addition, photooxidative stress caused by the formation of ROS by the light excitation of bacteriochlorophyll destroys Fe-S clusters. The *isc-suf* operon is an important operon for the assembly of Fe-S cluster in *R. sphaeroides*, and has multiple promoters as predicted from the RNA-seq data, three sense promoters and two anti-sense promoters. The first gene *iscR* of the operon encodes the IscR protein that is homologous to the main regulator for genes related to Fe-S assembly in *E. coli*, but the amino acid residues of IscR that bind the Fe-S cluster are completely different. The details of the mechanisms of *isc-suf* operon regulation in *R. sphaeroides* for photosynthetic complexes and iron-dependent

regulators (Irr, IscR, Fur/Mur, RirA) and oxidative stress-dependent regulator (OxyR) under different stress and growth conditions will be investigated to further improve our previous global regulatory net.

2. Materials

2.1 Chemicals and reagents

Chemicals and reagents used in this study, listed alphabetically with manufacturers.

Products	Manufacturer
Agarose FMC	Rockland USA
Ammonium peroxydisulfate (APS)	Sigma Aldrich
Acetic acid	Roth
Acrylamide (30% w/v)/ bisacryet lamide (0.8% w/v)	Roth
Agarose (LE agarose Biozym)	Roche
Bromophenol blue	Merck
Biotin	Serva
Bacto-Agar Difco	Detroit USA
Boric acid (H_3BO_4)	Sigma Aldrich
Bovine serum albumin (BSA)	Roth
Bromophenol	Sigma Aldrich
β-mercaptoethanol	Roth
Calcium chloride ($CaCl_2$)	Roth
Coomassie Brilliant Blue G-250	Difco
Deoxyribonucleoside triphosphates (dNTPs)	Serva
Diethyl-pyrocarbonate (DEPC)	Sigma Aldrich
DTT, 1,4-Dithiothreitol	Sigma Aldrich
Dimethyl sulfoxide (DMSO)	Roth
Ethanol	Roth
Ethidium bromide (EB)	Serva
Ethanolamine	Sigma Aldrich
Ethidium bromide	Roth
Ethylene-diamine tetraacetate (EDTA)	Roth
Formaldehyde (37%)	Applichem
Formamid	Applichem
Fe-(II)-citrate	Sigma Aldrich
Glycerol	Roth
Glycine	Roth
Glutathione	Sigma Aldrich
Glucose	Merck
GeneRuler 1kb DNA Ladder Plus	Fermentas
GeneRuler 100 bp DNA Ladder	Fermentas
Hydrogen peroxide	Roth
Imidazole	Sigma Aldrich
Isopropyl-β-D-thiogalactoside (IPTG)	Roth
Magnesium chloride ($MgCl_2$)	Roth
Magnesium sulphate ($MgSO_4$)	Merck

Methanol	Roth
Methylene blue	Sigma Aldrich
Nickel NTA	Qiagen
N-2-hydroxyethylpiperazine-N'-2- ethanesulfonic acid	Roth
N, N, N ', N'-tetramethylene diamine	Roth
Ortho-Nitrophenyl-β-galactoside (ONPG)	Serva
Prestained Protein Marker	NEB
Ponceau-Red	Sigma Aldrich
Phenyl-methyl-sulfonylfluoride (PMSF)	Sigma Aldrich
Potassium dihytrogen phosphate	Roth
Potassium chloride	Roth
Phenol (water grade)	Applichem
Phenol/Chloroform	Applichem
Polyvinylpyrolidon	Sigma Aldrich
(γ-32P)ATP (10 µCi/µl)	Hartmann Analytik
Roti-Quant (Bradford-Reagent)	Roth
Sepermidine	Sigma Aldrich
Sodiumthiosulphate $\times 5H_2O$	Merck
Spurenelenmente (RÄ-medium)	Sigma
Sodium carbonate Na_2CO_3 (> 99.8%)	Merck
Sodium chloride, NaCl (> 99.8%)	Roth
Sodium hydroxide, NaOH (> 99%)	Pearls Roth
Sodium dodecyl sulphate (SDS)	Roth
Sulfosalicylic acid dihydrate	Sigma Aldrich
Standard I nutrient broth (STI-medium)	Merck
Sodium dihydrogen phosphate (NaH_2PO_4)	Merck
SYBR Green	Sigma Aldrich
Tri-sodium citrate	Merck
Tert-butyl hydroperoxide	Sigma
Tris-(hydroxymethyl)-aminomethane	Roth
Trypton	Difco
Urea	Roth
Xylene cyanol	Sigma Aldrich
Yeast extract	Gibco

2.2 Enzymes

Products	Manufacturer
TURBO DNaseI	Invitrogen
Lysozyme	Sigma Aldrich
Taq DNA polymerase	QIAGEN
T4 DNA ligase	NEB
T4 polynucleotide kinase (T4 PNK)	NEB
Restriction endonucleases	Fermentas
phusion DNA polymerase	QIAGEN

Proteinase K	Roth
RNase A	QIAGEN

2.3 Antibiotics

Final concentration added to bacterial cultures (Sterilized by 0.22 μm filter)

Antibiotic	stock(mg/ml)	Solvent	*E.coli*(μg/ml)	*R.sphaeroides*(μg/ml)
Ampicilin(Ap)	100	ddH_2O	200	-
Kanamycin(Km)	10	ddH_2O	25	25
Gentamycin (Gm)	4	ddH_2O	10	10
Spectinomycin(Sp)	10	ddH_2O	10	10
Tetracycline(Tc)	10	75% Ethanol	20	1.5
Trimethoprim(Tp)	25	Dimethyl-Form amide	-	50

2.4 Strains

R. sphaeroides and *E. coli* strains used in this study

Strains	Relevant features	References
R.sphaeroides		
2.4.1	*Rhodobacter sphaeroides* wild type	(van Niel, 1944)
2.4.1	*Rhodobacter sphaeroides* wild type	ATCC collection
Δ*pucBA2BA*	*puc1BA* and *puc2BA* deletion strain	Xiaohua Zeng(2003)
BCHE	Km^r, *bchE* deletion strain	Gomelsky. (1995)
APP11	Tp^r, *appA* deletion strain	Gomelsky. (1995)
Gad C_2	Sp^r, *Cyt* C_2 deletion strain	Caffrey et al. (1992)
2.4.1 Δ*iscR*	Sp^r, *iscR* deletion strain	(Remes *et al.*, 2015)
2.4.1 Δ*fur/mur*	Sp^r, *fur/mur* deletion strain	(Peuser *et al.*, 2011)
2.4.1 Δ*oxyR*	Sp^r, *oxyR* deletion strain	(Zeller and Klug, 2004)
2.4.1 Δ*irr*	Km^r, *irr* deletion strain	(Peuser *et al.*, 2012)
2.4.1 ΔRSP_2888	Km^r, *rirA* homolog deletion strain	This study
2.4.1 ΔRSP_3341	Sp^r, *rirA* homolog deletion strain	This study
2.4.1 ΔRSP_2888+3341	Km^r, Sp^r, rirA homolog double deletion strain	This study
E. coli		
JM109	Host strain for cloning procedures	(Yanischperron *et al.*, 1985)
S17-1	Strain for diparental conjugation, tra^+	(Simon *et al.*, 1986)
M15(pREP4/pQEoxyR)	M15 containing pQE30::*oxyR*, Km^r, Ap^r, used for OxyR overexpression	(Zeller *et al.*, 2007)
M15(pREP4/pQE*iscR*)	M15 containing pQE30::*iscR*, Km^r, Ap^r, used for IscR overexpression	(Remes *et al.*, 2015)
M15(pREP4/pQE*irr*)	M15 containing pQE30::*irr*, Km^r, Ap^r, used for Irr overexpression	(Peuser *et al.*, 2012)

Sp^r, spectinomycin-resistant; Ap^r, ampicillin-resistant; Km^r, kanamycin resistant; when required, antibiotics were added in the following concentrations: spectinomycin (10 μg·ml^{-1}) and kanamycin (25 μg·ml^{-1}) for *R. sphaeroides*; ampicillin (200 μg·ml^{-1}) and kanamycin (25 μg·ml^{-1}) for *E. coli*

2.5 Plasmids

Plasmids used in this study

Plasmid names	Relevant features	Source
pJET1.2/ blunt	Ap^r, 2.97 kb, PCR cloning vector	Fermentas
pPHU281	Tc^r, *lacZ mob*(RP4), suicide vector for knock-out construction	(Hubner *et al.*, 1991)
PRK4352	Tc^r, 16S vector with terminator for antisense promoter construction	(Keen *et al.*, 1988)
PRK4352-asP2	Tc^r, antisense of Promoter 2 from *isc suf* operon on PRK4352	This study
pBBR1-MCS5-*lacZ*	Gm^r, broad-host-range cloning vector	(Kovach *et al.*, 1995)
pBBR1-MCS5-*lacZ*-P2	Gm^r, promoter 2 from *isc suf* operon on pBBR1-MCS5-*lacZ*	This study
pBBR1-MCS5-*lacZ*-P25-88	Gm^r, promoter 2 and 5 (88 nt upstream) from *isc suf* operon on pBBR1-MCS5-*lacZ*	This study
pBBR1-MCS3-*lacZ*	Tc^r, broad-host-range cloning vector	(Kovach *et al.*, 1995)
pBBR1-MCS3-*lacZ*-P1	Tc^r, promoter 1 from *isc suf* operon on pBBR1-MCS3-*lacZ*	This study
pBBR1-MCS3-*lacZ*-P2	Tc^r, promoter 2 from *isc suf* operon on pBBR1-MCS3-*lacZ*	This study
pBBR1-MCS3-*lacZ*-P3	Tc^r, promoter 3 from *isc suf* operon on pBBR1-MCS3-*lacZ*	This study
pBBR1-MCS3-*lacZ*-P4-60	Tc^r, promoter 4(60 nt upstream) from *isc suf* operon on pBBR1-MCS3-*lacZ*	This study
pBBR1-MCS3-*lacZ*-P4-98	Tc^r, promoter 4(98 nt upstream) from *isc suf* operon on pBBR1-MCS3-*lacZ*	This study
pBBR1-MCS3-*lacZ*-P5-88	Tc^r, promoter 5(88 nt upstream) from *isc suf* operon on pBBR1-MCS3-*lacZ*	This study
pBBR1-MCS3-*lacZ*-P5-112	Tc^r, promoter 5(112 nt upstream) from *isc suf* operon on pBBR1-MCS3-*lacZ*	This study
pBBR1-MCS3-*lacZ*-P12	Tc^r, promoter 1 and 2 from *isc suf* operon on pBBR1-MCS3-*lacZ*	This study
pBBR1-MCS3-*lacZ*-P25-88	Tc^r, promoter 2 and 5 (88 nt upstream) from *isc suf* operon on pBBR1-MCS3-*lacZ*	This study
pBBR1-MCS3-*lacZ*-P25-112	Tc^r, promoter 2 and 5 (112 nt upstream) from *isc suf* operon on pBBR1-MCS3-*lacZ*	This study
pBBR1-MCS3-*lacZ*-P125-88	Tc^r, Promoter 1, 2 and 5 (88 nt upstream) from *isc suf* operon on pBBR1-MCS3-*lacZ*	This study

pBBR1-MCS3-*lacZ*-P125-112	Tc^r, promoter 1, 2 and 5 (112 nt upstream) from *isc suf* operon on pBBR1-MCS3-*lacZ*	This study
pBBR1-MCS3-*lacZ*-P254-60	Tc^r, promoter 2, 5 and 4(60 nt upstream) from *isc suf* operon on pBBR1-MCS3-*lacZ*	This study
pBBR1-MCS3-*lacZ*-P254-98	Tc^r, promoter 2, 5 and 4(98 nt upstream) from *isc suf* operon on pBBR1-MCS3-*lacZ*	This study
pBBR1-MCS3-*lacZ*-P1254-60	Tc^r, promoter 1, 2, 5 and 4(60 nt upstream) from *isc suf* operon on pBBR1-MCS3-*lacZ*	This study
pBBR1-MCS3-*lacZ*-P12543	Tc^r, promoter 1, 2, 5, 4 and 3 from *isc suf* operon on pBBR1-MCS3-*lacZ*	This study
pJET1.2-mut P5-88	Ap^r, mutated promoter 5 (88 nt upstream) from *isc suf* operon on pJET1.2	This study
pJET1.2-mut P25-88	Ap^r, mutated promoter 5 of P25 (88 nt upstream) from *isc suf* operon on pJET1.2	This study
pJET1.2-mut P4-60	Ap^r, mutated promoter 4 (60 nt upstream) from *isc suf* operon on pJET1.2	This study
pJET1.2-mut P4-98	Ap^r, mutated Promoter 4 (98 nt upstream) from *isc suf* operon on pJET1.2	This study
pJET1.2-mut P254-60	Ap^r, mutated Promoter 4 of P254 (60 nt upstream) from *isc suf* operon on pJET1.2	This study
pJET1.2-mut P254-98	Ap^r, mutated Promoter 4 of P254 (98 nt upstream) from *isc suf* operon on pJET1.2	This study
pBBR1-MCS3-*lacZ*-mut P5-88	Tc^r, mutated promoter 5 (88 nt upstream) from *isc suf* operon on pBBR1-MCS3-*lacZ*	This study
pBBR1-MCS3-*lacZ*-mut P25-88	Tc^r, mutated promoter 5 of P25 (88 nt upstream) from *isc suf* operon on pBBR1-MCS3-*lacZ*	This study
pBBR1-MCS3-*lacZ*-mut P4-60	Tc^r, mutated promoter 4 (60 nt upstream) from *isc suf* operon on pBBR1-MCS3-*lacZ*	This study
pBBR1-MCS3-*lacZ*-mut P4-98	Tc^r, mutated promoter 4 (98 nt upstream) from *isc suf* operon on pBBR1-MCS3-*lacZ*	This study
pBBR1-MCS3-*lacZ*-mutP254-60	Tc^r, mutated promoter 4 of P254 (60 nt upstream) from *isc suf* operon on pBBR1-MCS3-*lacZ*	This study
pBBR1-MCS3-*lacZ*-mutP254-98	Tc^r, mutated promoter 4 of P254 (98 nt upstream) from *isc suf* operon on pBBR1-MCS3-*lacZ*	This study
pPHU281ΔRSP_3341	Tc^r, pPHU281 containing RSP_3341 gene with flanking sites	This study
pPHU281ΔRSP_3341::Sp	Tc^r, Sp^r, pPHU281ΔRSP_3341 containing Sp^r cassette	This study
pPHU281ΔRSP_2888	Tc^r, pPHU281 containing RSP_2888 gene with flanking sites	This study
pPHU281ΔRSP_2888::Km	Tc^r, Km^r, pPHU281ΔRSP_3341 containing Km^r cassette	This study
pPH45_Ω	Sp^r, source of Ω-Sp^r cassette	(Prentki *et al.*, 1991)

pPH45_Km	Km^r, source of Km^r cassette	(Prentki *et al.*, 1991)

Sp^r, spectinomycin-resistant; Ap^r, ampicillin-resistant; Tc^r, tetracycline-resistant; Km^r, kanamycin resistant

2.6 Oligonucleotides

Name	Sequence (5'→3')	Purpose
P1_136_fwd	TCTAGATGCAGGTAATCGAGCGC	promoter 1(136 nt upstream) of *isc-suf*-operon cloning
P1_95_fwd	TCTAGAGATGCCCTGATCGTACTCGC	promoter 1(95 nt upstream) of *isc-suf*-operon cloning
P1_rev	CTGCAGTTGCCATCGTGCTGCAC	promoter 1 of *isc-suf*-operon cloning
P2_fwd	TCTAGAAAATCACTTCGGGCATCGC	promoter 2 of *isc-suf*-operon cloning
P2_rev	CTGCAGTCGTTACGGTTCCGGGC	promoter 2 of *isc-suf*-operon cloning
P25_rev	CTGCAGGCGCGAGATCCACCAGC	promoter 25(88 nt upstream) of *isc-suf*-operon cloning
P3_fwd	CCCGGGAAAACCTGATCGGGATCGC	promoter 3 of *isc-suf*-operon cloning
P3_rev	CTGCAGTGACGAGGCAGAGCGTGTT	promoter 3 of *isc-suf*-operon cloning
P4as_fwd	TCTAGACAAGGATTGTGCACGCGAG	promoter 4(98 nt upstream) of *isc-suf*-operon cloning
P4as_rev	CTGCAGCGGCTACAAGCTCGCGC	promoter 4 of *isc-suf*-operon cloning
nP4as_fwd	TCTAGACACCAGCACCGGTATGCATC	promoter 4(60 nt upstream) of *isc-suf*-operon cloning
nP4as_fwd-2	CTGCAGCACCAGCACCGGTATGCATC	promoter 4(60 nt upstream) of *isc-suf*-operon cloning
P5as_fwd	TCTAGAGCGCGAGATCCACCAGC	promoter 5(112 nt upstream) of *isc-suf*-operon cloning
P5as_rev	CTGCAGAACCATTCCACCTGGGCG	promoter 5 of *isc-suf*-operon cloning
newP5as_fwd	TCTAGATCGCATACCGACCCTTGG	promoter 5(88 nt upstream) of *isc-suf*-operon cloning
P12345_fwd	ACTAGTTGCAGGTAATCGAGCGC	promoter 12543 of *isc-suf*-operon cloning
P12345_rev	CCCGGGTGACGAGGCAGAGCGTGTT	promoter 12543 of *isc-suf*-operon cloning
asP2_fwd	TCTAGATTCCGGGCGGATGCAC	antisense of promoter 2 of *isc-suf*-operon cloning
asP2-rev	GGATCCCGCGTCGCGATCCTTCT	antisense of promoter 2 of *isc-suf*-operon cloning
RT-asP2_fwd	TTCCGGGCGGATGCAC	antisense of promoter 2 of *isc-suf*-operon RT-PCR
RT-asP2_rev	CGCGTCGCGATCCTTCT	antisense of promoter 2 of *isc-suf*-operon RT-PCR
RT_RSP_1669_A	ATCGCGGAAGAGACCCAGAG	RSP_1669 (*rpoZ*) real-time RT-PCR
RT_RSP_1669_B	GAGCAGCGCCATCTGATCCT	RSP_1669 (*rpoZ*) real-time RT-PCR
RT_RSP_0799_A	GAACAATTACGCCTTCTC	RSP_0799 (*gloB*) real-time RT-PCR
RT_RSP_0799_B	CATCAGCTGGTAGCTCTC	RSP_0799 (*gloB*) real-time RT-PCR
3341up_r	GGATCCGTAGATCGAGGCGGTCTC	knock-out of RSP_3341-RirA Homolog 1
3341dn_f	GGATCCTTCATGGACACGCTCG	knock-out of RSP_3341-RirA Homolog 1
3341dn_r	AAGCTTACATCAACCCGCTGTTCAGC	knock-out of RSP_3341-RirA Homolog 1
2888up_f	GGTACCGTAGCAAAAGCTGTCCGAG	knock-out of RSP_2888-RirA Homolog 2
2888up_r	GGATCCTCATCGCGAGATTGGTG	knock-out of RSP_2888-RirA Homolog 2
2888dn_f	GGATCCTTCTACGGCACGCTCGA	knock-out of RSP_2888-RirA Homolog 2
2888dn_r	AAGCTTACGAGGAGATCGGCCTCG	knock-out of RSP_2888-RirA Homolog 2
3341_670upst_f	ACGACGAAACTCGCGGAAGACG	knock-out of RSP_3341-RirA Homolog 1
3341_721upst_f	CGAGATCTTCGGGGTGAGC	knock-out of RSP_3341-RirA Homolog 1
3341_dn2_r	GGTCAACTGGGGGATCTATGTCTG	knock-out of RSP_3341-RirA Homolog 1
2888_675upst_f	GAACCAGGGCTCCATGATCC	knock-out of RSP_2888-RirA Homolog 2
2888_630upst_f	CATCCGCCAGTCATAGAGGCT	knock-out of RSP_2888-RirA Homolog 2
2888_dn2_r	GGCCAAGACGATCCGCTATT	knock-out of RSP_2888-RirA Homolog 2

Prom5_TTG_to_AAA	AAATCCAAAAACGCCAAGCGGCAGGCCG	rolling cycle/inverse PCR for mutation of P5 and P25 of *isc-suf* operon
Prom5_TTG_to_AAA	TGGCGTTTTTGGATTTGGCGGGAACCGG	rolling cycle/inverse PCR for mutation of P5 and P25 of *isc-suf* operon
Prom254_AAC-TTT	AGACGGTTTTTGCGATGCATACCGGTGC	rolling cycle/inverse PCR for mutation of P4 and P254 of *isc-suf* operon
Prom254_AAC-TTT	ATCGCAAAAACCGTCTCTTCCACCGCTT	rolling cycle/inverse PCR for mutation of P4 and P254 of *isc-suf* operon
pucB_fwd	CGAAGCCGAAGAAGTTCA	RSP_0314 (*pucB*) real-time RT-PCR
pucB_rev	TTCACCACGAGCCAGATT	RSP_0314 (*pucB*) real-time RT-PCR
pufL_fwd	ACACCTACGGCAACTTCC	RSP_0257 (*pufL*) real-time RT-PCR
pufL _rev	ATCGAGTAGCCGACCAGA	RSP_0257 (*pufL*) real-time RT-PCR
puhA_fwd	AAGCCCAAGACCTTCATCCT	RSP_0291 (*puhA*) real-time RT-PCR
puhA _rev	TCATCGGCTTGATCTTGTTG	RSP_0291 (*puhA*) real-time RT-PCR
bchY_fwd	CAATTCGGAATCGCTCGT	RSP_0261 (*bchY*) real-time RT-PCR
bchY _rev	ACGCAGAGGTTCGTCACC	RSP_0261 (*bchY*) real-time RT-PCR
crtI_fwd	CGAGATCCTCGTCGAGAA	RSP_0271 (*crtI)* real-time RT-PCR
crtI _rev	CAGAAGCCGCATGTAGGT	RSP_0271 (*crtI*) real-time RT-PCR
hemA_fwd	GCACCACGCTCTATCACA	RSP_2984 (*hemA*) real-time RT-PCR
hemA _rev	CAGGTCGTCGAGGTCATT	RSP_2984 (*hemA*) real-time RT-PCR
hemP_fwd	ATGACCGACCCGATGGAG	RSP_6006 (*hemP*) real-time RT-PCR
hemP _rev	AGTAGATCTGCCCGTCGAG	RSP_6006 (*hemP*) real-time RT-PCR

2.7 Culturing media

2.7.1. Standard I medium

Standard I liquid medium

Standard I Nutrient medium	25 g
Add ddH_2O up to	1000 ml

Strandard I agar plates

Bacto Agar (1.6%)	8.0 g
Add ddH_2O up to	500 ml

2.7.2 RÄ medium

2.7.2.1 Trace elements solution

Fe-(II)-citrate	500 mg (2 mM) (not in RÄ-Fe medium)
$MgCl_2$ x 4 H_2O	20 mg (0.05 mM)
$ZnCl_2$	5 mg (0.03 mM)
LiCl	5 mg (0.1 mM)
KI	2.5 mg (0.02 mM)
KBr	2.5 mg (0.02 mM)
$CuSO_4$	0.15 mg (0.9 µM)
Na_2MoO_4 x 2 H_2O	1 mg (0.002 mM)

$CoC1_2$ x 6 H_2O	5 mg (0.02 mM)
$SnCl_2$ x 2 H_2O	0.5 mg (0.002 mM)
$BaCl_2$	0.5 mg (0.002 mM)
$AlCl_3$	1 mg (0.007 mM)
H_3BO_4	10 mg (0.1 mM)
EDTA	20 mg (0.06 mM)
Add ddH_2O up to	1000 ml
	Autoclave

2.7.2.2 Vitamins

Niacin	200 mg (24 mM)
Thiamine hydrochloride	400 mg (3.5 mM)
Nicotinamide	200 mg (1.6 mM)
Biotin	8 mg (0.3 mM)
Add ddH_2O up to	1000 ml
	sterilized by 0.22 μm filter

2.7.2.3 Phosphate solution

	45 g (260 mM)
Potassium phosphate dibasic	35g (250 mM)
Potassium phosphate monobasic	1000 ml
Add ddH_2O up to	Autoclave

2.7.2.4 RÄ liquid medium

Malic acid	3 g (20 mM)
Ammonium sulphate	1.2 g (9 mM)
Magnesium sulphate-7-dihydrate	0.2 g (0.8 mM)
Calciumchloride dihydrate	0.07 g (0.4 mM)
Trace elements solution (RÄ-Fe liquid medium without Fe(II) citrate)	1.5 ml
Add ddH_2O up to	1000 ml
	pH 7.0 autoclave
Vitamins	8 ml
Phosphate	20ml

RÄ agar plates

Bacto Agar (1.6%)	8.0 g
Add RÄ liquid medium	500 ml

2.7.3 PY medium

PY liquid medium

Trypton	10 g
Yeast extract	0.5 g

$CaCl_2$ (1M)	2.0 ml
$MgCl_2$ (1M)	2.0 ml
$FeSO_4$ (0.5%)	2.4 ml
Add ddH_2O up to	1000 ml
	pH 7.0 autoclave

PY agar plates

Bacto Agar (1.6%)	8.0 g
Add PY liquid medium	500 ml

2.8 Molecular biological kits

Kit	Purpose	Manufacturer
Plasmid Isolation KIT	Plasmid extraction	Qiagen
Brilliant III Ultra-Fast SYBRR Green QPCR	RT-PCR	Agilent
innuPREP DOUBLEpure	DNA gel extraction and PCR purification	Analytik Jena
CloneJET PCR cloning kit	Gene cloning	Fermentas
peqGOLD TriFastTM Kit	RNA isolation	PEQLAB

2.9 Standard buffers and solutions

2.9.1 Commercial reaction buffers

10 × NEB buffer NEB
10 × T4 ligase buffer NEB
10 ×BSA for restriction endonucleases NEB
10 × T4 PNK buffer NEB
10 × T4 ligase buffer NEB
10 × PCR buffer QIAGEN

2.9.2 Other buffers and solutions

TBE (10 ×)	890 mM Tris/HCl
	890 mM sodium borate
	25 mM EDTA
	pH 8.3
TAE (10 ×)	400 mM Tris/HCl
	400 mM acetic acid
	4 mM EDTA
	pH 8.0
Separation buffer (4 ×)	1.5 M Tris/HCl
	0.4% (w/v) SDS
	pH 8.8
Stacking buffer (4 ×)	0.5 M Tris/HCl
	0.4% (w/v) SDS
	pH 6.8

Stacking gel	0.2 ml 40% PAA
	0.5 ml stacking buffer (4 ×)
	10 µl 10% APS
	2 µl TEMED
	1.3 ml H_2O
Separation gel	1.5 ml 40% PAA
	1.25 ml stacking buffer (4 ×)
	40 µl 10% APS
	4 µl TEMED
	2.2 ml H_2O
Laemmli buffer(10 ×)	250 mM Tris/HCl
	1.92 M Glycin
	1% (w/v) SDS
	pH 8.2
SDS-loading dye	200 mM Tris-Cl (pH 6.8)
	400 mM DTT
	8% SDS
	0.4% bromophenol blue
	40% glycerol
	pH 8.2
Lysis buffer for purification of OxyR	20 mM Tris-Cl (pH 7.5)
	500 mM NaCl
	50 mM KCl
	5 mM MgCl2
	0.5 mM EDTA
Fresh lysis buffer for purification of OxyR	30 ml lysis buffer
	30 µl DTT (1M)
	1.2 ml lysozyme (25mg/ml)
	60µl PMSF (100 mM)
	50 mM Tris-Cl (pH 7.5)
Wash buffer for purification of OxyR	250 mM NaCl
	20 mM imidazole
	50 mM Tris-Cl (pH 7.5)
Elution buffer for purification of OxyR	250 mM NaCl
	150 mM imidazole
	50 mM HEPES (pH 8.0)
Z-buffer for purification of OxyR	0.5 mM EDTA (pH 8.0)
	10 mM MgCl2
	100 mM KCl
	80 mM Tris-Cl (pH 8.0)
Binding buffer for EMSA of OxyR	400 mM NaCl
	8 mM EDTA
	40% glycerol
Lysis buffer for purification of IscR/Irr	50 mM NaH_2PO4

	300 mM NaCl
	10 mM imidazole
	pH 8.0
Wash buffer for purification of IscR/Irr	50 mM NaH_2PO4
	300 mM NaCl
	20 mM imidazole
	pH 8.0
	50 mM NaH_2PO4
Elution buffer for purification of IscR/Irr	300 mM NaCl
	250 mM imidazole
	pH 8.0
	5% glycerol
	100 mM potassium glutamate
Binding buffer for EMSA of IscR	1 mM EDTA
	10 mM potassium phosphate (K_2HPO_4)
	50 ug/ml bovine serum albumin (BSA)
	50 uM dithiothreitol (DTT)
	10 mM MgCl2
	3 mM Tris (pH 8.0)
TB buffer (445mM)	5.4 g Tris ($MrC_4H_{11}NO_3$:121.14)
	2.75 g boric acid
	PH 7.8, add ddH_2O up to 100 ml
TE buffer	10 mM Tris-HCl (pH 8.0)
	1 mM EDTA
	add ddH_2O up to 100 ml
10% CTAB w/V in 0.7 M NaCl	
Sodium chloride	4.1 g (0.7 M)
ddH_2O	80 ml
Cetrimonium bromide	10 g (10%)
	stir and heat (65 ℃) until dissolved
	add ddH_2O up to 100 ml
Binding buffer for EMSA of Irr	0.12 M TB buffer
	0.01 M DTT
	80% glycerol
	0.1 ug/μl bovine serum albumin (BSA)
Z-Buffer for β-galactosidase assay	0.06 M $Na_2HPO_4 \times H_2O$
	0.04 M $NaH_2PO_4 \times H_2O$
	0.01 M KCl
	0.001 M $MgSO_4 \times 7\ H_2O$
	Add β-mercaptoethanol fresh
	pH 7.0
Coomassie staining solution	
Methanol	40% (w/v)

Acetic acid	10% (w/v)
Coomassie Brilliant Blue (G-250)	0.2% (w/v)
ddH_2O	50% (w/v)
Coomassie destaining solution	
Methanol	20% (w/v)
Acetic acid	10% (w/v)
ddH_2O	70% (w/v)
0.1% SDS w/v	1 g sodium dodecyl sulfate
	add ddH_2O up to 1000 ml
STE buffer	100 mM NaCl
	20 mM Tris HCl (pH 7.5)
	0.01 M EDTA (disodium salt)
1M Tris HCl, various pH (100 ml)	12.1 g Tris
	ddH_2O 80 ml
	adjust the pH with 5M HCl
	add ddH_2O up to 100 ml
Lysis solution I	50 mM glucose
	25 mM Tris-HCl (pH 8.0)
	10 mM EDTA (pH 8.0)
	add ddH_2O up to 100 ml
	add fresh 4 µl/ml RNase A (100 mg/ml)
	and store at 4 ℃
Lysis solution II	0.2 M NaOH
	1% (w/v) SDS
	store at RT
Lysis solution III	60 ml 5 M potassium acetate
	11.5 ml glacial acetic acid
	28.5 ml H_2O
	store at 4 ℃

2.10 Other Material and Equipments

Material and Equipments	Manufacturer
CFX96 Real-Time PCR	Bio-Rad
Centricon 10 membrane	Millipore
Cooling centrifuge, Sorvall RC-5C+	Kendro
Cooling centrifuge, Sorvall -5B	Kendro
Cooling centrifuge Z 323K	Hermle
Electroporator (Micro Pulser)	Biorad
Filter paper, Whatman	Hartenstein
Fusion SL4 –Chemiluminasence detector	Vilber Lourmart
Glass wool	Serva
Halogen lamp	Conrad

Incubator Shaker (Model G 25)	New Brunswick Scientific
Microcon (MWCO 3000)	Millipore
MicroSpin G-50 Columns	GE Healthcare
Microarray scanner	Agilent technologies
Nitrocellulose membrane (BA Protran)	Schleicher & Schuell
NanoDrop 1000 spectrophotometer	Peq Lab
PCR cycler S100	Bio-Rad (Li-Cor)
Phosphoimager (Molecular Imager FX)	Biorad
Phosphoimager Screens	Biorad/Fuji
pH meter	Schott
Screen Eraser K	Biorad
Semi dry blot- Apparatus(Novablot)	Pharmacia
Sterile filter 0.22/0.45 μm	Nalagene
SpeedVac SC 110	ThermoScientific
SuperdexTM75,HiLoadTM16/60 (Gel filtration)	Pharmacia
Scintillation counter (LS 6500)	Beckman Coulter
Tabletop centrifuge Biofuge 13 and fresco , Uni Gen MR	Herolab
Ultrasound machine Sonoplus GM70 (Sonifier)	Bandelin
UV-StratalinkerTM 1800	Stratagene
Vacuum-blotter	Appligene
ÄKTA pure	Amersham Pharmacia

3. Methods

3.1 Microbiological methods

3.1.1 *E. coli* plating culture

All *E. coli* strains were cultivated on solid Standard I growth medium in 9 cm diameter Petri dish at 37 ℃ in the dark, which contained 1.6% (w/v) agar. Depending on the cultivated strain the antibiotics were added (see 2.3) to the solid growth media.

3.1.2 *E. coli* liquid culture

All *E. coli* strains were cultivated in Erlenmeyers with liquid Standard I growth medium on a shaker at a speed of 180 rpm at 37 ℃ in the dark. Depending on the cultivated strain the antibiotics were added (see 2.3) to the liquid growth media. The optical density of *E. coli* was measured by spectrophotometer at 600 nm.

3.1.3 *R. sphaeroides* plate culture

All *R. sphaeroides* strains were cultivated on solid RÄ growth medium in 9 cm diameter Petri dish at 32 ℃ in the dark, which contained 1.6% (w/v) agar. Depending on the cultivated strain the antibiotics were added (see 2.3) to the solid growth media.

3.1.4 *R. sphaeroides* liquid culture

3.1.4.1 Aerobic growth condition (high oxygen)

For aerobic growth conditions, all *R. sphaeroides* strains were cultivated in 100 ml Erlenmeyer baffled flasks containing 25 ml RÄ medium (aerobic conditions with 160 to 180 µM dissolved oxygen) on a shaker at a speed of 140 rpm in the dark at 32 °C. The optical density of *R. sphaeroides* was measured by spectrophotometer at 660 nm.

3.1.4.2 Microaerobic growth condition (low oxygen, iron depletion)

For microaerobic growth condition, all *R. sphaeroides* strains were cultivated in 50 ml Erlenmeyer flasks (non-baffle-flask) containing 40 ml RÄ medium (microaerobic growth with 25-30 µM dissolved oxygen) on a shaker at a speed of 140 rpm in the dark at 32 ℃. Depending on the cultivated strain the antibiotics were added (see 2.3) to the liquid growth media.

3.1.4.3 Anaerobic growth condition (anaerobic dark)

For anaerobic growth conditions in the dark, all *R. sphaeroides* strain were cultivated and filled up to 55 ml airtight sealed Meplat bottles containing 60 mM of dimethyl sulfoxide (DMSO) as a terminal electron acceptor without shaking in the dark at 32 ℃.

3.1.4.4 Anaerobic growth condition (phototrophy)

For phototrophic growth conditions in the light, all *R. sphaeroides* strains were cultivated and filled up to 55 ml airtight sealed Meplat bottles containing 55 ml RÄ medium without shaking in the white light (60 W/m^2) at 32 ℃. In this condition, the strains will perform anoxygenic photosynthesis.

3.1.4.5 Iron depletion growth condition

For iron depletion growth condition, all *R. sphaeroides* strains were cultivated in 50 ml Erlenmeyer flasks (non-baffle-flask) containing 40 ml RÄ-Fe medium (without the addition of Fe(II) citrate) on a shaker at a speed of 140 rpm in the dark at 32 ℃. The cells were grown overnight and then transferred to new RÄ-Fe medium three times more (the iron chelator 2,2'-dipyridyl (Merck) is added to the last culture in a final concentration of 30 μM) before harvesting (Remes *et al.*, 2014; Peuser *et al.*, 2011). Depending on the cultivated strain the antibiotics were added (see 2.3) to the liquid growth media.

3.1.4.6 Oxidative stress experiment

For generating oxidative stress, all *R. sphaeroides* strains were cultivated under microaerobic growth condition and were treated with 1 mM (final concentration) hydrogen peroxide (H_2O_2) or 100 μM (final concentration) tertiary butyl-alcohol (tBOOH) for 7 min or 30 min at an $OD_{660\,nm}$ of 0.5 (exponential growth phase). H_2O_2 and tBOOH are oxidative stress agents. tBOOH represents organic peroxides which are generated in the cell e.g. upon singlet oxygen exposure.

3.1.5 Preparation of glycerol stocks for the -80 ℃ strain collection

Cells from liquid overnight culture of *E. coli* (4 ml) or *R. sphaeroides* (10 ml) in late

exponential growth phase were harvested by centrifugation (5,000rpm), and then the pellets were resuspended by 1 ml relevant medium and 800 µl 80% autoclaved glycerol. At last, the suspensions were transferred into cryo-tubes, freezed in liquid nitrogen first and then stored into -80 ℃.

3.1.6 Transfer of plasmids into *R. sphaeroides* by diparental conjugation

E. coli S17-1 (donor strain) containing plasmid was inoculated on the solid Standard I growth medium. *R. sphaeroides* (acceptor strain) in exponential growth phase was harvested by centrifugation (5,000 rpm). The pellet was resuspended by 100 µl medium with the strains of S17-1 into the resuspension to mix them. The mixture was transferred onto membrane filter (0.45µm, ø25mm, Carl-Roth) and incubated on the solid PY plates at 32 ℃ for at least 5 hours (the best is overnight). Afterwards, all the cells were washed from the membrane by 1 ml RÄ-medium with different amount of cells into RÄ plates with appropriate antibiotics and incubate at 32 ℃ for three days.

3.1.7 β-galactosidase assays in *R. sphaeroides*

The cultures in the exponential growth phase (OD_{660nm} is about 0.5) were harvested by centrifugation (10,000 rpm, 10 min, 4 °C) for the measurement of β-galactosidase activity of transcriptional *lacZ* fusions by hydrolysis with O-nitrophenyl-β-D-galactopyranoside (ONPG) and expressed as Miller Units (Fenton, 1894) as described in (Klug *et al.*, 1997). The pellets were stored at -20 ℃ overnight. The second day, the pellets were dissolved in 750 µl of Z-buffer (with fresh 2.7 µl /ml β-mercaptoethanol) by vortex for 15s, and then 20 µl of chloroform and 10 µl of 0.1% SDS were added for lysis. The lysates were vortexed for 30 s. The samples and ONPG (4 mg/ml) were pre-heated for 5 min at 28 ℃. Afterwards, 200 µl of ONPG were added into pre-heated samples to start the color reaction for 5 min (exactly) at 28 ℃, and then the reactions were stopped by adding 500 µl of Na_2CO_3 (1 M) and the samples were centrifuged at 13,000 rpm for 3 min. Finally, the absorbance of the supernatants was measured photometrically at 420 nm and 550 nm. The sample volume (100 µl to 1 ml) depends on the activities of the promoters (A_{420} should not be

higher than 1). Therefore, different volumes of the promoter fusion should be tested in advance. β-galactosidase activities were calculated by the following formula:

Formula for Miller units = $(1000 \times (A_{420}\text{-}1.82 \times A_{550}) / OD_{660nm} \times V \times T$

A_{420} = absorbance of the yellow colour

A_{550} = absorbance from cell debris

T = reaction time in min (5 min)

V = culture volume (100 µl - 1 ml)

OD_{660nm} = reflects cell density

3.1.8 Full-cell spectrum of *R. sphaeroides*

1 ml of liquid cultures in the exponential growth phase (OD_{660nm} is about 0.5) were measured in the quartz cuvettes for the full-cell spectrum. The spectrum from 350 to 950 nm is taken and 1 ml of RÄ-medium is used as reference.

3.1.9 Cell-free spectrum of *R. sphaeroides*

20 ml liquid cultures in the exponential growth phase (OD_{660nm} is about 0.5) were harvested by centrifugation (8,000 rpm, 15 min, 4 ℃) and the cell pellets were resuspended in RÄ-medium, cells were breaken by sonication (parameters: Power MS 72/D, cycle 70%, 30 sec/time, 3 times). For the measurement of free-cell spectrum, the spectrum from 350 to 950 nm is taken. The same amounts of cells were harvested for the sonication and spectrum measurement.

3.1.10 Photopigments measurement of *R. sphaeroides*

1 ml of liquid cultures in the exponential growth phase (OD_{660nm} is about 0.5) were harvested by centrifugation (13,000 rpm, 5 min, RT) and the pellets were resuspended in 50 µl Roth H_2O. The photopigments are extracted with 500 µl of a mixture of acetone and methanol (7:2, v/v) from the pellets. After vortexing the samples for 10 seconds and centrifugation (13,000 rpm, 5 min, RT), the absorption of the supernatant is measured in a quartz cuvette at 484 nm and 770 nm. The mixture of the acetone and methanol (7:2, mixture) is used as reference. The concentration of the bacteriochlorophyll and the carotenoids are respectively calculated using the

extinction coefficient of 76 mM^{-1} cm^{-1} and 128 mM^{-1} cm^{-1} at 770 nm and 484 nm (Clayton, 1966) as follows:

BChl (μM) / OD_{660} = (OD_{770} × 1000 × $V_{acetone\text{-}methanol}$ ml) / (76 mM^{-1} cm^{-1} × 1 cm × V_{cell} ml × OD_{660})

Crt (μM) / OD_{660} = (OD_{484} × 1000 × $V_{acetone\text{-}methanol}$ ml) / (128 mM^{-1} cm^{-1} × 1 cm × V_{cell} ml × OD_{660})

V = Volume.

3.2 Molecular method

3.2.1 DNA preparation

3.2.1.1 Chromosomal DNA isolation

4 ml wild-type cells from *R. sphaeroides* in the exponential growth phase (OD_{660nm} is about 0.6) were harvested by centrifugation (8,000 rpm, 10 min, 4 ℃) for chromosomal DNA isolation. The pellets were washed with 700 μl TE buffer containing 1 mg/ml lysozyme and incubated for 10 min at 37 ℃. 30 μl 10% SDS and 16 μl 20 mg/ml proteinase K were added into the sample and then incubated for 1 h at 37 ℃. After incubation, 12 μl of 5M sodium chloride (NaCl) and 95 μl cetrimonium bromide (CTAB; detergent) with NaCl were added for 10 min at 65 ℃ in the heating block. Afterwards, 750 μl of a chloroform/isoamyl alcohol mixture (24:1) was added to precipitate the cell debris and proteins by centrifugation (13,000 rpm, 5 min, RT). Chromosomal DNA from the upper, aqueous phase was transferred into a new tube and mixed with one volume of a phenol/chloroform/isoamyl alcohol mixture (25:24:1; AppliChem), and then centrifuged (8,000 rpm, 10 min, 4 ℃). Chromosomal DNA from the upper, aqueous phase was further precipitated with 0.6 volume of isopropanol by incubation for 5 min at RT and centrifugation (4,000 rpm, 4 min, RT). The pellets were washed by 200 μl of cold 70% ethanol and dried in the SpeedVac (vacuum dryer, Eppendorf) for 7 min and then dissolved in 50 μl TE buffer.

3.2.1.2 Plasmid minipreparation

Cultures were centrifuged at 8,000 rpm for 5 min at RT, and then extracted by plasmid Miniprep Kit II (Peqlab) according to the manufacturer's instruction.

3.2.1.3 Extraction of DNA fragment and vectors from agarose gels

DNA fragments and vectors were extracted from agarose gels by using QIAEX II Gel Extraction Kit or QIA quick Gel Extraction Kit (QIAGEN) according to the manufacturer's instruction

3.2.2 RNA preparation

3.2.2.1 Total RNA isolation

20 ml cells from *R. sphaeroides* in the exponential growth phase (OD_{660nm} is about 0.6) were harvested by centrifugation (10,000 rpm, 10 min, 4 ℃). The isolation of total RNA from *R. sphaeroides* for real time RT-PCR was performed by using peqGOLD TriFastTM Kit (PEQLAB) as described in the manufacturer's manual.

3.2.2.2 RNA purification

Remaining DNA needs to be removed from the total RNA. All potential remaining traces of DNA were removed by the TURBO DNaseI (Invitrogen) as described in the manufacturer's manual.

3.2.2.3 Detection of remaining DNA

To further confirm the absence of DNA, PCR was performed targeting *gloB* (RSP_0799) with the primers listed and measure the concentration by Nano-Drop 1000 spectrophotometer (Peq Lab)

3.2.3 Agarose gel electrophoresis of DNA

TAE or TBE agarose gels were used to separate DNA fragments according to their size. The agarose powder was dissolved by boiling in TAE/TBE buffer in the microwave and cooled in the chamber with a comb. As running buffer 1x TAE or 1x TBE is used, respectively. DNA samples were mixed with 6 × DNA loading dye (15% of the total volume) before loading into the pockets of the gel. Electrophoresis was performed at 120 mA for 20 min. DNA bands were visualized by staining with ethidium bromide solution (1ug/ml) for 10 min and detected and photographed on a UV-transilluminator (UVT-20 M/W, HeroLab).

3.2.4 Polymerase chain reaction (PCR)

3.2.4.1 Standard PCR

Reaction components	Volume
H_2O	6.7 µl
5x GC buffer	2 µl
dNTPs (10 mM)	0.2 µl
Primer-forward (10 pmol/µl)	0.5 µl
PrimerB-reverse (10 pmol/µl)	0.5 µl
Phusion	0.1 µl
Template (DNA: chromosomal (100 ng/µl); plasmid (30 ng/µl))	0.5 µl
	Total :10.5 µl

Programme:

98 ℃ 5 min

98 ℃ 30 s

annealing temperature 30 s } 34 Cycles

72 ℃ 30 s/kb

72 ℃ 10 min

4°C ∞

PCR products were purified by the kit (innuPREP DOUBLEpure Kit) according to the manufacture's instruction

3.2.4.2 Site-specific mutagenesis by reverse PCR

To exchange the desired nucleotides, a primer pair containing the mutated nucleotides was designed. This primer pair and the plasmids containing the DNA sequence to be changed as template were used for inverse PCR. The primer pair prolong in different directions to amplify the whole plasmid so that the PCR results in a plasmid containing the mutated DNA sequence. The unmutated plasmid templates were digested by the enzyme DpnI.

3.2.5 Restriction of DNA

The restriction of DNA sequences was performed by restriction enzymes from

Fermentas. The restriction was carried out according to the manufactures manual based on the definition that 1 unit restriction enzyme cuts 1 μg of DNA in 1 h in a 50 μl reaction.

3.2.6 Ligation

For the ligation of DNA fragments and vectors, both were restricted by identical restriction enzymes, a molar ratio of 3:1 insert to vector was used.

Reaction components	Volume
Vector	30 fmoles
Insert	90 fmoles
T4 DNA ligase	1 unit
10 ×T4 ligase buffer	2 μl
	add H_2O to 20μl

After the ligation reactions were incubated overnight at 15℃ in the water bath, the mixtures were heated for 5 min at 65℃ to inactivate the enzyme for transformation. Ligation of the pJET 1.2 vector is followed as described in the manufacturer's manual.

3.2.7 Preparation of *E. coli* competent cells for electroporation

5 ml of fresh overnight *E. coli* (eg. DH5α, JM109, S17-1) culture were transferred into 500 ml Standard I liquid medium and cultivated on the shaker at 37℃ until the OD_{600} nm reached 0.5~1.0 (in the exponential growth phase). The pellets were harvested by centrifugation (5,000 rpm, 10 min, 4 ℃) and washed with cold sterile ddH_2O in the same volume (500 ml). The pellets were repeated to wash with cold sterile ddH_2O in the half volume (250ml). Then the pellets were washed with 10 ml 10% ice-cold sterile glycerol and were subsequently washed again with 2 ml 10% ice-cold sterile glycerol. Finally, the suspension was immediately frozen in aliquots in liquid nitrogen and stored at -80℃. The whole process should be on the ice all the time. Electro-competent *E. coli* cells are used for transformation of plasmid DNA and ligation products.

3.2.8 Transformation by electroporation

50-100 ng of plasmid DNA or 5-10 µl of ligation products were mixed with melted *E. coli* competent cells on ice and transferred into the sterilized Gene Pulser cuvette (Bio-rad) UV-Stratalinker 1800 (Stratagene) using programme "Auto Crosslink" twice and chill it on ice before use. A pulse of electricity (2.5 KV, 5 ms) was applied to the mixtures in Pulser (Bio-rad). Immediately the mixtures were resuspended with 1 ml Standard I liquid medium without any antibiotics and cultivated on the shaker for 1 hour at 37 ℃. Finally, 10-100 µl or pellets of the mixtures were plated on the solid Standard I plates containing appropriate antibiotics.

3.2.9 Quantitative real-time RT-PCR

Quantitative RT-PCR was performed in a Bio-Rad CFX96 Real Time system as described in the manufacturer's manual of One-Step Brilliant III QRT-PCR Master Mix Kit (Agilent). The total RNA for RT-PCR were isolated by using peqGOLD TriFastTM Kit (PEQLAB).

Reaction components	Volume
Enzyme Mix	5 µl
RT block	0.4 µl
DTT	0.1 µl
Primer-forward (10 pmol/µl)	1 µl
PrimerB-reverse (10 pmol/µl)	1 µl
Roth H_2O	0.5 µl
Template (RNA: 20 ng/µl)	2 µl
	Total :10 µl

Enzyme Mix, RT block, DTT is from One-Step Brilliant III QRT-PCR Master Mix Kit (Agilent)

Programme:

50 ℃ 10 min

95 ℃ 3 min

95 ℃ 10 s
58 ℃ 5 s
60 ℃ 10 s
+ Plate Read
} 39 Cycles
annealing temperature 30 s
72 ℃ 10 min
melt curve 65.0 to 95.0 C, increment 0.5 C, 0:05 + Plate Read, END

Besides a RT-PCR run for the target mRNA, another RT-PCR run for the house-keeping gene *rpoZ* (reference) encoding the ω-subunit of RNA polymerase of *R. sphaeroides* was also performed for normalization (Pappas et al., 2004). The relative expression ratio (R) of a target gene was calculated based on real-time PCR efficiency (E) and threshold cycle (Ct) of reference gene and target genes (Pfaffl, 2001).

3.3 Protein techniques

3.3.1 Protein purification

3.3.1.1 *E. coli* culture growth for preparative purification (1 liter)

E. coli M15 for over-expression of His-tag Irr/OxyR/IscR protein were cultivated overnight in a flask with liquid Standard I growth medium containing appropriate antibiotics on a shaker at a speed of 180 rpm at 37 ℃ in the dark. The non-induced overnight culture was inoculated by 1:100 into 1 liter of fresh culture and shaken at 37 ℃ until an OD_{600} of 0.5 was reached. Afterwards, IPTG (final concentration:1mM) was added to induce the expression of the protein Irr/OxyR/IscR. The culture were kept at 20 ℃ for an additional 2 h or overnight, or at 37 ℃ for 3 hours (for the detail of each protein, refer (Zeller *et al.*, 2007; Peuser *et al.*, 2012; Remes *et al.*, 2015).After induction, the cells were harvested by centrifugation (8,000 rpm, 15 min, 4 ℃) and the pellets were frozen at -20 ℃.

3.3.1.2 Purification of His-tagged proteins

The frozen pellets were put on ice and resuspended in 10 ml lysis buffer. The lysates were sonicated on ice using a sonicator equipped with a microtip (use six 30 s bursts at 70% with a 30 s break on ice between each burst). The cleared supernatant

containing the proteins were harvested by centrifugation (12,000 rpm, 20 min, 4 ℃) and gently mixed with 1 ml of the 50% Ni-NTA slurry in the column (Prewash in lysis buffer to remove the ethanol, polypropylene columns, 10 ml, QIAGEN) with the bottom outlet capped by rotation at 4 ℃ for 3-6 hours. After incubation, the cap was removed and the flow-through was collected and the column was washed with 25 ml wash buffer to remove free proteins. Finally, the proteins were eluted 4~8 times with 1~2 ml elution buffer and stored at 4 ℃. The proteins were further purified by ÄKTA pure (Amersham Pharmacia) with Z-buffer (OxyR) or dialyze overnight with lysis buffer (Irr/IscR) to remove the imidazole. The concentration was measured by Nanodrop 1000 spectrophotometer (Peq Lab).

3.3.2 SDS-polyacrylamide gel electrophoresis

The protein samples were mixed with 4 × SDS loading dye in a ratio of 4:1 (v/v) and denatured at 95 ℃ for 5 min. The samples were loaded in an SDS-polyacrylamide gel (separating and stacking gel) of appropriate percentage and run the gel in at 100~150 volts for 1~2 hours.

3.3.3 Coomassie blue staining and destaining of SDS-PAGE

The gel was stained with coomassie staining solution (see 2.9.2) for 30 min on a shaker, and then destained by water overnight or destaining solution (see 2.9.2) until the background is nearly clear.

3.3.4 Radioactive labeling and purification of DNA

Fragments were produced via normal PCR and purified using the double PURE INNU prep kit (Jena Analytik) and then the concentration was measured using the Nanodrop 1000 spectrophotometer (Peq Lab). For hybridisation probes, single stranded oligonucleotide was end-labeled by using the enzyme polynucleotide kinase (PNK). For the labelling reaction, the DNA fragments (30 ng) was mixed with PNK (10 U/µl) and PNK buffer A (Thermo Scientific) and γ^{32P} dATP (30 µCi, Hartmann Analytic). The reaction was incubated for 1 h in a heating block at 37 ℃. Afterwards, the reaction was stopped by adding 40 µl STE buffer which results in a volume of 50 µl.

The mixtures were purified using a MicroSpin G50 illustra column (GE Healthcare) to remove the remaining enzyme, buffer and free dATPs.

Reaction components	Volume
DNA fragment	30 ng
PNK buffer A	1 µl
(10 U/µl) polynucleotide kinase (PNK)	1 µl
	add H_2O to 7 µl
(γ32P)dATP (10 µCi/µl)	3 µl (30 µCi)
	Total: 10 µl

3.3.5 Purification of radioactively labelled nucleic acids

The radioactively labelled nucleic acids was purified using MicroSpin G50 illustra columns manufactured by GE Healthcare to get rid of free radioactive nucleotides and salt from the buffer and labeling reaction. The G50 columns were used for nucleic acids larger than 30 bases in length. First the resin inside the column was resuspended by vortexing 15s, and the bottom closure of the column was removed. The storage buffer was removed into a collector tube by centrifugation (2,600 rpm, 2 min, RT). The mixtures (50 µl) were purified twice through the column containing the resin by centrifugation (2,600 rpm, 2 min, RT). 2 µl of purified fragments were measured by the scintillation counter (Beckman Coulter). The rest of radioactively labeled fragments can be stored at -20 ℃ for two weeks. For gel mobility shift analysis, the labeled fragments were diluted into 1000 cpm.

3.3.6 Gel mobility shift analysis (EMSA)

The purified protein and a (γ32P)dATP-labeled DNA fragment were mixed with 1 µg uncompetitive salmon sperm DNA (sonified, 1µg/µl) or competitive DNA fragments in 15-20 µl binding solution respectively (µl).

OxyR-oxidative reaction for EMSA:

Reaction components	Volume						
	A	B	C	D	E(1:1)	F(1:10)	G(1:100)
H_2O	14.5	13.5	12.5	11.5	10.5	10.5	10.5
Binding buffer (OxyR)	2.5	2.5	2.5	2.5	2.5	2.5	2.5
Salmon sperm DNA (1μg/μl)	1	1	1	1	1	1	1
OxyR (150 ng)	0	1	2	3	2	2	2
Cold (new) P5	0	0	0	0	2	2	2
Lalbeled (new) P5 (1000 cpm)	2	2	2	2	2	2	2
Total	20						

OxyR-reduced reaction for EMSA:

Reaction components	Volume						
	A	B	C	D	E(1:1)	F(1:10)	G(1:100)
H_2O	14.5	9.5	8.5	7.5	6.5	6.5	6.5
Binding buffer (OxyR)	2.5	2.5	2.5	2.5	2.5	2.5	2.5
Salmon sperm DNA (1μg/μl)	1	1	1	1	1	1	1
DTT (1M)	0	4	4	4	4	4	4
OxyR(150 ng)	0	1	2	3	2	2	2
Cold (new) P5	0	0	0	0	2	2	2
Lalbeled (new) P5 (1000 cpm)	2	2	2	2	2	2	2
Total	20						

IscR reaction for EMSA:

Reaction components	Volume							
	A	B	C	D	E (1:1)	F (1:10)	G (1:400)	H (1:600)
H_2O	4.5	3.5	2.5	1.5	2.5	0.5	0.5	0.5
Binding buffer (IscR)	7.5	7.5	7.5	7.5	7.5	7.5	7.5	7.5
Salmon sperm DNA (1μg/μl)	1	1	1	1	1	1	1	1

IscR (250 ng)	0	1	2	3	2	2	2	2
Cold P3 or 0019	0	0	0	0	2	2	2	2
Lalbeled P3 or 0019 (1000 cpm)	2	2	2	2	2	2	2	2
Total	15							

Irr reaction for EMSA:

Reaction components	Volume						
	A	B	C	D	E(1:1)	F(1:10)	G(1:100)
H_2O	5.5	4.5	3.5	2.5	1.5	1.5	1.5
TB (0.12M)	2.5	2.5	2.5	2.5	2.5	2.5	2.5
10 ×BSA (1 mg/μl)	1.5	1.5	1.5	1.5	1.5	1.5	1.5
DTT (0.01M)	1.5	1.5	1.5	1.5	1.5	1.5	1.5
80% glycerol	1	1	1	1	1	1	1
Salmon sperm DNA (1μg/μl)	1	1	1	1	1	1	1
Irr (200 ng)	0	1	2	3	2	2	2
Cold P1 or P2	0	0	0	0	2	2	2
Lalbeled P1 or P2 (1000 cpm)	2	2	2	2	2	2	2
Total	15						

The reactions were performed at 4 ℃ or 32 ℃ for 30 min and the samples were loaded on a 4% or 6% polyacrylamide gel and run (130-160V for 2-5 hours) in TBE buffer at 4 ℃ or room temperature. The gels were dried on a gel dryer for 1 hour and then exposed overnight. The signals were scanned by the phosphoimaging system (Molecular Imager® FX; Bio-Rad) and the appropriate software (QUANTITY ONE; Bio-Rad).

4. Results

4.1 Prediction of promoters for the *isc-suf* operon based on dRNA-seq analysis

Previously RNA-seq was performed by (Remes *et al.*, 2017). RNA-seq data indicated *R. sphaeroides* has a cluster of genes, with *isc* and *suf* homologues, and called *isc-suf* operon. The genes of *isc-suf* operon are co-transcription. The important regulator IscR (RSP_0443) related to Fe-S assembly is encoded by the first gene *iscR* of *isc-suf* operon, which coordinates a Fe-S cluster with a unique Fe-S ligation scheme (Remes *et al.*, 2015). The other genes of the operon encode two cystein desulfurases (IscS and SufS), the membrane component of an iron-regulated ABC transporter (SufB), a hypothetical protein (RSP_0439), the ATPase subunit of an ATP transporter (SufC), an Fe-S cluster assembly protein (SufD), and two proteins of the Yip1 family (RSP_0433 and RSP_0432) (Fig. 4.1). And this co-transcription was also confirmed by further RT PCR experiments (Remes *et al.*, 2015).

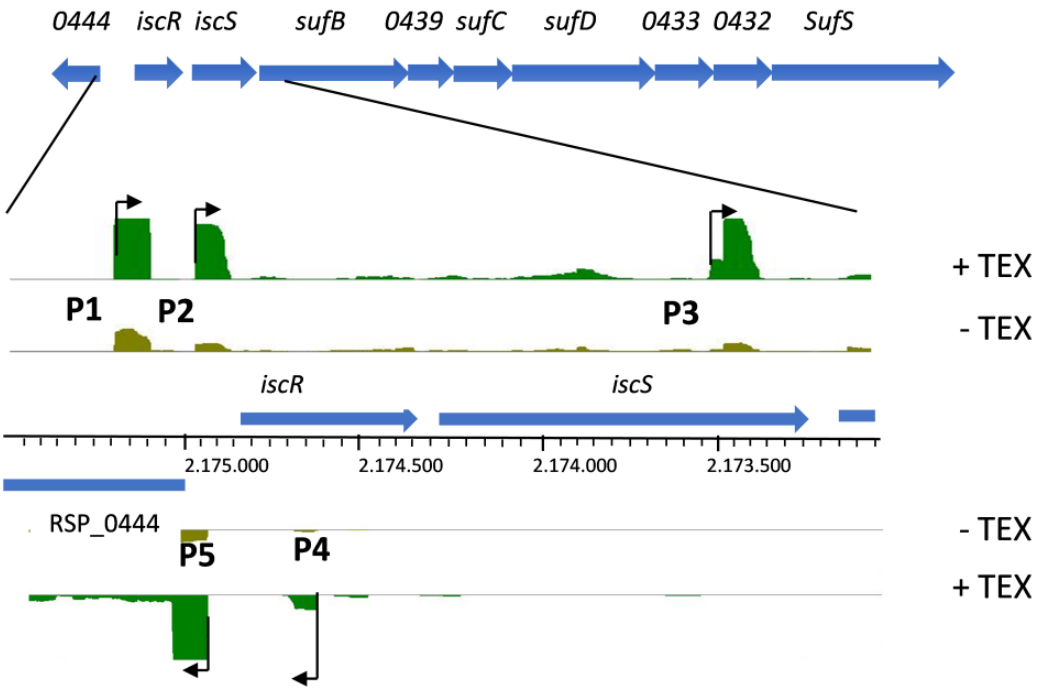

Fig. 4.1: Schematic overview of the *isc-suf* operon of *R. sphaeroides* and reads from RNA-seq for its 5 ŕegion in plus direction as displayed in the Integrated Genome Browser (Nie *et al.*, 2019).

Prediction of promoters for the *isc-suf* operon of *R. sphaeroides* was based on the RNA-seq analysis. The transcriptional start sites (TSS) were determined by differential dRNA-seq analysis by using RNA samples treated and untreated with terminator exonuclease (TEX) (Sharma *et al.*, 2010). Accumulation of primary transcripts with 5 ́triphosphate in the TEX-treated sample strongly supports the presence of a TSS at this position. From the dRNA-seq read coverage, there are five promoters in the *isc-suf* operon including three sense promoters and two anti-sense promoters. Two promoters (P1 and P2) are positioned upstream of *iscR* (RSP_0443), which is transcribed from the minus DNA strand (in Fig.4.1, 4.2, 4.3 shown on the plus strand). Another sense promoter (P3) starts in the middle of *iscS* (RSP_0443). Furthermore, there are two anti-sense promoters (P4 and P5) transcript on the another DNA strand. P4 leads to a transcript partially anti-sense to the *iscR* mRNA and was represented by a very low number of reads. P5 represents the promoter for transcription of RSP_0444. The transcript is anti-sense to a transcript initiating at P1 for the *isc-suf* operon (Fig. 4.1).

In *R. sphaeroides* most of the promoters have an A residue at position -10/-11 and a TTG around position -35 in regard to the TSS (Remes *et al.*, 2017). In the *isc-suf* operon, promoter 1 has an A residue at position -11, but a TTG around position -35 in regard to the TSS is absent. Promoter 2 is the promoter of *iscR* (RSP_0443) and has an A residue at positions -11 and a TTG around position -35. The promoter 3, in the middle of *iscS* has an A residue at position -10 and a TTG around position -34. Promoter 4 is very weak based on RNA-seq data and has a TTG around position -35, but no A residue is at position -10/-11. P5 also has a TTG around position -35, but no A residue is at position -10/-11 (Fig. 4.2).

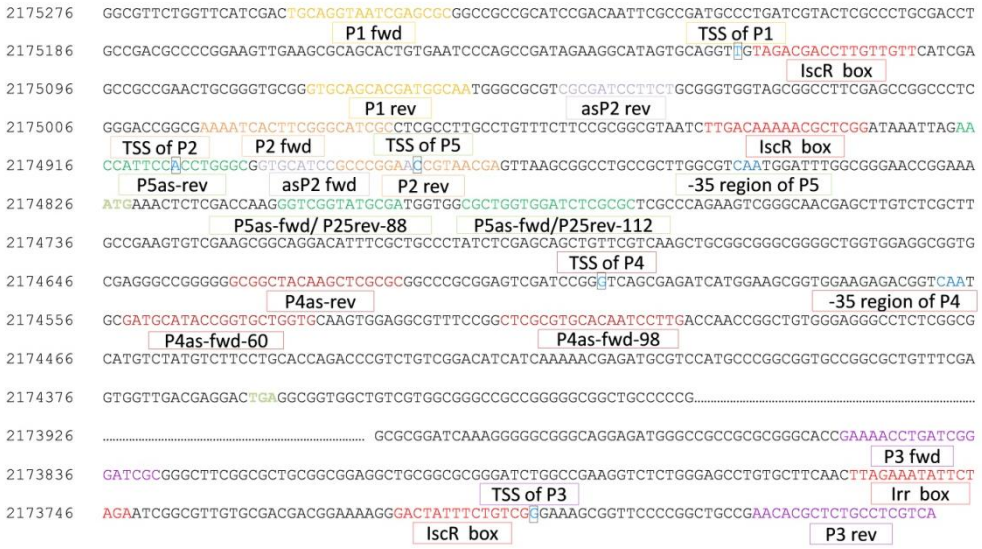

Fig. 4.2: Sequence of the 5 ŕegion of the *isc-suf* operon from *R. sphaeroides* shown in plus direction. The TSS for promoters P1-P5 are indicated (red, boxed), as well as the primer binding sequences for amplification of DNA fragments for reporter plansid construction. The ATG and the TGA of the IscR coding sequence are marked in bold green. The TTGs at position -35 of P4 and P5 that were mutated to AAA for our investigations are marked in blue (Nie *et al.*, 2019).

4.2 Construction of transcriptional reporter gene fusions for the *isc-suf* operon

Based on the data of the RNA-seq, different transcriptional fusions to the *lacZ* gene of the *isc-suf* sense and anti-sense promoters alone or in combination were constructed. These constructions were used to confirm the activity and interaction of the predicted promoters. An overview of the cloned strategy is shown in Fig. 4.3. Fragments of these different transcriptional fusions (sense and anti-sense promoters alone and in combination) containing 60-148 bp upstream or 34-63 bp downstream of these TSS as shown by dRNA-seq were inserted in front of the *lacZ* gene of plasmid pBBR1-MCS3-*lacZ* (Kovach *et al.*, 1995) by restriction enzyme and ligase. Each predicted TSS and exact positions of primers are shown in Fig. 4.2. These plasmids were transferred into competent cells S17-1 first and then further transferred into *R. sphaeroides* 2.4.1 wild type by diparental conjugation.

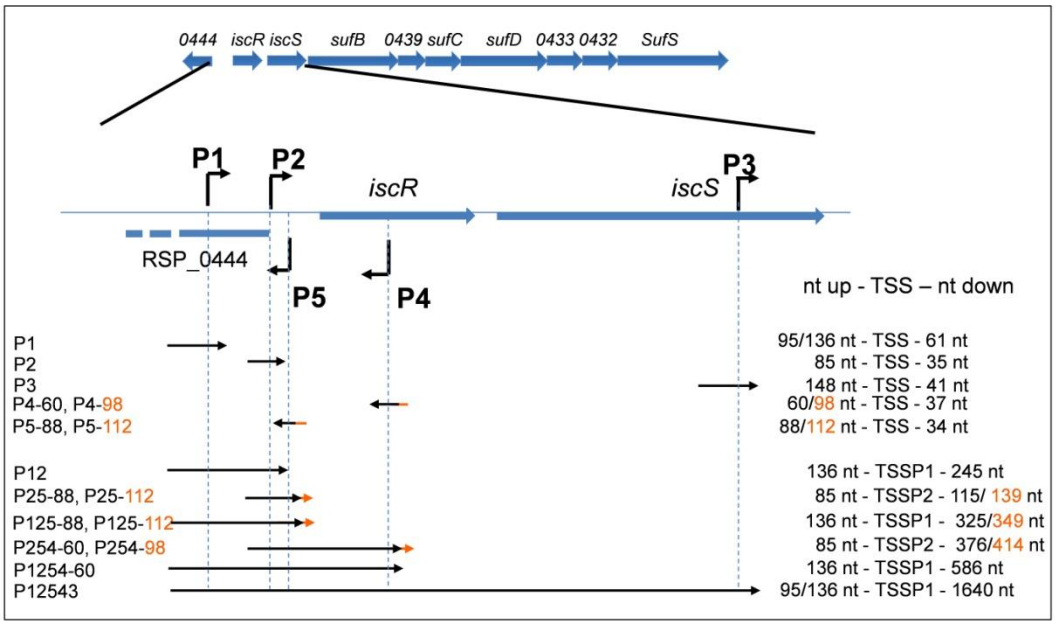

Fig. 4.3: strategies of fusion construction. The map of plasmid PBBR1-MCS3-*lacZ* and fragments used in the reporter assays to examine the promoter activity for all of the single promoters and combined promoter are indicated (Nie *et al.*, 2019).

4.3 Activities of transcriptional reporter gene fusions in the sense and anti-sens promoters alone and in combination under microaerobic condition

The β-galactosidase activities of the *isc-suf* sense and anti-sense promoters alone or in combination under microaerobic condition were measured for exponentially growing cultures. The β-galactosidase activities for the different promoter fusions alone or in combination showed great differences (Fig. 4.4). For single promoter fusions, P1-*lacZ* and P2-*lacZ* very weak activity of about 20-50 Miller Units (MU) was determinated, the P3-*lacZ* and P5-88-*lacZ* fusions showed about 150-200 MU, the P4-98-*lacZ* fusion showed about 400 MU under microaerobic conditions. But the P5-112-*lacZ* and the P4-60-*lacZ* fusions showed a lower activity than P5-88-*lacZ* and the P4-98-*lacZ* fusions. The high activity of P4-98-*lacZ* was different from the data of the RNA-seq that only showed a low number of reads from the P4. This indicates that the transcript initiating at P4 may be very unstable compared to the P4-98-*lacZ* fusion. But this high activity was reduced to about 30 MU, when the upstream fragments was reduced from 98 b to 60 bp. Similarly, the activity of P5 was also dependent on the length of the upstream fragments.

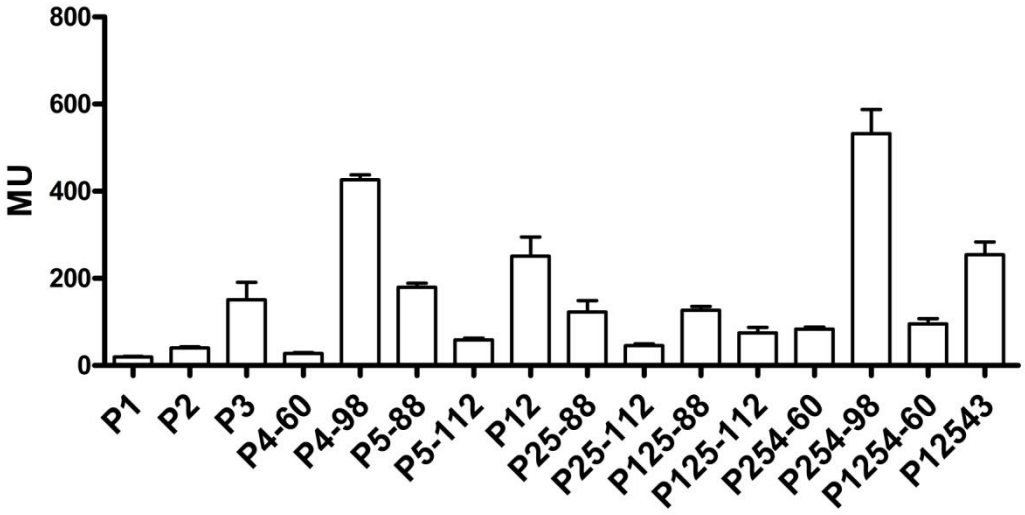

Fig. 4.4: Activity of single promoters and combined promoters as determined by *lacZ* reporter assays and quantified by measuring the β-galactosidase activity in Miller Units (MU) under microaerobic condition (iron repletion). The bars represent the average of technical duplicates from biological tripliates and the standard deviation is indicated.

Based on the arrangement of the different promoters on the *isc-suf* operon on the chromosome, it is conceivable that sense promoters P1, P2, and P3 mainly contribute to *isc-suf* operon transcription and that the anti-sense transcripts may influence the activity of sense promoters on the *isc-suf* operon transcription. To confirm this hypothesis, we applied the same primers as used for the single promoter fusions to construct combined transcriptional fusion that have different combinations of the different promoters (Fig. 4.3). Our results confirmed that the precence of additional promoters can influence the activity of a single promoter (Fig. 4.4). When P1 and P2 were transcribed together, the activity was obviously higher than the single promoter fusions. The P25-88-*lacZ* fusions showed a higher activity than P2 alone. Maybe P25-88 produces the 28 bp anti-sense transcripts at the 5´end of *iscR* that led to the increases of P2 activity. But this increase did not happen in the P25-112-*lacZ* fusions. When P4-98 was added into the P25-*lacZ* fusions it led to a strong increase of the activity, but nothing happened after the addition of P4-60. Comparing all the combined fusions with P1, the P1 seems to have no influence of the other promoters. A 1777 nt fragment harbouring all five promoters P12543 showed lower β-galactosidase activity was than P254 and nearly as the P12 activity under microaerobic conditions (Fig. 4.4).

4.4 An anti-sense promoter stimulates transcription of the *isc-suf* operon

As shown in Fig. 4.4, the anti-sense promoter P5 influences on P2 activity. Because of the addition of P5, the P25-88-*lacZ* fusion shown a higher activity than P2 alone. It is conceivable that the prolonged DNA fragments fused to *lacZ* may include other elements that can affect the β-galactosidase activity. Because the DNA fragment of P2 fused to *lacZ* was prolonged by 80 bp in P25-88 *lacZ* fusions, the DNA fragment of P25 fused to *lacZ* was prolonged by 275 bp in P254-98 *lacZ* fusions. To confirm these two possibilities that the P4/P5 really affect the activity of P2 or the prolonged fragments affect the activity of P2, the respective point mutations of the -35 promoter regions of P4 and P5 were constructed by inverse PCR (see method 3.2.4.2) to abolish their activity. Exact positions of mutations are shown in Fig. 4.2. These mutated plasmids were transferred into S17-1 competent cells first and then further transferred into *R. sphaeroides* 2.4.1 wild type by diparental conjugation. The β-galactosidase activities of these fusions harbouring mutations under microaerobic condition were measured for exponentially growing cultures. As shown in Fig. 4.5, the activity of the point mutation in the -35 promoter regions of P5 (mutP5-88) was indeed nearly abolished compared to the activity of P5-88. The addition of the P5-88 fragment induced P2 activity, but no effect of the mutated P5-88 fragment on P2 activity was observed. The fact that P5 indeed affects the activity of P2 was confirmed. It indicates that the anti-sense promoter 5 can affect the transcription of the minus DNA strand in the *isc-suf* operon.

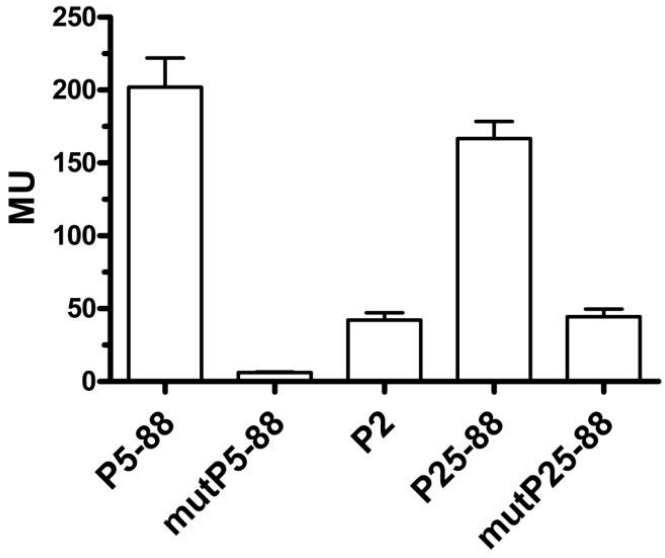

Fig. 4.5: Effects of the anti-sense promoter P5 on activity of P2 as determined in the *lacZ*-reporter assay (β-galactosidase activity in Miller units). The activity of single promoters (mut) P5 or P2 or the combined (mut) P25 fragment. The numbers indicate the length of the DNA sequence upstream of the TSS. "mut" indicates that the TTG at postion -35 of promoter P5 was changed to AAA.

There are two possibilities, how P5 affects the activity of P2: i) through the production of an anti-sense transcript of P5, or ii) through changing the local DNA topology by its promoter activity. Another plasmid (pRK4352-asP2) was constructed and introduced into the strain to discriminate between these two possibilities. This plasmid (pRK4352-asP2) can produce much more anti-sense RNA as produced by P5 initiating at the strong 16S promoter. These two different plasmids were transferred respectively into competent cell S17-1 first and then further transferred together into *R. sphaeroides* 2.4.1 wild type by diparental conjugation. The β-galactosidase activities under microaerobic conditions were measured for exponentially growing cultures. As shown in Fig. 4.6A, the production of this anti-sense RNA did not affect activity of P2. The construction used in these assays (P2 Gm) was placed into another vector with gentamicin resistance not tetracycline to allow over-expression of the anti-sense RNA asP2 from vector PRK4352 with tetracycline resistance. Furthermore, real time RT-PCR proved that the plasmid pRK4352-asP2 can indeed produce a lot of the anti-sense RNA asP2 of about 30-fold higher than in a strain lacking this plasmid (Fig. 4.6B).

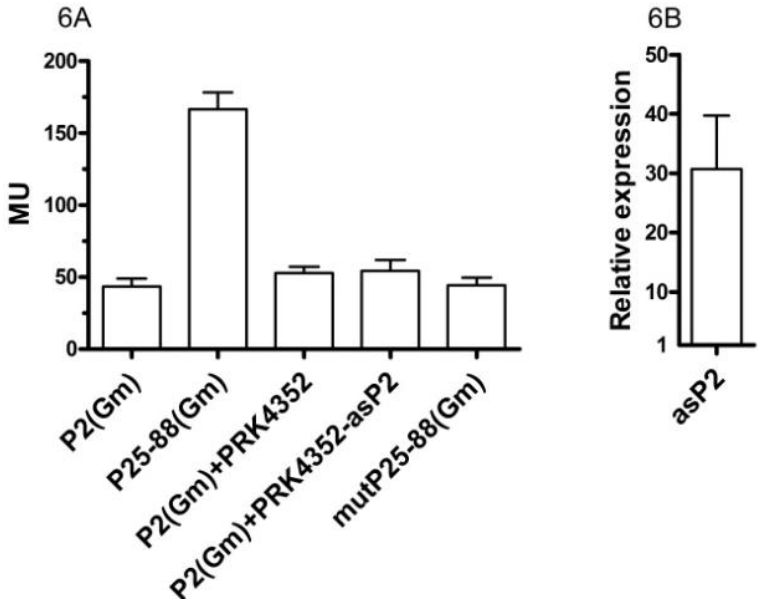

Fig. 4.6: Effects of the anti-sense promoters P5 on activity of P2 as determined in the *lacZ*-reporter assay (β-galactosidase activity in Miller units). A: Effect of elevated levels of RNA anti-sense to P2 on activity of P5 as determined in the *lacZ*-reporter assay. B: Change of the level of RNA anitisense to P2 in the wild type containing the P2 reporter plasmid and plasmid pRK4352-asP2 compare to a strain just containing the P2 promoter. RNA level was determined by real time RT PCR and the bar represents the average level of technical triplicates from biological triplicates with standard deviation.

The same strategy was applied to measure the effect of P4 in different length (P4-60 and P4-98) on P2 activity. However, mutation of the TTG at the -35 region of P4-98 only slightly decreased β-galactosidase activity in the mutP4-98-*lacZ* fusion (Fig. 4.7A). The addition of P4-98 in the P254-*lacZ* led to a strong increase of P25 activity, but the addition of the mutated P4-98 in the mutP254-98-*lacZ* would still increase the activity of the P25 fusion, even though the activity was a little lower than P254-98-*lacZ* fusion (Fig 4.7A). The fact that P4-98 has no effects on the activity of P2 was confirmed. It indicates that the promoter of anti-sense P4-98 can not affect the transcription of the minus DNA strand in the *isc-suf* operon. The increased activity in the P254-*lacZ* may come from the unknown specificity of the P4-98 fragment. However, the P4-60-*lacZ* fusion had strongly reduced activity compared to P4-98-*lacZ* fusion and the low activity of P4-60 was almost abolished by the mutation of the -35 region of P4-60. The addition of P4-60 to the P25-*lacZ* would reduced slightly the activity of the P25 fusion, but no significant difference. So the P4-60 has still no effects on the activity of P2. However, the addition of the mutation of P4-60 into the

P25-*lacZ* would strongly increase the activity of the P25 fusion compared to P254-60-*lacZ* fusion (Fig 4.7B). It indicates that sequences in the -98 to -60 upstream of the P4 are responsible for the strong activity of P4-98 and for the influence of P4 on P25.

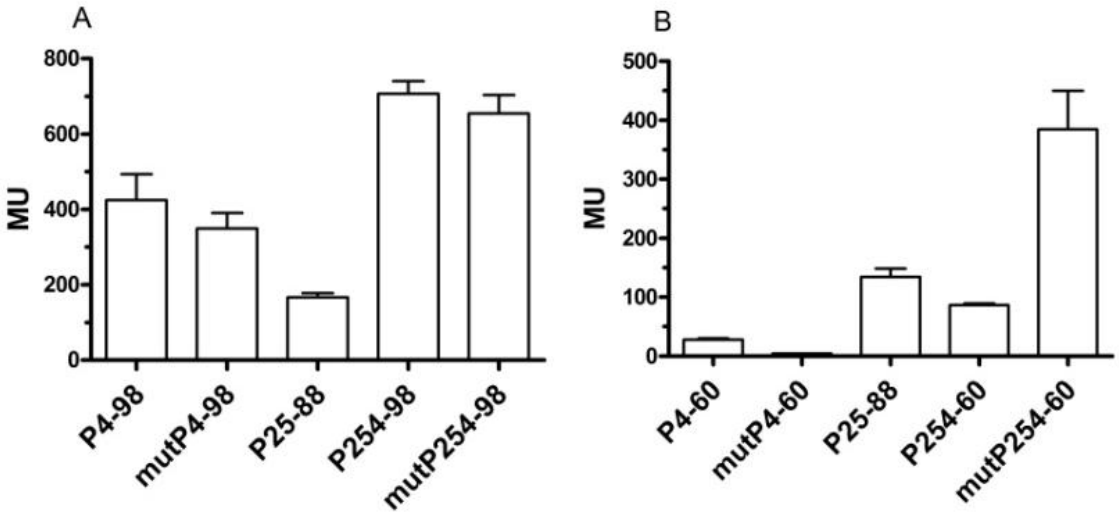

Fig. 4.7: Effects of the anti-sense promoters P4 on activity of P2 as determined in the *lacZ*-reporter assay (β-galactosidase activity in Miller units). The activity of single promoter (mut)P4 or the combined P25 and (mut)P254 fragment. The numbers indicate the length of the DNA sequence upstream of the TSS. "mut" indicates that the TTG at postion -35 of promoter P4 was changed to AAA.

4.5 Activities of transcriptional reporter gene fusions under aerobic conditions

The β-galactosidase activities of the *isc-suf* sense and anti-sense promoters alone or in combination were measured together for exponentially growing cultures that were incubated under aerobic and microaerobic conditions to analyse the influence of the environment (oxygen concentration). As shown in Fig. 4.8, P3 is the only promoter with changed activity under aerobic conditions. The activity of P3 under aerobic conditions was significantly higher (increase > 1.5 fold and $p < 0.01$) than the activity of P3 under microaerobic conditions. For the combined promoters, the activity of the P12543 was also significantly increased under aerobic conditions compared to microaerobic conditions, while the other single promoters and combined promoters were independent of the oxygen concentration. These significant differences were statistically significant, but the increase of the activity under aerobic conditions was not strong (slightly more than 1.5-fold).

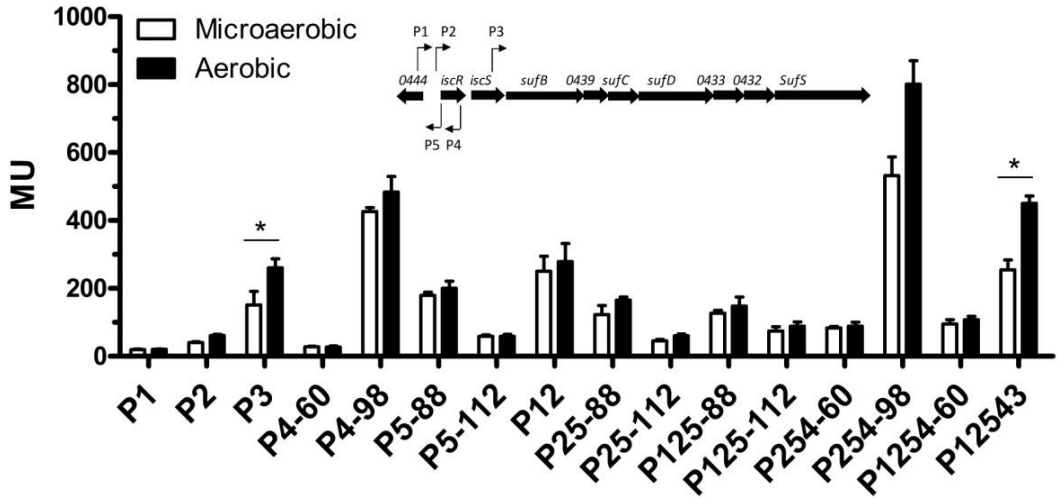

Fig. 4.8: The activity of single promoters and combined promoters as determined by *lacZ* reporter assays and quantified by measuring the β-galactosidase activity in Miller Units (MU). The bars represent the average of technical duplicates from biological tripliates and the standard deviation is indicated. *: the significant difference between the values for microaerobic and aerobic conditions is > 1.5 fold with a p-value of < 0.01.

4.6 Effect of oxidative stress on the activity of the promoters of the *isc-suf* operon

Previous microarrays and RNA-seq experiments revealed that expression of the *isc-suf* genes was affected by oxidative stress (Zeller *et al.*, 2005; Zeller *et al.*, 2007). In this study, the activities of the different reporter fusions were measured, and then analysed whether the single or combined promoters were affected by these external factors (oxidative stress). Two different kinds of oxidative stress agents, hydrogen peroxide (H_2O_2) and tertiary butyl alcohol (tBOOH), were applied to produce the different oxidative stress.

4.6.1 Effect of hydrogen peroxide on the activity of the promoters

The β-galactosidase activities of the *isc-suf* sense and anti-sense promoters alone or in combination under microaerobic conditions were measured after the addition of the hydrogen peroxide (H_2O_2, final concentration: 1 mM) for exponentially growing cultures to analyse the influence of oxidative stress. Hydrogen peroxide itself is a reactive oxygen species and may be partially reduced to hydroxyl radical (•OH) that is an even more reactive oxygen species. As shown in Fig. 4.9, all the single promoters and combined promoters had no significant difference after addition of hydrogen

peroxide (Fig. 4.9).

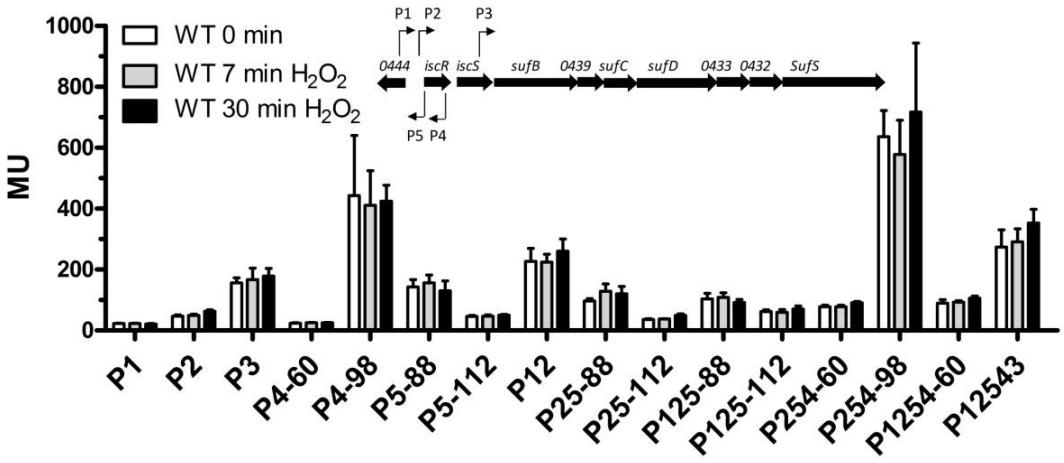

Fig. 4.9: The activity of single promoters and combined promoters as determined by *lacZ* reporter assays and quantified by measuring the β-galactosidase activity in Miller Units (MU). β-galactosidase activity was measured before, 7 min, and 30 min after addition of H_2O_2 (1 mM final concentration) to the wild type. The bars represent the average of technical duplicates from biological tripliates and the standard deviation is indicated. *: the signigicant difference is > 1.5 fold with a p-value of < 0.01.

4.6.2 Effect of tertiary butyl alcohol on the activity of the promoters

The β-galactosidase activities of the *isc-suf* sense and anti-sense promoters alone or in combination under microaerobic conditions were measured by the addition of tertiary butyl alcohol (tBOOH, final concentration: 100 μM) for exponentially growing cultures to analyse the influence of another reagent causing oxidative stress. tBOOH represents organic peroxides that are produced in the cell e.g. upon singlet oxygen exposure. As shown in Fig. 4.10, the addition of tBOOH led to significantly increased activities of some promoters after 30 min. Only P2 of the single promoter fusions was affected by tBOOH 30 min after the addition of tBOOH. P25-88 had significant difference after 30 min of the addition of tBOOH. The changes in activity were however less than 2-fold (Fig. 4.10). It indicates that P2 and P25-88 had a significant tBOOH-dependent expression, even though the changes were slight and less than 2-fold (Fig. 4.10).

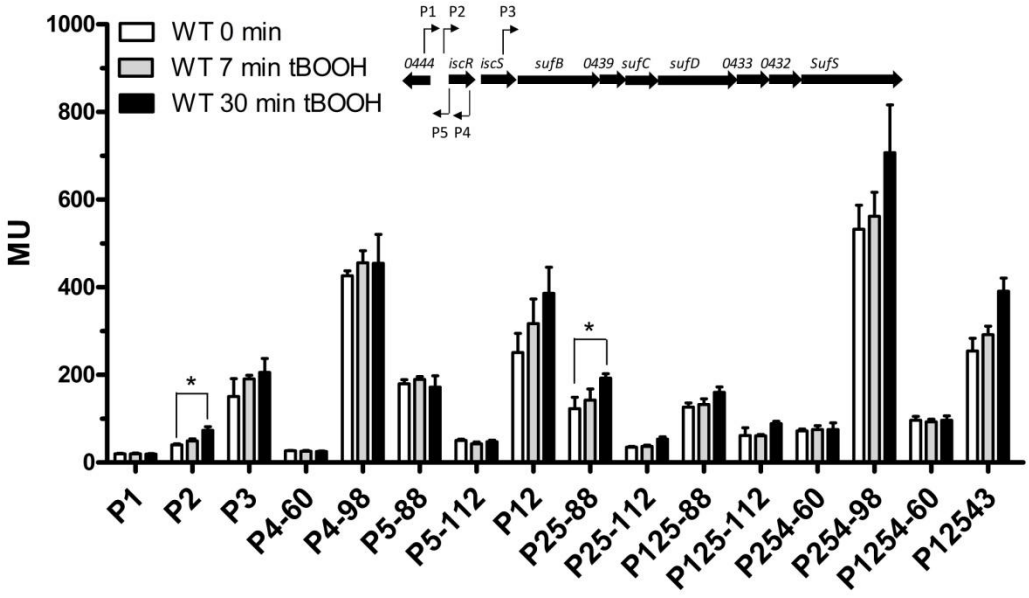

Fig. 4.10: The activity of single promoters and combined promoters as determined by *lacZ* reporter assays and quantified by measuring the β–galactosidase activity in Miller Units (MU). The β-galactosidase activity was measured before, 7 min, and 30 min after addition of tBOOH (100 μM final concentration). The bars represent the average of technical duplicates from biological tripliates and the standard deviation is indicated. *: the significant difference is > 1.5 fold with a p-value of < 0.01.

4.7 Effect of iron availability on the activity of the promoters of the *isc-suf* operon

Previous microarrays and RNA-seq experiments revealed that expression of the *isc-suf* genes is affected by iron availability (Remes *et al.*, 2014; Peuser *et al.*, 2011). The β-galactosidase activities of the *isc-suf* sense and anti-sense promoters alone or in combination under microaerobic conditions (iron-repletion) and under iron-depletion were measured for exponentially growing cultures to analyse the influence of the external factors, iron availability. As shown in Fig. 4.11, a strong increase of P2 activity (about 5-fold) under iron depletion was observed compared to iron repletion in this study, and the increase activities of all of the other fusions containing P2, including the long fusion extending to P3 were more or less also observed (Fig. 4.11). It indicates that P2 contributes to all of the increase on the expression under iron depletion condition. It is consistent with a previous study showing that the *iscR* transcript level increases upon iron depletion (Remes *et al.*, 2015). But no significant difference for the activities of P1, P3, P4 or P5 were observed under iron repletion or iron depletion (Fig. 4.11).

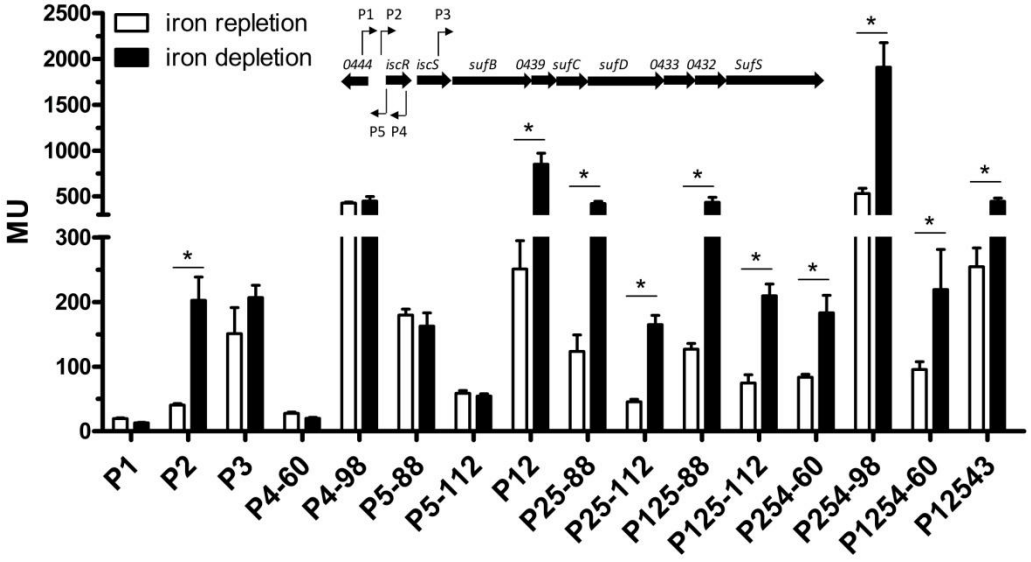

Fig. 4.11: The activity of single promoters and combined promoters as determined by *lacZ* reporter assays and quantified by measuring the β-galactosidase activity in Miller Units (MU). The β-galactosidase activities were determined under iron repletion and the iron depletion conditions. The bars represent the average of technical duplicates from biological tripliates and the standard deviation is indicated. *: the significant difference is > 1.5 fold with a p-value of < 0.01.

4.8 The RirA proteins have no effect on *isc-suf* expression in *R. sphaeroides*

Even though the Fur protein is the dominant iron regulator in gamma-proteobacteria, other proteins also paly an important role in iron-dependent regulation in alpha-proteobacteria (Rodionov *et al.*, 2006).

4.8.1 RirA have no effect on the growth

The RirA protein is an another transcriptional regulator of the Rrf2 protein family besides the IscR protein, and was confirmed to play an important role in the iron regulation in *Rhizobia* (Imam *et al.*, 2014). The genes RSP_2888 and RSP_3341 of *R. sphaeroides* 2.4.1 have 59-63% identity to *rirA* from *Rhizobium leguminosarum* or *Agrobacterium tumefaciens* (*Rhizobium radiobacter*). The knock out strains of *R. sphaeroides* that lack either RSP_2888 or RSP_3341 or both genes (*rirA*) together were constructed. Firstly, the growth curves of the double mutant were measured for 24 hours. As shown in Fig. 4.12, the double mutant RirA showed nearly identical growth curves compared to the wild type under iron repletion and iron depletion. It indicates that the lack of double *rirA* genes have no effect on the growth, and maybe also have no

effect on iron regulation in *R. sphaeroides*.

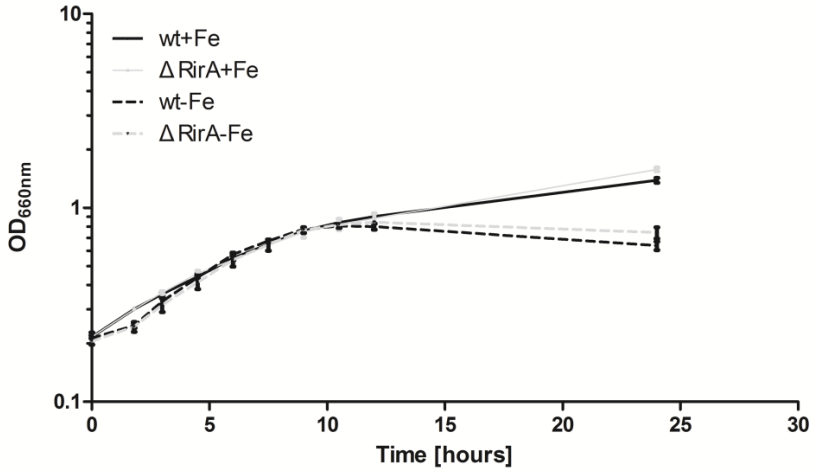

Fig. 4.12: Growth curves for the wild type and the RirA double mutant under iron repletion and iron depletion conditions. Growth curves of the *R. sphaeroides* wild type (black) and the RirA double mutant (gray) under iron repletion (continuous line) and under iron depletion (dashed line) conditions are shown. The optical density at 660 nm (OD_{660nm}) of microaerobically grown *R. sphaeroides* cultures were determined time by time. The data represent the mean of three independent experiments and error bars indicate standard deviation of the mean.

4.8.2 Effect of iron availability on the activity of the promoters of the *isc-suf* operon in RirA mutant

The β-galactosidase activities of the *isc-suf* sense and anti-sense promoters alone or in combination under microaerobic conditions (iron-repletion) and under iron-depletion were measured for exponentially growing cultures of wild type and the double mutant RirA. As shown in Fig. 4.13, all the single and combined promoters of the *isc-suf* operon showed very similar activities in the wild type and the double mutant, and also the effect of iron depletion on promoter activity was very similar in the wild type and the double mutant. It indicates that the double RirA homologues of *R. sphaeroides* play no major role in iron-dependent regulation of the *isc-suf* operon.

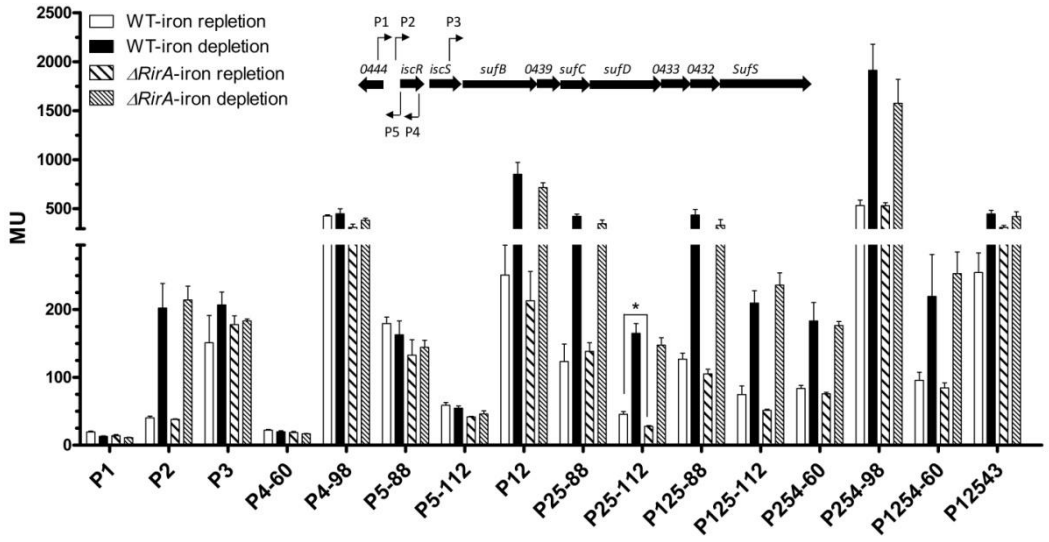

Fig. 4.13: The activity of single promoters and combined promote as determined by *lacZ* reporter assays and quantified by measuring the β-galactosidase activity in Miller Units (MU). β-galactosidase activity was compared for the wild type and the RirA double mutant under iron repletion and iron depletion. The bars represent the average of technical duplicates from biological tripliates and the standard deviation is indicated. *: the significant difference is > 1.5 fold with a p-value of < 0.01.

4.8.3 Effect of tBOOH on the activity of the promoters of the *isc-suf* operon in RirA

The β-galactosidase activities of the *isc-suf* sense and anti-sense promoters alone or in combination under microaerobic conditions were measured by the addition of tertiary butyl alcohol (tBOOH, final concentration: 100 μM) to exponentially growing cultures of the double mutant RirA. As shown in Fig. 4.14, all the single promoters and combined promoters of the *isc-suf* operon showed no significant difference in activity after addition of tBOOH.

From all of the above results, we conclude that the RirA homologues of *R. sphaeroides* play no major role in the oxidative stress and iron-dependent regulation of the *isc-suf* operon.

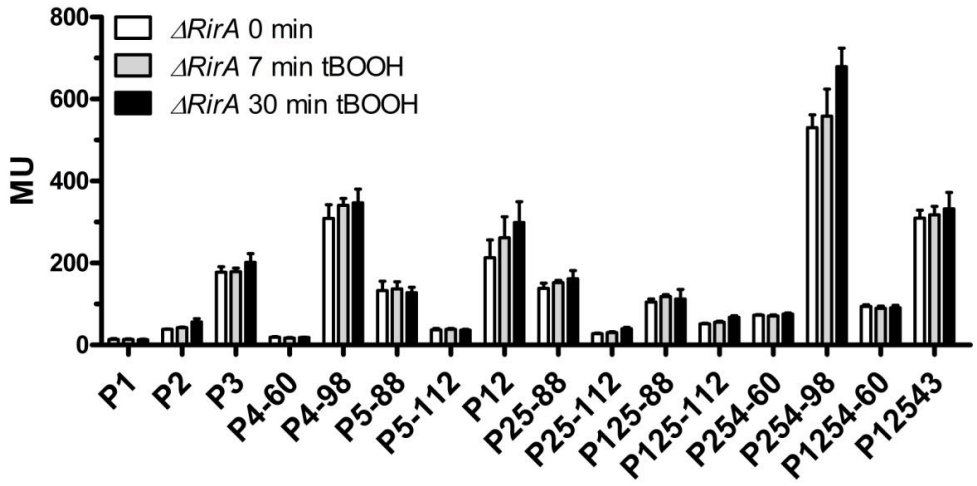

Fig. 4.14: The activity of single promoters and combined promoters as determined by *lacZ* reporter assays and quantified by measuring the β-galactosidase activity in Miller Units (MU). β-galactosidase activity was measured before, 7 min, and 30 min after addition of tBOOH (100 μM final concentration) to the double mutant RirA. The bars represent the average of technical duplicates from biological tripliates and the standard deviation is indicated. *: the difference is > 1.5 fold with a p-value of < 0.01.

4.9 Protein regulators of the *isc-suf* operon

Previous microarray, RNA-seq, bioinformatic analyses and experiments revealed that some protein regulators (IscR, Irr, OxyR, Fur/Mur) play a role in regulation of *isc-suf* operon expression. Therefore, we tested the effects of these regulators on the *isc-suf* promoters.

4.9.1 The effects of IscR on the *isc-suf* promoters

The IscR protein is a main regulator of the *isc* operon in *E. coli* (Giel *et al.*, 2006) and owns a similar function in regulation of the *isc-suf* operon of *R. sphaeroides.*

4.9.1.1 Effect of iron availability on the activity of the promoters in the IscR mutant

The β-galactosidase activities of the *isc-suf* sense and anti-sense promoters alone or in combination under microaerobic conditions (iron-repletion) and under iron-depletion were measured together for exponentially growing cultures of wild type and IscR mutant to analyse the influence of iron. As shown in Fig. 4.15, of all single promoters, only P2 and P3 showed strong increased activities in the wild type and the IscR mutant under iron-repletion and under iron-depletion. All of the combined promoters of the *isc-suf* operon containing P2 except P12543 also showed strong

increased activities in the wild type and the IscR mutant under iron-repletion and under iron-depletion. `The fact that the increased activities were due to P2 is consistent with previous results showing that the IscR protein is a strong repressor of P2.

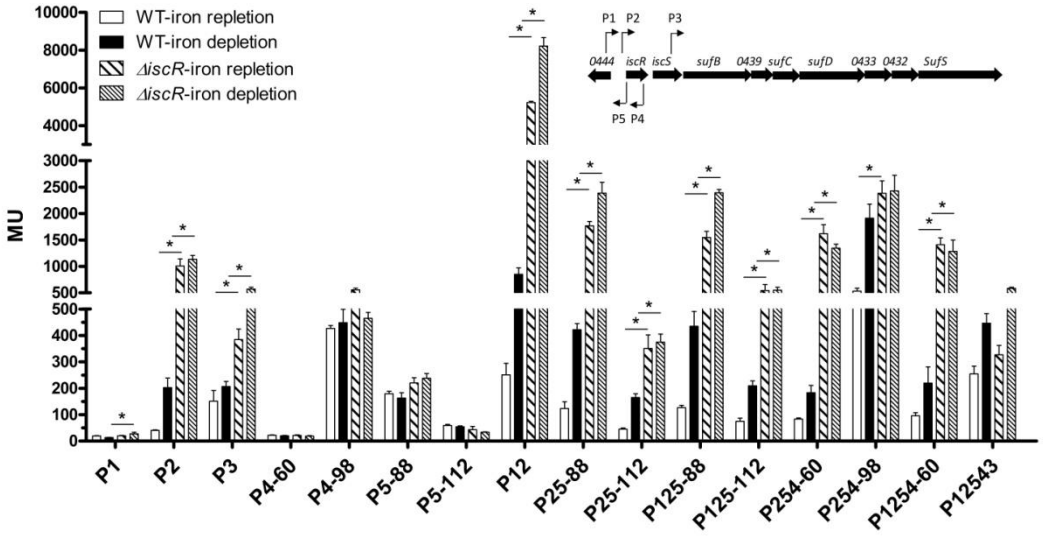

Fig. 4.15: The activity of single promoters and combined promoter as determined by *lacZ* reporter assays and quantified by measuring the β-galactosidase activity in Miller Units (MU). β-galactosidase activity was compared for the wild type and the IscR mutant under iron repletion and iron depletion. The bars represent the average of technical duplicates from biological tripliates and the standard deviation is indicated. *: the significant difference is > 1.5 fold with a p-value of < 0.01.

4.9.1.2 Gel mobility shift analysis with IscR protein and promoter 3

Previous bioinformatic analysis predicted IscR binding sites in the upstream of the *iscR* genes and the predicted IscR box spans the positions -36 to -19 in relation to the TSS at P2 (Rodionov *et al.*, 2006) (Fig. 4.16, TSS indicated in red). Binding of IscR to the upstream region of the *iscR* gene (Promoter 2) was experimentally verified previously (Remes *et al.*, 2015).

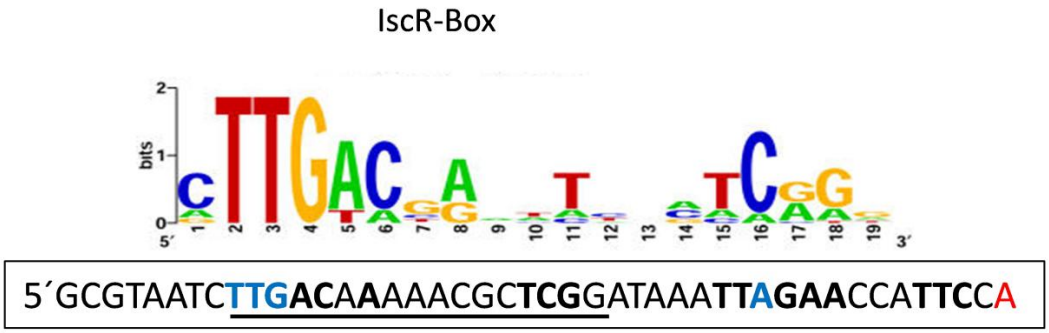

Fig. 4.16 The consensus IscR boxes as presented by (Rodionov *et al.*, 2006) are shown together with the sequence of the P2 promoter (shown in plus orientation). The IscR box is underlined, matching bases are

shown in bold. The transcriptional start site is shown in red, the A at position -11 and the TTG around -35 hehare shown in blue.

Similar to P2, P3 also had an increased activity in the IscR mutant under iron depletion and iron repletion. Analyses of the sequence upstream of the predicted TSS of P3 revealed a specific motif (**GA**CT**ATT**TCT**GT)** with good similarity to the IscR box (Fig. 4.2). But P3 in the wild type is had no significant response to iron (Fig. 4.15). The above analyses implied that the P3 may bind IscR protein, the gel mobility shift analysis (EMSA) with purified IscR-His-tag protein was performed to confirm this possibility. As shown in Fig. 4.17, IscR indeed showed a specific binding to P3 (a DNA fragment containing the probable binding site). Addition of increasing amounts of IscR resulted in a shift of DNA fragment P3. Addition of an excess of the unlabeled specific DNA fragments lead to decrease of shift due to specific competition with the labeled fragments in EMSA assay. This result strongly supports that IscR can indeed bind to P3. This showes that not only the IscR protein regulates its own gene *iscR*, but also regulates the expression of promoter 3 by direct binding.

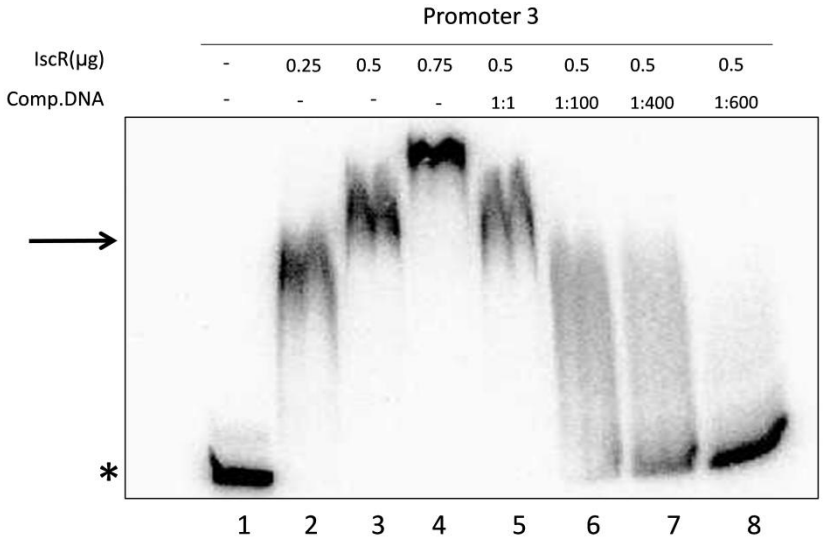

Fig. 4.17: Electrophoretic mobility shift assays showing the interaction of IscR to the P3 promoter region (190 bp fragment). The star labels the radiolabeled input DNA fragment, the arrow points to the shifted bands of the DNA protein complexes. The amount of the protein input is given for each lane and the molar ratio of specific, unlabelled competitor DNA.

4.9.1.3 Gel mobility shift analysis with IscR protein and promoter 1

P1 had similar activity as the wild type in the IscR mutant under iron repletion but about 2-fold increased activity under iron depletion. A sequence with some similarity to

the IscR box is present at the transcriptional start site of P1 (TAGACGACCTTGTTGTT, Fig. 4.2). Because the IscR protein maybe bind to P1, the gel mobility shift analysis (EMSA) with purified IscR-His-tag protein was performed to confirm this possibility. As shown in Fig. 4.18, the gel retardation indeed showed that IscR has a specific interaction to the P1 promoter region (a DNA fragment containing the probable binding site). Addition of increasing amounts of IscR protein resulted in a shift of DNA fragments P1. Addition of an excess of the unlabeled specific competitor DNA fragments resulted in decrease of shift due to specific competition with the labeled fragments in EMSA assay. This result strongly supports that IscR can indeed bind to P1. It indicates that not only the IscR protein regulates its own gene *iscR* and P3, but also regulates the expression of promoter 1.

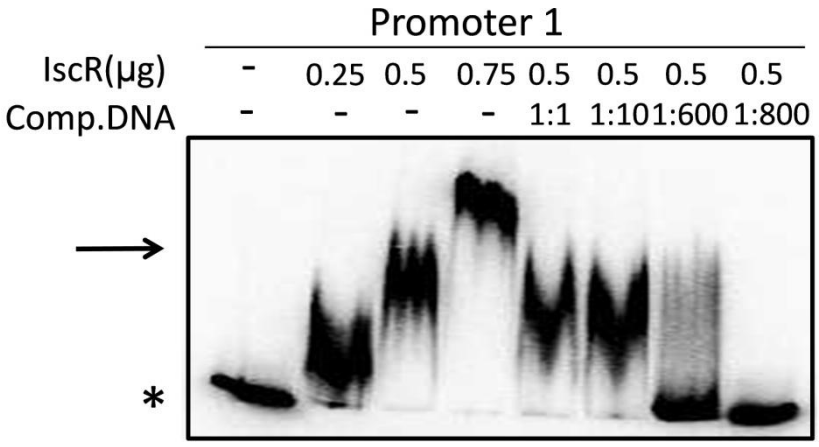

Fig. 4.18: Electrophoretic mobility shift assays showing the interaction of IscR to the P1 promoter region (201 bp fragment). The star labels the radiolabeled input DNA fragment, the arrow points to the shifted bands of the DNA protein complexes. The amount of the protein input is given for each lane and the molar ration of specific, unlabelled competitor DNA.

4.9.1.4 Effect of tBOOH on the activity of the promoters in IscR mutant

The β-galactosidase activities of the *isc-suf* sense and anti-sense promoters alone or in combination under microaerobic conditions were measured by the addition of tertiary butyl alcohol (tBOOH, final concentration: 100 μM) for exponentially growing cultures of the IscR mutant to analyse the influence of the oxidative stress (tertiary butyl alcohol) of the IscR mutant. As shown in Fig. 4.19, all the single promoters and combined promoters of the *isc-suf* operon have no significant difference after addition of tBOOH were observed. This indicates that were no effect of tBOOH on the activities

of the promoters of the *isc-suf* operon in the IscR mutant. But the activity of P2 was elevated after the addition of tBOOH in wild type (Fig. 4.10), this response of P2 to tBOOH was disappeared in the IscR mutant (Fig. 4.19). IscR maybe abolish the effect of P2 on the tBOOH under microaerobic conditions.

From all of the above results, we concluded that the IscR of *R. sphaeroides* plays no major role in the oxidative stress regulation of the *isc-suf* operon, but it may contribute the abolished effect on the tBOOH.

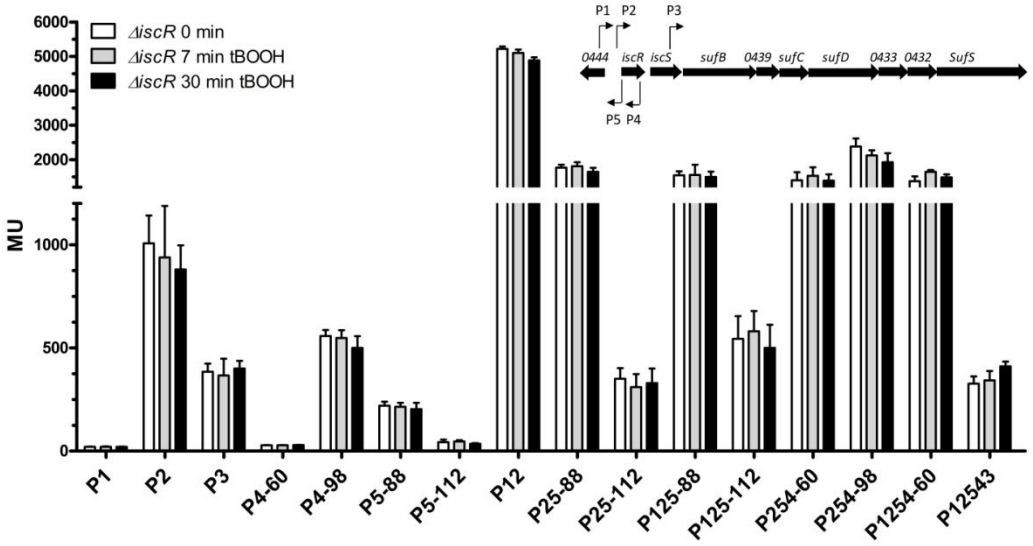

Fig. 4.19: The activity of single promoters and combined promoters as determined by *lacZ* reporter assays and quantified by measuring the β-galactosidase activity in Miller Units (MU). β-galactosidase activity was measured before, 7 min, and 30 min after addition of tBOOH (100 μM final concentration) to the IscR mutant. The bars represent the average of technical duplicates from biological tripliates and the standard deviation is indicated. *: the difference is > 1.5 fold with a p-value of < 0.01.

4.9.2 The effects of Irr on the *isc-suf* promoters

A role of Irr in expression of the *suf* genes was revealed by microarray analysis (Peuser *et al.*, 2012), but the binding of the Irr protein to the *iscR* promoter region of *R. sphaer*oides was not performed.

4.9.2.1 Effect of iron availabity on the activity of the promoters in Irr mutant

The β-galactosidase activities of the *isc-suf* sense and anti-sense promoters alone or in combination under microaerobic conditions (iron-repletion) and under iron-depletion were measured together for exponentially growing cultures of wild type and Irr mutant to analyse the influence of iron availability. As shown in Fig. 4.20, of all

single promoters of the *isc-suf* operon, only P2 of the *isc-suf* operon had a significantly decreased activities in the Irr mutant compared to the wild type under iron repletion condition. Of all the combined promoters of the *isc-suf* operon, only the full fusions P12543 showed strong increased activities in the IscR mutant under iron depletion condition. So the effect of iron depletion on the activity of the promoters only happen in P12543. The activity of P1 was nearly1.5-fold lower in the Irr mutant than in the wild type under iron repletion, but the activity of P3 was elevated in the Irr mutant under iron depletion but only by a factor of 1.3-fold (Fig. 4.20). The activity of the reporter fusion harbouring P12345 was strongly induced in the Irr mutant under iron depletion. This indicates that the Irr protein of *R. sphaeroides* can bind to P3.

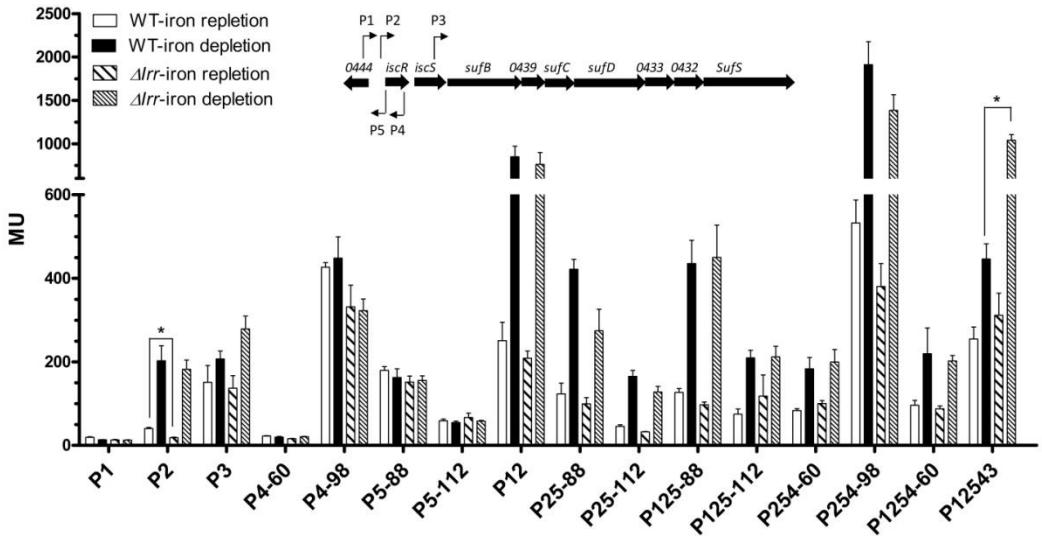

Fig. 4.20: The activity of single promoters and combined promote as determined by *lacZ* reporter assays and quantified by measuring the β-galactosidase activity in Miller Units (MU). β-galactosidase activity was compared for the wild type and the Irr mutant under iron repletion and iron depletion. The bars represent the average of technical duplicates from biological tripliates and the standard deviation is indicated. *: the significant difference is > 1.5 fold with a p-value of < 0.01.

4.9.2.2 Gel mobility shift analysis with Irr protein and promoter 2

Because of the significantly decreased activity of P2 in the Irr mutant under iron repletion (Fig. 4.20), the binding of Irr to P2 (the upstream region of the *iscR* gene) was performed by using the gel mobility shift assay (EMSA) with DNA fragments containing the sequence of P2 and Irr protein. No shift was detected in this study. The *mbfA* (0850) fragment was used as the positive control in this EMSA (Fig. 4.21),

proving that the purified Irr protein had DNA binding capacity.

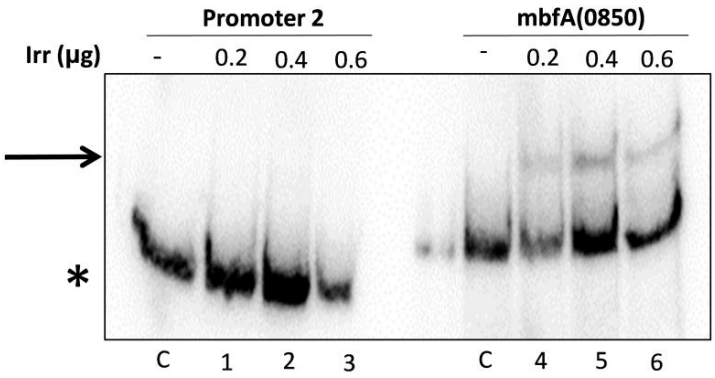

Fig. 4.21: Electrophoretic mobility shift assays testing the interaction of Irr to the P2 promoter region (121 bp fragment). The promoter region of the *mbfA* gene (180 bp fragment) that was known to bind Irr (Peuser *et al.*, 2012) was used as a positive control. The star labels the radiolabeled input DNA fragment, the arrow points to the shifted bands of the DNA protein complexes. The amount of the protein input is given for each lane and the molar ration of specific, unlabelled competitor DNA.

4.9.2.3 Gel mobility shift analysis with Irr protein and promoter 1

Previous bioinformatic analysis predicted an Irr binding site in the upstream of the *iscR* gene (Rodionov *et al.*, 2006). The predicted position of the Irr box positions -13 to +1 in relation to the TSS at P2 (Fig. 4.22, TSS indicated in red). A sequence (**TAGAA**GGCA**T**AGTGC) with similarity to the Irr-box was detected upstream of the TSS of P1 (Fig. 4.2).

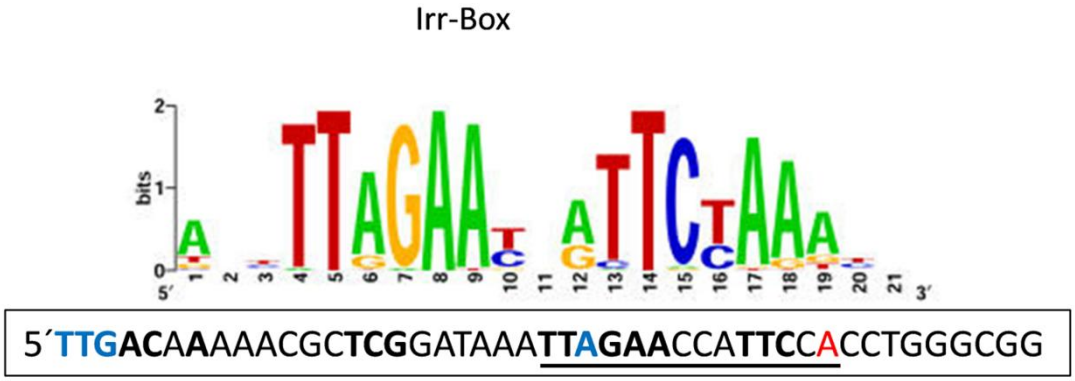

Fig. 4.22 The consensus Irr boxes as presented by (Rodionov *et al.*, 2006) are shown together with the sequence of the P2 promoter (shown in plus orientation). The Irr boxes are underlined, matching bases are shown in bold. The transcriptional start site is shown in red, the A at position -11 and the TTG around -35 are shown in blue.

No significant effect of Irr on the activity of P1 was observed, but the decrease was nearly1.5-fold lower in the Irr mutant than in the wild type under iron repletion.

Based on the similarity of the sequence to the Irr box and the nearly significant effect on P1 in the Irr mutant, the gel mobility shift analysis (EMSA) with purified Irr-His-tag protein was performed to test the hypothesis that Irr binds to the P1 promoter region. As shown in Fig. 4.23, no binding of Irr to P1 was detected in vitro. The *mbfA* (0850) fragment was used as the positive control in this EMSA.

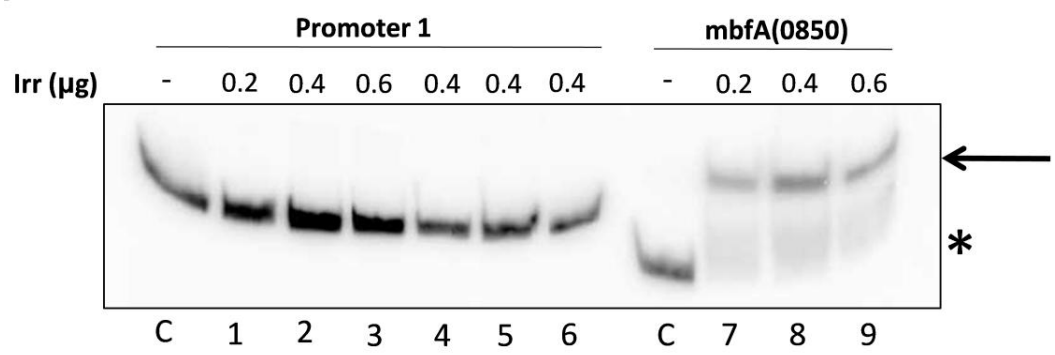

Fig. 4.23: Electrophoretic mobility shift assays testing the interaction of Irr to the P1 promoter region (199 bp fragment). The promoter region of the *mbfA* gene (180 bp fragment) that was known to bind Irr (Peuser *et al.*, 2012) was used as a positive control. The star labels the radiolabeled input DNA fragment, the arrow points to the shifted bands of the DNA protein complexes. The amount of the protein input is given for each lane and the molar ration of specific, unlabelled competitor DNA.

Neither binding of Irr to the P2 promoter nor to the P1 promoter *in vitro* were detected, while in a positive control assay binding to the *mbf*A promoter as described in (Peuser *et al.*, 2012) could be observed. All of the above results indicate that the influence of Irr on P1 may be indirect and that Irr does not play a major role in the regulation of *isc-suf* operon.

4.9.2.4 Gel mobility shift analysis with Irr protein and promoter 3

There is a significant increase in P12345 activity (about 2.3-fold increase) in the strain lacking Irr under iron depletion compared to wild type. Since Irr can not bind to P1 and P2, significant increase may come from P3. Indeed, P3 activity has a significant increase (2-fold increase) in the strain lacking Irr under iron depletion compared to the iron repletion. This agrees with our previous microarray data: the iron dependency of *suf* transcript levels is more pronounced in a strain lacking Irr than in the wild type (Klug *et al.*, 1997; Peuser *et al.*, 2011; Peuser *et al.*, 2012; Remes *et al.*, 2014; Remes *et al.*, 2015). Analysis of the sequence upstream of the predicted TSS of P3 revealed a

putative Irr binding site (**TTAGAA**AT**ATTCTA**G**A**) is about 50 nt upstream of the TSS of P3 (Fig. 4.2), which is a same distance to the TSS as observe for *ccpA* (Peuser *et al.*, 2012). This implies that the the Irr protein may bind P3. Gel mobility shift analysis (EMSA) with purified Irr-His-tag protein was performed to confirm this possibility. As shown in Fig. 4.24, Irr indeed showed a specific binding to P3 (a DNA fragment containing the probable binding site). Addition of increasing amounts of IscR resulted in a shift of DNA fragments P3. Addition of an excess of the unlabeled specific competitor DNA fragments led to decrease of the shift due to specific competition with the labeled fragments in the EMSA assay. This result strongly supports that Irr can indeed bind to P3.

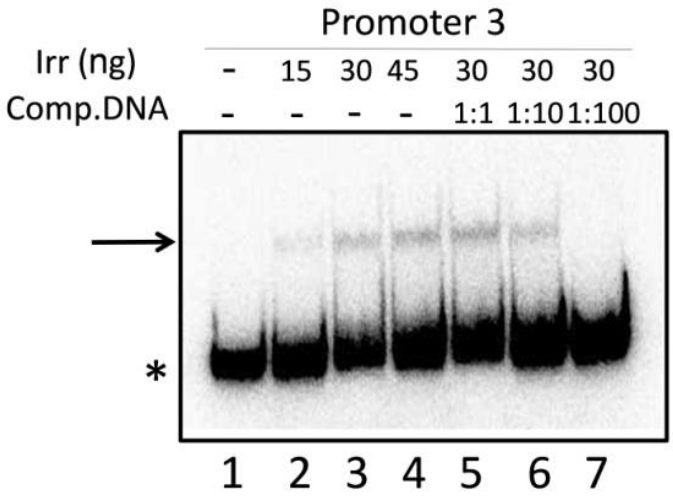

Fig. 4.24: Electrophoretic mobility shift assays testing the interaction of Irr to the P3 promoter region (190 bp fragment). The star labels the radiolabeled input DNA fragment, the arrow points to the shifted bands of the DNA protein complexes. The amount of the protein input is given for each lane and the molar ration of specific, unlabelled competitor DNA.

4.9.2.5 Effect of tBOOH on the activity of the promoters in Irr mutant

The β-galactosidase activities of the *isc-suf* sense and anti-sense promoters alone or in combination under microaerobic conditions were measured by the addition of tertiary butyl alcohol (tBOOH, final concentration: 100 μM) for exponentially growing cultures of the Irr mutant to analyse the influence of the oxidative stress (tertiary butyl alcohol). As shown in Fig. 4.25, the addition of tBOOH led to the significantly increased activities of some promoters after 30 min. Only P2 among all of single promoters fusion was affected by tBOOH after 30 min of the addition of tBOOH. Also

only P12 of the combined promoters had significant increase after 30 min of the addition of tBOOH. It is nearly consistent with the response of wild type to tBOOH (Fig. 4.10).

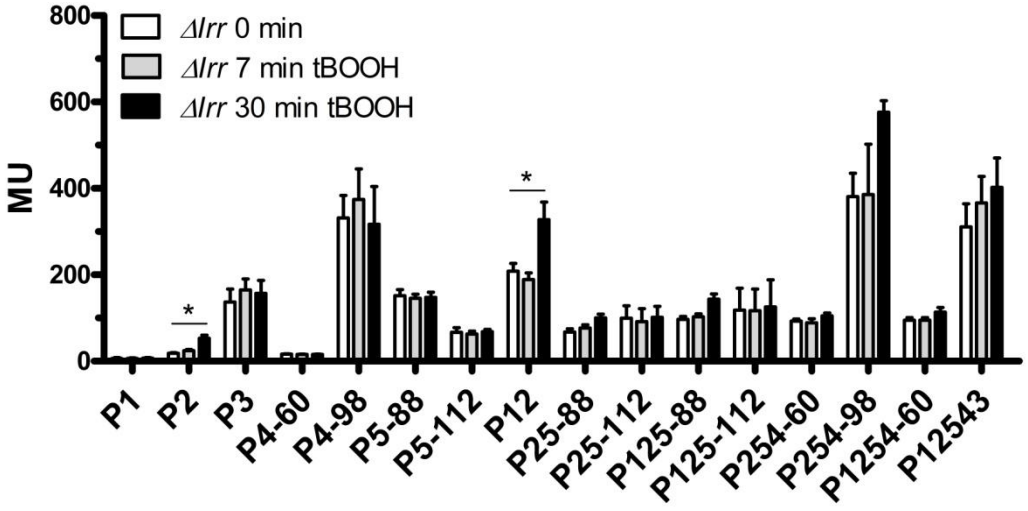

Fig. 4.25: The activity of single promoters and combined promoters as determined by *lacZ* reporter assays and quantified by measuring the β-galactosidase activity in Miller Units (MU). β-galactosidase activity was measured before, 7 min, and 30 min after addition of tBOOH (100 μM final concentration) to the Irr mutant. The bars represent the average of technical duplicates from biological tripliates and the standard deviation is indicated. *: the difference is > 1.5 fold with a p-value of < 0.01.

4.9.3 The effects of OxyR on the *isc-suf* promoters

OxyR is a known sensor for oxidative stress in *E. coli* and many other bacteria and acts as an activator of the *suf* operon (Lee *et al.*, 2004). Previous results suggested that OxyR also serves this function in *R. sphaeroides* and activates genes for iron metabolism in response to H_2O_2 and an effect of the OxyR regulator on *isc-suf* expression was observed (Zeller *et al.*, 2007).

4.9.3.1 Effect of iron availability on the activity of the promoters in OxyR mutant

The β-galactosidase activities of the *isc-suf* sense and anti-sense promoters alone or in combination under microaerobic conditions (iron-repletion) and under iron-depletion were measured together for exponentially growing cultures of wild type and OxyR mutant to analyse the influence of iron. As shown in Fig. 4.26, in all of the single promoters of the *isc-suf* operon, OxyR just had a small effect on P2 (1.6 folds) under iron depletion condition, and P5-112 had a significantly increased activity (about 3-4 folds) in the OxyR mutant compared to the wild type under iron repletion and

depletion condition. It implied that maybe the OxyR protein and P5-112 can interact. However, this effect on P5 activity was not present with only 88 bp upstream of the TSS of P5. Of all the combined promoters of the *isc-suf* operon, P25-112 and P125-112 showed a significantly decreased activity in the OxyR mutant under iron depletion condition. The reporter fusion harbouring P12543 had no significant difference, but showed about 1.4-fold increased activity under iron repletion in the OxyR mutant and similar activity under iron depletion in the wild type and OxyR mutant (Fig. 4.26).

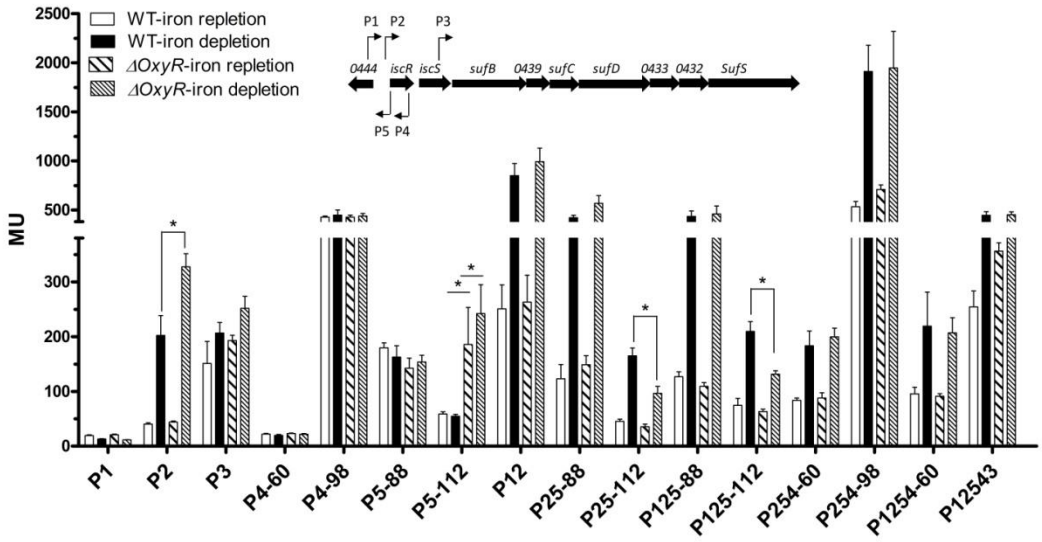

Fig. 4.26: The activity of single promoters and combined promote as determined by *lacZ* reporter assays and quantified by measuring the β-galactosidase activity in Miller Units (MU). β-galactosidase activity was compared for the wild type and the OxyR mutant under iron repletion and iron depletion. The bars represent the average of technical duplicates from biological tripliates and the standard deviation is indicated. *: the significant difference is > 1.5 fold with a p-value of < 0.01.

4.9.3.2 Gel mobility shift analysis with OxyR protein and promoter 5-112

Because P5-112 showed a strong increased activity in the OxyR mutant under iron repletion condition, the OxyR protein maybe bind the P5-112 each other. The gel mobility shift analysis with OxyR protein and P5-112 was performed to confirm whether OxyR is able to bind to P5-112 directly. As shown in Fig. 4.27, addition of increasing amounts of oxidized OxyR led to a shift of DNA fragment P5-112. Addition of an excess of the unlabeled specific competitor DNA fragments led to decrease of shift due to specific competition with the labeled fragments in EMSA assay. This result strongly supports that OxyR can indeed bind to the P5-112. The same result was

detected with reduced OxyR protein (Fig. 4.28).

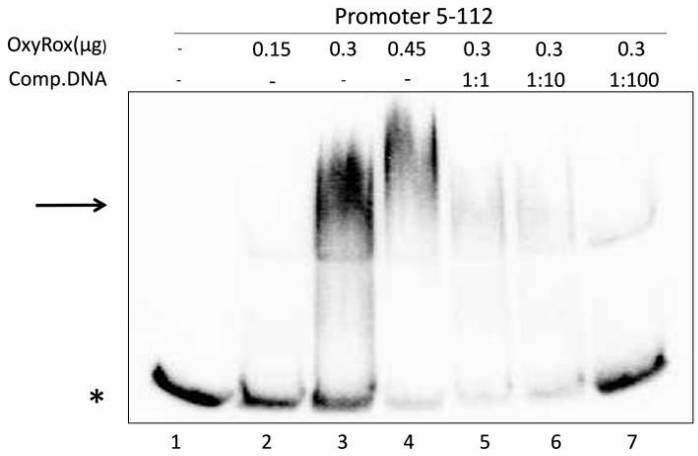

Fig. 4.27: Electrophoretic mobility shift assays showing the interaction of oxidized OxyR to the P5-112 promoter region (147 bp fragment). The star labels the radiolabeled input DNA fragment, the arrow points to the shifted bands of the DNA protein complexes. The amount of the protein input is given for each lane and the molar ration of specific, unlabelled competitor DNA.

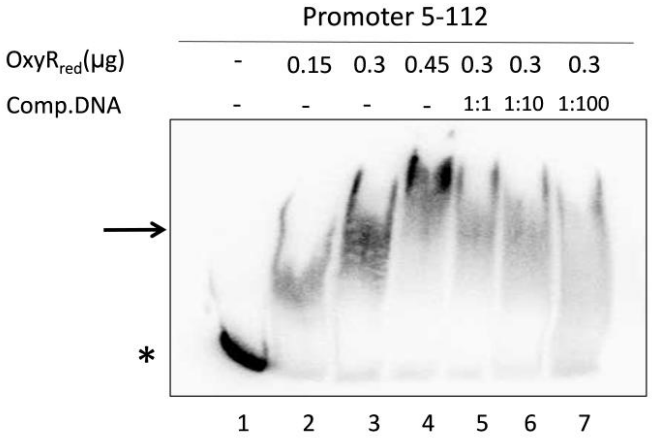

Fig. 4.28: Electrophoretic mobility shift assays showing the interaction of reduced OxyR to the P5-112 promoter region (147 bp fragment). The star labels the radiolabeled input DNA fragment, the arrow points to the shifted bands of the DNA protein complexes. The amount of the protein input is given for each lane and the molar ration of specific, unlabelled competitor DNA.

4.9.3.3 Gel mobility shift analysis with OxyR protein and promoter 5-88

Since P5-88 had no different activity in the OxyR mutant, another gel mobility shift analysis with OxyR protein and P5-88 was performed to distinguish which part of sequence is essential for the binding. As shown in Fig. 4.29, addition of increasing amounts of oxidized OxyR also resulted in a shift of DNA fragments P5-88. Addition of an excess of the unlabeled specific competitor DNA fragments led to decrease of shift due to specific competition with the labeled fragments in EMSA assay. This result

supports that OxyR can also bind to the P5-88. The same result was also detected with reduced OxyR protein (Fig. 4.30). It indicates that the difference of the sequence between P5-88 and P5-112 only affects the activity of fusions but no a specific binding to P5.

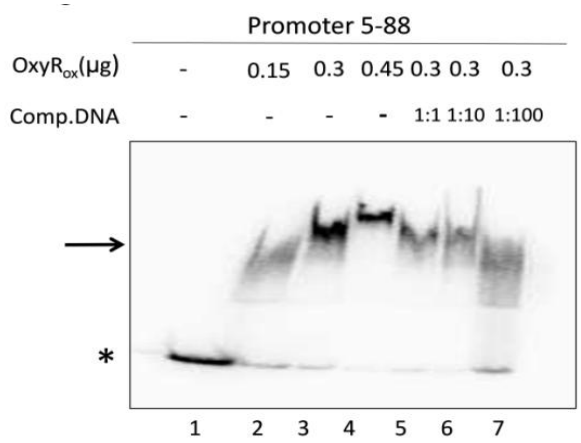

Fig. 4.29: Electrophoretic mobility shift assays showing the interaction of oxidized OxyR to the P5-88 promoter region (123 bp fragment). The star labels the radiolabeled input DNA fragment, the arrow points to the shifted bands of the DNA protein complexes. The amount of the protein input is given for each lane and the molar ration of specific, unlabelled competitor DNA.

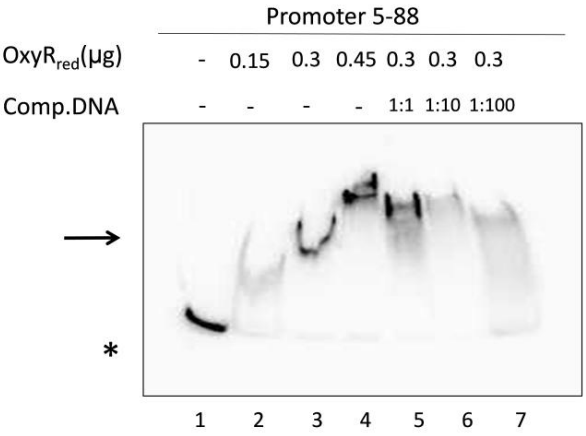

Fig. 4.30: Electrophoretic mobility shift assays showing the interaction of reduced OxyR to the P5-88 promoter region (123 bp fragment). The star labels the radiolabeled input DNA fragment, the arrow points to the shifted bands of the DNA protein complexes. The amount of the protein input is given for each lane and the molar ration of specific, unlabelled competitor DNA.

4.9.3.4 Effect of tBOOH on the activity of the promoters in the OxyR mutant

The β-galactosidase activities of the *isc-suf* sense and anti-sense promoters alone or in combination under microaerobic conditions were measured by the addition of tertiary butyl alcohol (tBOOH, final concentration: 100 μM) for exponentially growing cultures

of the OxyR mutant to analyse the influence of the oxidative stress (tertiary butyl alcohol). As shown in Fig. 4.31, the addition of tBOOH only led to the significantly increased activities of P2 after 30 min. It is nearly similar to the response of wild type to tBOOH (Fig. 4.10).

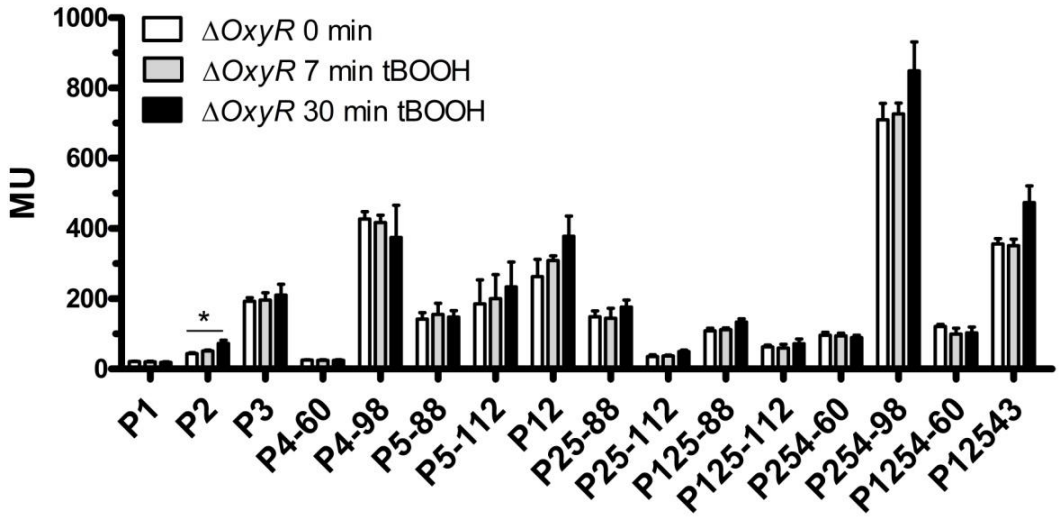

Fig. 4.31: The activity of single promoters and combined promoters as determined by *lacZ* reporter assays and quantified by measuring the β-galactosidase activity in Miller Units (MU). β-galactosidase activity was measured before, 7 min, and 30 min after addition of tBOOH (100 μM final concentration) to the OxyR mutant. The bars represent the average of technical duplicates from biological tripliates and the standard deviation is indicated. *: the difference is > 1.5 fold with a p-value of < 0.01.

4.9.4 The effects of Fur/Mur on the *isc-suf* promoters

Previous microarray analyses suggested a stronger effect of iron depletion on the *isc-suf* expression in a mutant lacking the Fur/Mur regulator. The Fur/Mur protein plays a major role in manganese-dependent regulation in *R. sphaeroides* but also show a significant impact on iron-dependent regulation (Peuser *et al.*, 2011).

4.9.4.1 Effect of iron availability on the activity of the promoters in the Fur/Mur mutant

The β-galactosidase activities of the *isc-suf* sense and anti-sense promoters alone or in combination under microaerobic conditions (iron-repletion) and under iron-depletion were measured together for exponentially growing cultures of wild type and Fur/Mur mutant to analyse the influence of iron. As shown in Fig. 4.32, of all of the single and combined promoters of the *isc-suf* operon, only P3 had a significantly decreased activity in the Fur/Mur mutant compared to the wild type under iron

depletion condition, but the decreased activity for P3 was slight (about 1.8-fold change) under iron depletion. All of the other changes were no more than 1.5-fold and/or statistically not significant. This indicates that only P3 maybe contribute to the decrease under iron depletion.

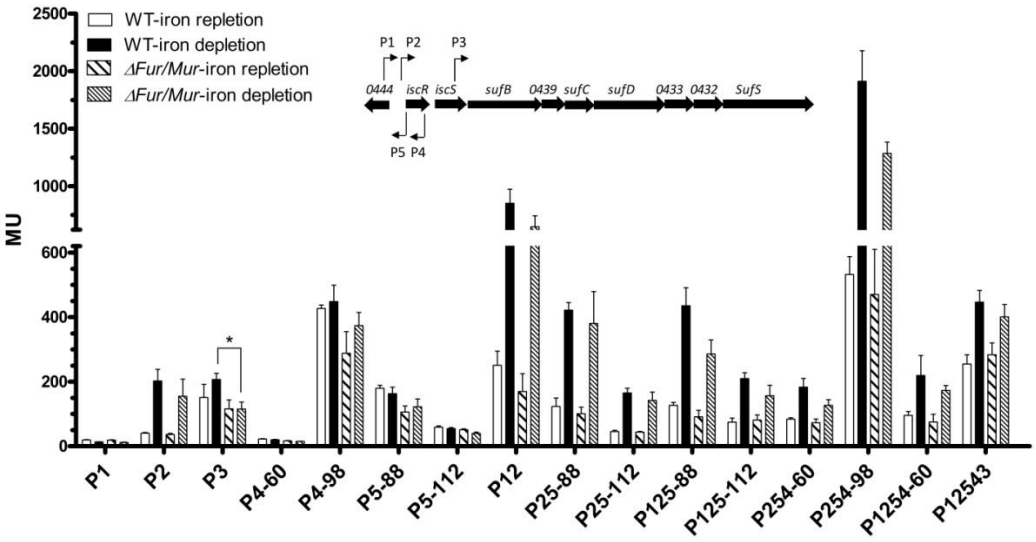

Fig. 4.32: The activity of single promoters and combined promote as determined by *lacZ* reporter assays and quantified by measuring the β-galactosidase activity in Miller Units (MU). β-galactosidase activity was compared for the wild type and the Fur/Mur mutant under iron repletion and iron depletion. The bars represent the average of technical duplicates from biological tripliates and the standard deviation is indicated. *: the significant difference is > 1.5 fold with a p-value of < 0.01.

4.9.4.2 Effect of tBOOH on the activity of the promoters in Fur/Mur mutant

The β-galactosidase activities of the *isc-suf* sense and anti-sense promoters alone or in combination under microaerobic conditions were measured by the addition of tertiary butyl alcohol (tBOOH, final concentration: 100 μM) for exponentially growing cultures of the Fur/Mur mutant to analyse the influence of the oxidative stress (tertiary butyl alcohol). As shown in Fig. 4.33, the addition of tBOOH only led to the significantly increased activities of P2 after 30 min. It is nearly similar to the response of wild type to tBOOH (Fig. 4.10).

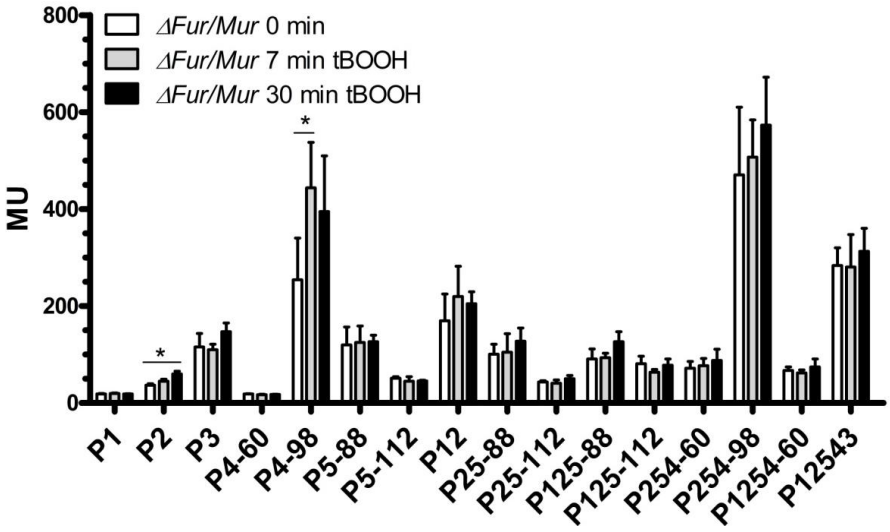

Fig. 4.33: The activity of single promoters and combined promoters as determined by *lacZ* reporter assays and quantified by measuring the β-galactosidase activity in Miller Units (MU). β-galactosidase activity was measured before, 7 min, and 30 min after addition of tBOOH (100 μM final concentration) to the Fur/Mur mutant. The bars represent the average of technical duplicates from biological tripliates and the standard deviation is indicated. *: the difference is > 1.5 fold with a p-value of < 0.01.

4.10 Interplay between formation of photosynthetic complexes and regulation of genes for Fe-S cluster assembly

4.10.1 Influence of growth conditions on the formation of photosynthetic complexes

The growth conditions strongly affect the amounts of the fomation of photosynthetic complexes in *R. sphaeroides*. The spectrum of the liquid cultures in the exponential growth phase was measured in the quartz cuvettes ranging from 350 to 950 nm. Fig. 4.34 showed the representative spectrum for wild type cultures grown under four conditions to the identical optical density.

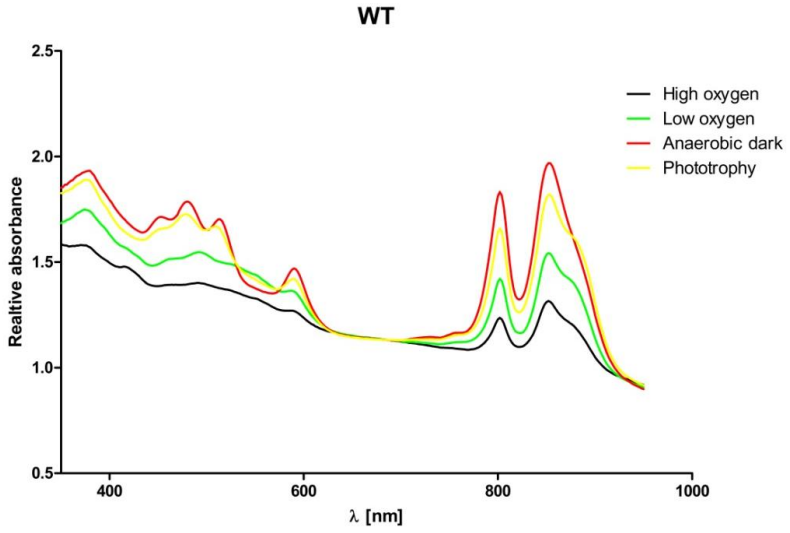

Fig. 4.34: Whole cells spectra from wild tpye cultures grown under different growth conditions. The same amount of cells was applied for each condition.

The formation of photosynthetic complexes was low under high oxygen condition. However, in the other three growth conditions, the formation of photosynthetic complexes was higher than under high oxygen condition. The highest amounts were detected under anaerobic dark conditions. Since photosynthetic complexes in high oxygen condition should not be synthesized, these pigments may be synthesized from low oxygen preculture. Both samples grown under anaerobic dark and phototrophy had a nearly similar absorption. These data suggested that the formation of high amounts of photosynthetic complexes under anaerobic conditions did not lead to transcriptional activation of *isc-suf* genes.

4.10.2 Influence of growth conditions on the concentration of pigments

The majority of bacteriochlorophyll and carotenoids are bound to the photosynthetic LHI/LHII complexes. The concentration of bacteriochlorophyll and carotenoids were measured after extraction.

The bacteriochlorophyll and carotenoids were synthesized at the lowest level in high oxygen condition. Similar to the spectrum of photosynthetic complexes, these detected pigments from the high oxygen condition may come from low oxygen preculture. The concentration of bacteriochlorophyll and carotenoids under all other conditions were higher than that in high oxygen condition. The highest amounts were detected in the anaerobic dark conditions (Fig. 4.35). These data revealed that the concentration of the pigments was consistent to the formation of high amounts of photosynthetic complexes in the same growth conditions.

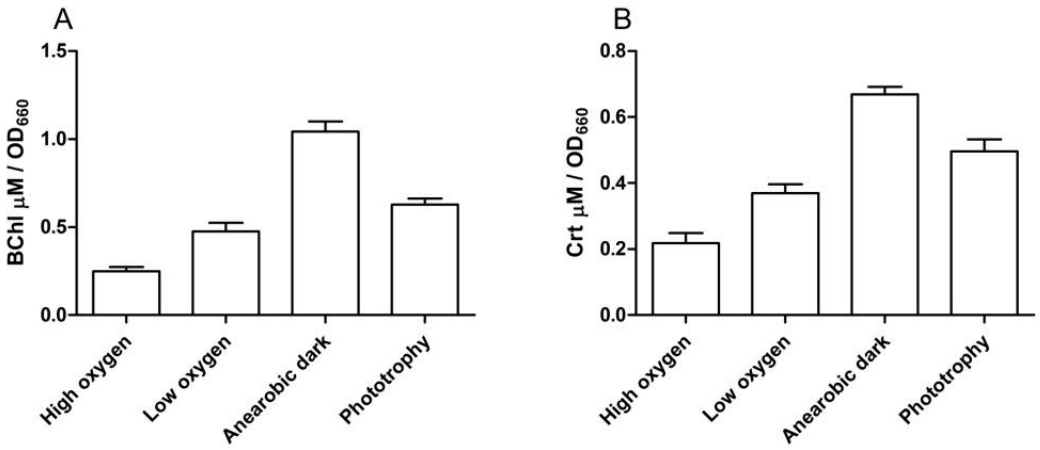

Fig. 4.35: The concentration of bacteriochlorophyll and the carotenoids in the wild tpye.

4.10.3 Influence of growth conditions on activity of the *isc-suf* promoters

Oxygen concentration strongly affects the amounts of photosynthetic complexes in *R. sphaeroides*. The formation of photosynthetic complexes requires much more Fe-S cluster. So we hypothesized that the expression of the *isc-suf* operon may be influenced by different oxygen tension. The activities of the promoters in the *isc-suf* operon in exponential phase cells from wild type (new) were measured under high oxygen, low oxygen, anaerobic growth in the dark with DMSO as terminal electron acceptor and anaerobic growth in the light (phototrophic growth 60W/m^{2}of light) to analyse the influence caused by the light and oxygen tension (Fig. 4.36).

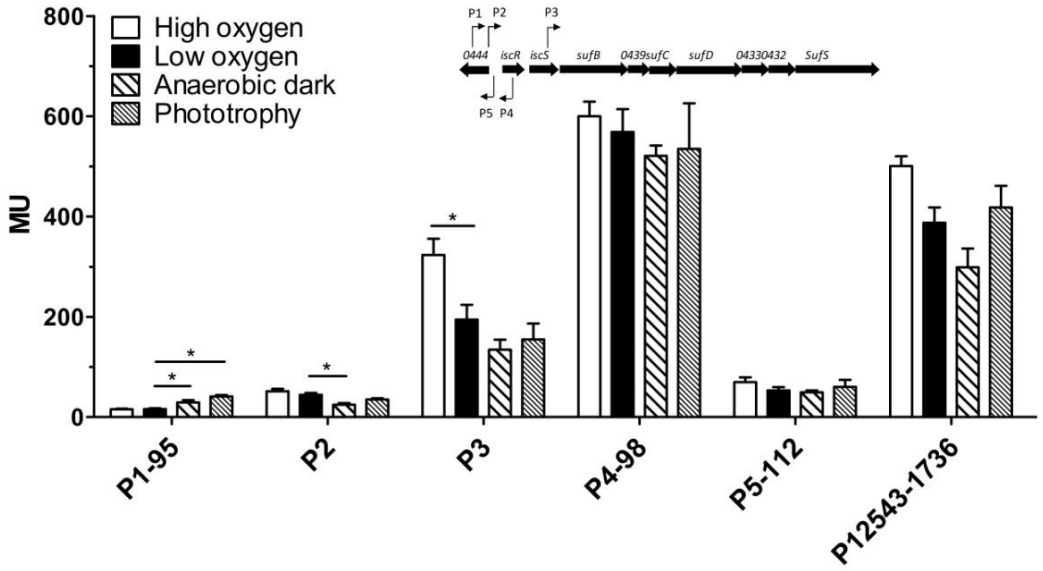

Fig. 4.36: The activity of single promoters and combined promoters as determined by *lacZ* reporter

assays and quantified by measuring the β-galactosidase activity in Miller Units (MU). β-galactosidase activity was measured in high oxygen, low oxygen, anaerobic dark and phototrophy to the wild type new. The bars represent the average of technical duplicates from biological tripliates and the standard deviation is indicated. *: the difference is > 1.5 fold with a p-value of < 0.01.

As shown in Fig. 4.36, of all the single promoters and P12543, only P1 that is the weakest one of the five promoters had a significantly increased activity in the wild type under anaerobic growth condition compared to low oxygen. There are no significant changes or slight decrease was measured under anaerobic growth conditions compared to aerobic growth in all the of the single promoters and P12543. Increased activity of P3 was measured under high oxygen, which was consistent with previous measurement (Fig. 4.8). However, there is no consistent with previous measurement, which P12543 was not activated. It was probably due to the shorter P1 (1736bp compared to 1777bp). The activities for anaerobic dark conditions were similar to phototrophic conditions in all measured promoters.

4.10.4 Influence of different mutants on the formation of photosynthetic complexes and the concentration of pigments

Most of the bacteriochlorophyll and carotenoids are bound to the LHI complexes (absorbance at 875 nm) and LHII complexes (absorbance at 800 and 850 nm). The amount of the LHI and LHII complexes is proportional to the concentration of the bacteriochlorophyll and carotenoids. Therefore, the spectrum of photosynthetic complexes and the concentration of the bacteriochlorophyll and carotenoids in the different mutants were measured to investigae the influence of different factors on the formation of photosynthetic complexes and the concentration of pigments.

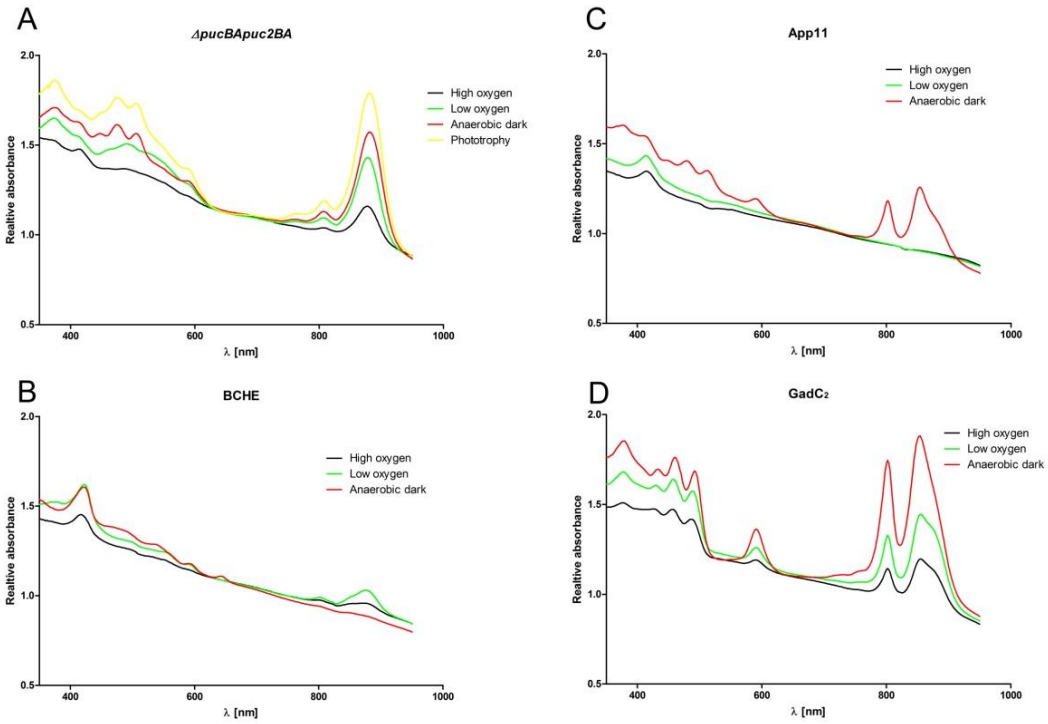

Fig. 4.37: Whole cell spectrum of different mutants under different growth conditions. The identical amount of cells was applied for the different strains and conditions. A: *ΔpucBApuc2BA*; B: BCHE; C: App11; D: Gadc2.

Both *pucBA and puc2BA* operons encode the LHII protein and have been deleted from the chromosome in the mutant *2.4.1ΔpucBApuc2BA.* Therefore, this mutant can only synthesize the reaction center (RC, absorbance at 803 nm) and LHI complex (absorbance at 875 nm). As a consequence, it contains less bacteriochlorphyll and carotenoids (Fig. 4.38) in the mutant *2.4.1ΔpucBApuc2BA* compared to the wild type.

The *bchE* encodes Mg-protoporphyrin IX monomethylester oxidative cyclase, which is one of the enzymes required for the synthesis of bacteriochlorphyll has been deleted in the mutant BCHE. Therefore, the mutant is unable to synthesize bacteriochlorophyll and consequently can not synthesize the photosynthetic complexes and thus can not grow photosynthetically (Fig. 4.37B and Fig. 4.38A).

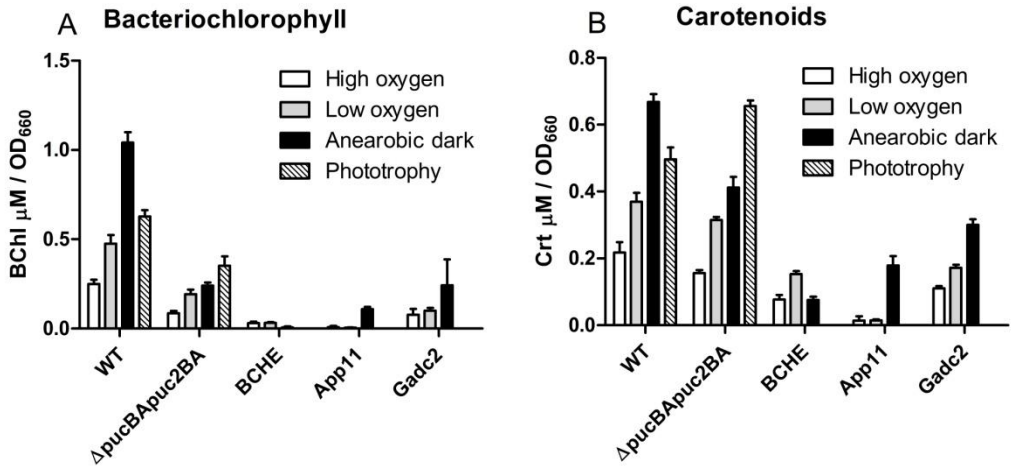

Fig. 4.38: The concentration of bacteriochlorophyll and carotenoids in different strains grown under different conditions. The bars represent the average of technical duplicates from biological tripliates and the standard deviation is indicated. A: bacteriochlorophyll; B: carotenoids.

The *appA* gene has been deleted in the mutant App11 which consequently can not form the anti-repressor AppA. The repressor PpsR is strongly activated to repress photosynthesis genes and the amounts of photosynthetic complexes (Fig. 4.37C and Fig. 4.38), since the anti-repressor AppA is not present. The mutant can not grow photosynthetically.

The *cycA* gene for cytochrome c2 has been deleted in the mutant Gadc2. The mutant is severely impeded in reducing the photo-oxidized reaction center and can not grow photosynthetically, but can form normal amounts of photosynthetic complexes (Fig. 4.37D and Fig. 4.38). Since the mutants BCHE, App11 and Gadc2 can not grow photosynthetically, phototrophic growth condition could not be used for all the measurements. Only wild type and the mutant *2.4.1ΔpucBApuc2BA* was used in the phototrophic growth condition.

4.10.5 Influence of different mutants on activity of the *isc-suf* promoters

The above data from wild tpye showed that in the different growth conditions not only the amounts of photosynthetic complexes, pigments and the activities of the *isc-suf* promoters changed, but also the amounts of photosynthetic complexes and pigments in the different mutants also changed. To further analyze whether formation

of photosynthetic complexes affects *isc-suf* promoters, the activities of *isc-suf* promoters were tested in selected mutants to compare the isogenic wild type in the identical growth conditions.

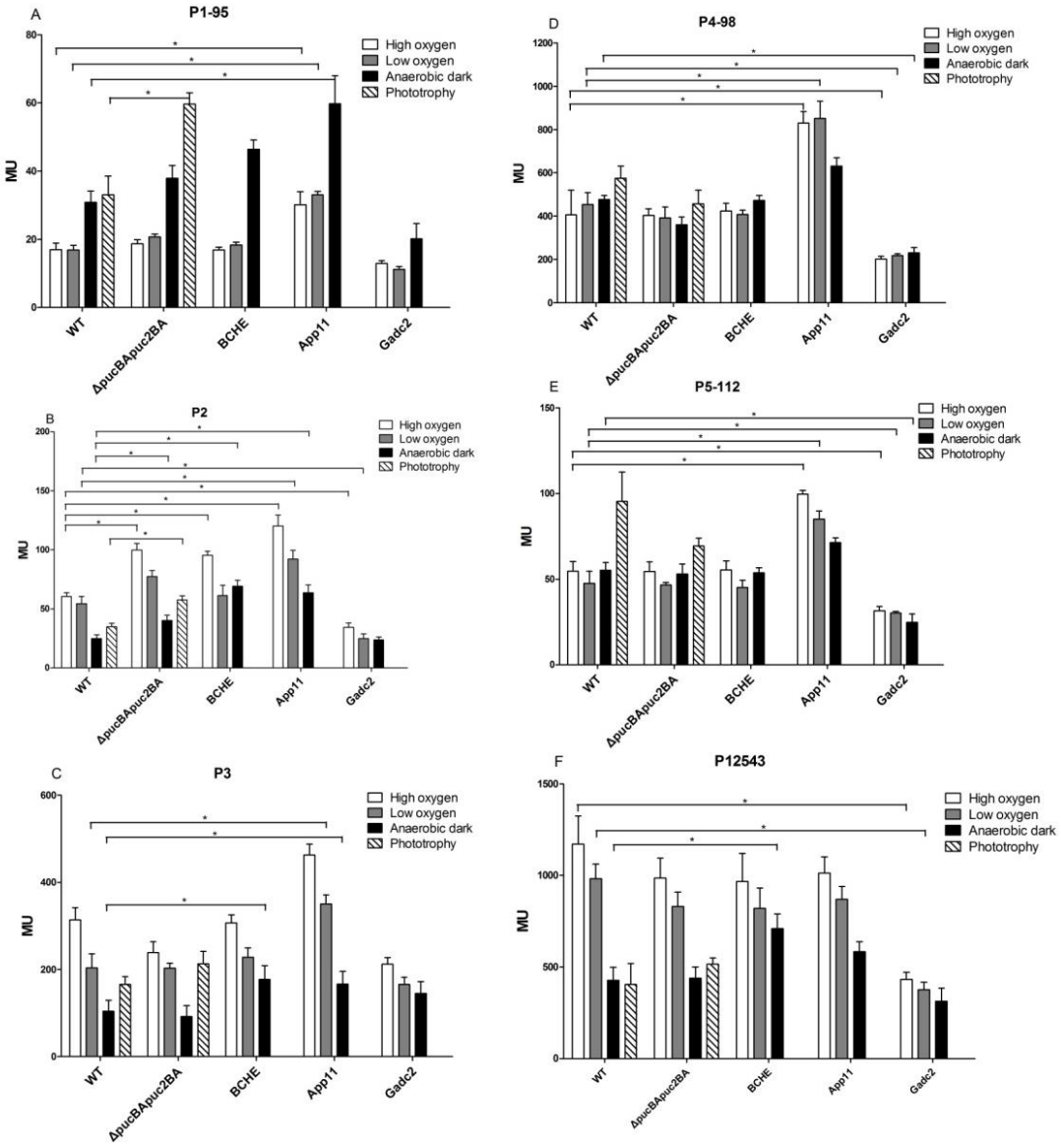

Fig. 4.39: Activity of the individual promoters and of P12543 as determined by *lacZ* reporter assays and quantified by measuring the ß-galactosidase activity in Miller Units (MU) in the wild type and mutant strains under four different conditions. ß-galactosidase activity was measured in high oxygen, low oxygen, anaerobic dark and phototrophy to the wild type and different mutants. The bars represent the average of technical duplicates from biological tripliates and the standard deviation is indicated. *: the difference is > 1.5 fold with a p-value of < 0.01.

Significant difference of P1 activities between the mutant 2.4.1Δ*pucBApuc2BA* and BCHE and the wild type in high oxygen or low oxygen conditions (Fig. 4.39A) was not observed, while it was slightly increased (maximal 1.5 fold) in these two

mutants in anaerobic dark condition and it was 1.8 fold increased in the mutant 2.4.1Δ*pucBApuc2BA* in phototrophic condition. However, P1 activity was reduced (about 1.5 fold) under all of the conditions in the mutant Gadc2 (lacking Cytc2). However, the activity was increased (1.8-2.0 fold) in all conditions in the mutant App11 (lacking *appA*) (Fig. 4.39A).

The activity of P2 had no significant difference or was slightly increased under all conditions for all the mutants except Gadc2, where the activity was reduced under high oxygen and low oxygen conditions and nearly same in the anaerobic dark condition compared to the wild type (Fig. 4.39B).

The activity of P3, P4, and P5 in the all conditions showed no significant difference between wild type and strains *2.4.1ΔpucBApuc2BA* and BCHE except the increased activity of P3 in mutant BCHE in the anaerobic dark condition (Fig. 4.39C-E). However, there were some significant difference for the mutants App11 and Gadc2. The activity of P3 initiating *suf* gene transcription was increased in App11 under low oxygen and anaerobic dark conditions (Fig. 4.39C). However, the activity of P4 and P5 that are anti-sense promoters was increased in App11 under high oxygen and low oxygen conditions but decreased in Gadc2 under all conditions (Fig. 4.39D-E).

The activity of all the promoters combined (P12543) of the *isc* operon was also measured (Fig. 4.39F). No significant differences were observed for this construct between the wild type and mutant *2.4.1ΔpucBApuc2BA*. The activity of P12543 in the mutant BCHE was higher than in the wild type in the anaerobic dark condition. However, the activity of P12543 in the mutant Gadc2 was strongly decreased in the presence of oxygen and absence of oxygen (Fig. 4.39F).

4.10.6 Effect of an *iscR* deletion on the activity of photosynthesis genes

IscR is a repressor of the *isc-suf* operon that encodes many genes related to the assembly of the Fe-S cluster in *R. sphaeroides* and many photosynthetic complexes contains the Fe-S cluster. In presence of light and oxygen, excitation of

bacteriochlorophyll causes photooxidative stress to damage the Fe-S cluster, but the carotenoids quench the singlet oxygen. A transcriptome study revealed that *suf* mRNA levels were slightly increased (about 1.5 fold) in the IscR mutant, but IscR had no influence on the expression of the photosynthesis genes (Remes *et al.*, 2015). Reduced amounts of photosynthetic complexes were however observed in this mutant through the spectrum of the photosynthetic apparatus (Fig.4.40). Therefore, real time RT-PCR was performed for selected genes related to the formation of the photosynthetic complexes and pigments in the IscR mutant, which is more sensitive than the microarrays.

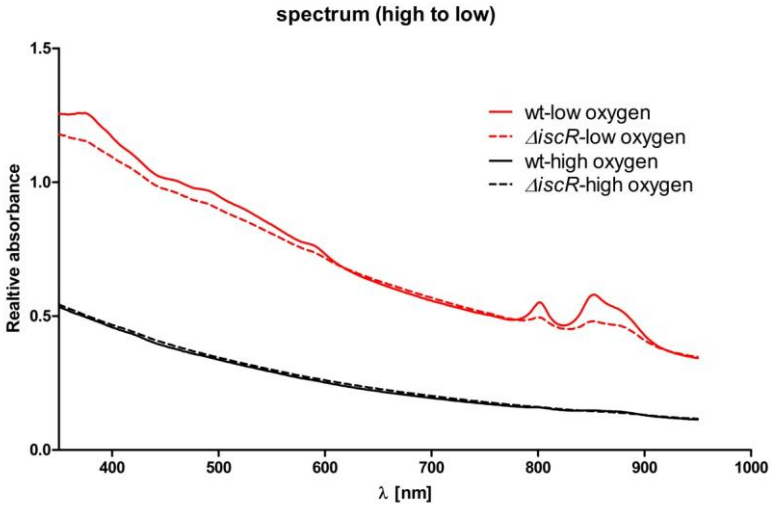

Fig. 4.40: The spectrum for the growth from high oxygen to low oxygen in the wild type and *iscR* mutant.

No significant differences were detected in the expression levels of photosynthesis genes and pigment genes between the IscR mutant and the wild type, which was consistent to previous microarray results (Fig.4.41). HemA catalyzes the synthesis of aminolevulinic acid, a precursor of protoporphyrin and HemP is a small hemin uptake protein not directly related to photosynthesis. The *hemP* (RSP_6006) mRNA level in both strains were quantified as a control for an IscR-dependent gene. The result was consistent to previous EMSA result that IscR could bind with the *hemP* promoter region (Remes *et al.*, 2015).

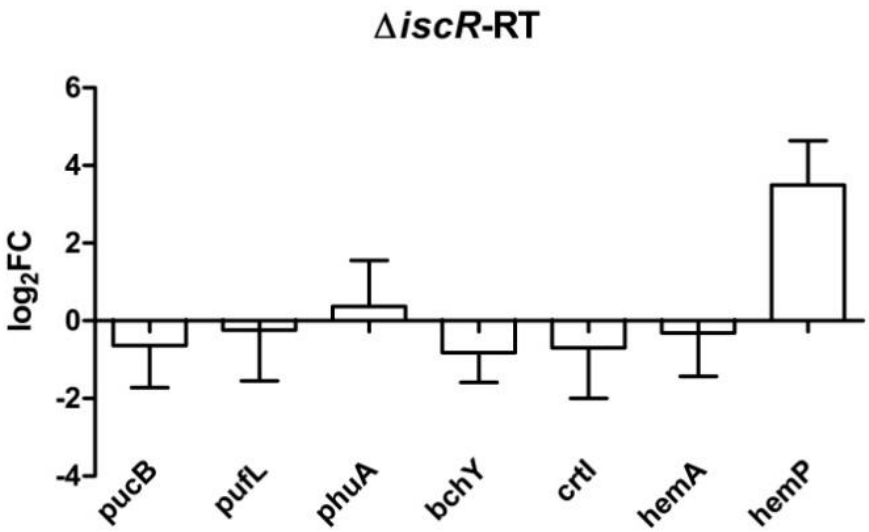

Fig. 4.41: The change of the level of photosynthetic complexes genes in the *iscR* deletion strain.

In summary, some differences were detected in the activity of the *isc-suf* promoters in the different mutants, but the amounts of photosynthetic complexes did not directly correlate with the activity. It is likely that coordination of the process occurs at post-transcriptional levels.

5 Discussion

Fe-S cluster is important components of many essential biological processes such as photosynthesis, respiration, N_2 fixation, gene regulation, oxygen transport, and DNA biosynthesis and so on. Consequently, the assembly of Fe-S cluster becomes an important cellular process in all living creatures. However, besides its beneficial functions, iron also has a threat to the cell from stress conditions as a source of ROS formation to destroy Fe-S cluster and consequently increase the need for Fe-S cluster assembly. In the present study, the facultative phototrophic bacterium *R. sphaeroides* was employed for the investigation of the assembly of Fe-S cluster.

5.1 The *isc-suf* operon in *R. sphaeroides*

R. sphaeroides is an excellent model organism for studying microbial photosynthesis. The facultative phototrophic bacterium is able to form high amounts of the photosynthetic complexes that need more additional Fe-S cluster for the synthesis of the $Cytbc_1$ complex and bacteriochlorophyll. However, bacteriochlorophyll can also cause photooxidative stress and thus destroy Fe-S cluster. So *R. sphaeroides* had to evolve some regulatory mechanisms to balance the damage and requirement of the assembly of Fe-S cluster.

The Isc system was identified as the main system for the regulation of the assembly of Fe-S cluster in most bacteria. *Rhodobacteracea* and *Rhizobiaceae* share some common features (Fig. 5.1), but it has been demonstrated that different species have their own regulatory mechanisms for the assembly of Fe-S cluster (Blanc *et al.*, 2015). In the model organism *E. coli*, the genes and proteins related to the assembly of Fe-S cluster are mainly encoded by the *isc* opreon and *suf* operon. However, different regulatory mechanisms may be present in *R. sphaeroides*. The synteny of *isc* and *suf* genes is conserved among *Rhodobacteracea* independently of the ability to perform photosynthesis and is also similar in *Rhizobiales* (Fig. 5.1). This suggests that the combined *isc-suf* operons arose early in evolution, in a common ancestor of these orders.

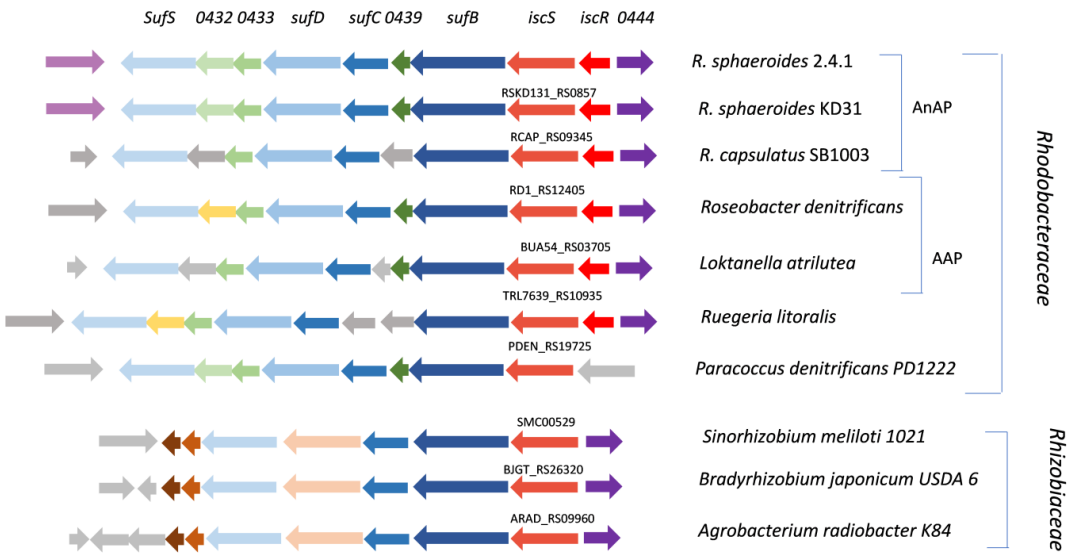

Fig. 5.1: Overview of the synteny of *suf* genes in selected bacterial genomes. All selected *suf* genes are annotated on the minus DNA strand and the figure displays the genome locations as displayed by genome browsers. Identical colors are used for the orthologs in different species. Grey color indicates no significant homology to the genes in the other species shown in the figure. AnAP: anaerobic anoxygenic phototrophs, AAP: aerobic anoxygenic phototrophs (Nie *et al.*, 2019).

5.1.1 The sense promoters of the *isc-suf* operon

As shown in Fig. 5.1, *R. sphaeroides* has an important operon called *isc-suf* operon for the assembly of the Fe-S cluster, which comprises *isc* and *suf* genes that are distributed to different operons in *E. coli*. In the *isc-suf* operon of *R. sphaeroides*, five promoters are predicted by dRNA-seq data: three sense promoters contributing to *isc-suf* transcription and two anti-sense promoters (Fig. 4.1), indicating a complex regulation at the transcriptional level.

The activities of the individual promoters and of the combinated promoters in the *isc-suf* operon were measured to verify their activities and to understand the contribution of the individual promoters and the interaction of the promoters, and the effect of oxygen, iron and oxidative stress on the activities by using reporter gene fusions. The results of the measurements showed that P1 was the weakest of the sense promoters and P3 was the strongest of the sense promoters. Both P1 and P2 together had a strong contribution to the expression of *isc-suf* operon (the activity of P12 was higher than P1 or P2) and P3 further contributed to the transcription of the *suf* genes. An extended upstream region of P3 including P1 and P2 further increased the activity and confered iron-dependent expression. Though the *isc-suf* operon is co-transcription,

a remotely additional promoter (P3) of the *isc-suf* operon for the *suf* genes may increase the higher expression of the required genes for the assembly of Fe-S cluster. The activity of P12543 was similar to P12 and was lower than P4-98 (P254-98). The P12543 fusion is the only reporter containing an intact copy of the *iscR* gene, which may lead to the increase of the amount of IscR in the cell.

Two cysteine desulfurases (IscS and SufS), the membrane component of an iron-regulated ABC transporter (SufB), the ATPase subunit of an ATPase transporter (SufC), an Fe-S cluster assembly protein (SufD), and two proteins of the Yip1 family (RSP_0433 and RSP_0432) that are encoded by the *isc-suf* operon locate in downstream of P3 (Fig.5.1). Both IscS and SufS are cysteine desulfurases that are required for the mobilization of sulfur from L-cystein. In *E. coli*, the role of the Suf system is exclusively restricted to the assembly of Fe−S cluster in the cell. SufS can not play the role of IscS in sulfur transfer for the formation of 2-thiouridine, 4-thiouridine, or the dithiolene group of molybdopterin (Buhning *et al.*, 2017). Since SufS may act as a main cysteine desulfurase that is encoded by downstream of P3 of the *isc-suf* operon, higher expression of the *iscS* may not be required. This arrangement with two cysteine desulfurases is conserved among *Rhodobacteraceae* and also found in *Rhizobiaceae* (Fig. 5.1). As known from previous data, the role of IscR in *R. sphaeroides* is as a transcriptional repressor for genes involved in iron metabolism by direct binding to the promoter region of genes preceded by a specific DNA-binding motif (Iron-Rhodo-box). Since IscR plays a regulatory function, the amount of the expression of the *iscR* gene may not be required in high amount.

The function of the upstream region of P3 is the regulation of the assembly of Fe-S cluster. However, the function of the downstream of P3 is for the expression of the components of the assembly of Fe-S cluster.

5.1.2 The anti-sense promoters of *isc-suf* operon

dRNA-seq data showed that there were two anti-sense promoters (P4 and P5) located in the downstream region of P2. P5 (promoter for RSP_0444, leading to a transcript anti-sense to the *iscR* promoter region) is closer to P2 and locates in the

upstream region of *iscR*. The gene product of RSP_0444 is annotated as a putative hydrolase, but no experimental data are available. RSP_0444 is also present on the chromosome in most of the *Rhodobacteraceae* and in *Rhizobiaceae*, but the upstream region of *iscS* has no *iscR* in *Rhizobiaceae* (Fig. 5.1). P4 locates within the *iscR* gene and leads to a transcript mostly anti-sense to the *iscR* mRNA. In this study the activity of P25 was higher than the activity of P2 initiating *iscR* transcrption, and the activity was even higher when P4 was present (P254-98). Both anti-sense promoter regions (P4 and P5) positively affected the transcription in sense direction. There are many kinds of anti-sense promoters in many different bacterial species and revealed remarkably different functions of the anti-sense transcripts (Yano *et al.*, 2010; Pernitzsch and Sharma, 2012; Sesto *et al.*, 2013). But in most cases, the anti-sense transcript decreases the expression of the sense transcripts. The transcription of the anti-sense normally produces some non-coding sRNAs that may interfere with translation and probably influence the stability of the sense mRNA. Anti-sense promoters may cause transcriptional interference by the reduction of the transcription or the attenuation of the transcription in sense direction (Bordoy and Chatterjee, 2015). So the anti-sense promoters are called "road blocks" for the transcription of the sense direction in synthetic biology (Bordoy and Chatterjee, 2015). Another possibility is that the anti-sense transcript base pairing with the sense transcript may form a new binding site for a double-strand specific endoribonuclease or may protect the RNA from the attack of a single-strand specific RNase. Only the latter case leads to the higher transcript levels in the sense promoters as observed in this study.

A global mapping of cleavage sites of the single-strand specific RNase E on the transcriptome was performed in *R. sphaeroides* (Forstner *et al.*, 2018). It indicated that the main 5′end coinciding with the TSS of P2 was reduced in a rne^{ts} mutant at the non-permissive temperature, indicating that this 5′end partially stemmed from the processing of the transcript initiating at P1 (Fig. 5.2). The anti-sense RNAs interferes with the cleavage by RNase E and lead to stabilization of the sense mRNAs in *Prochlorococcus* MED4 upon phage infection (Stazic *et al.*, 2011). The transcripts of the anti-sense initiating at P5 probably interferes with the cleavage of RNase E at the

P2 in this study.

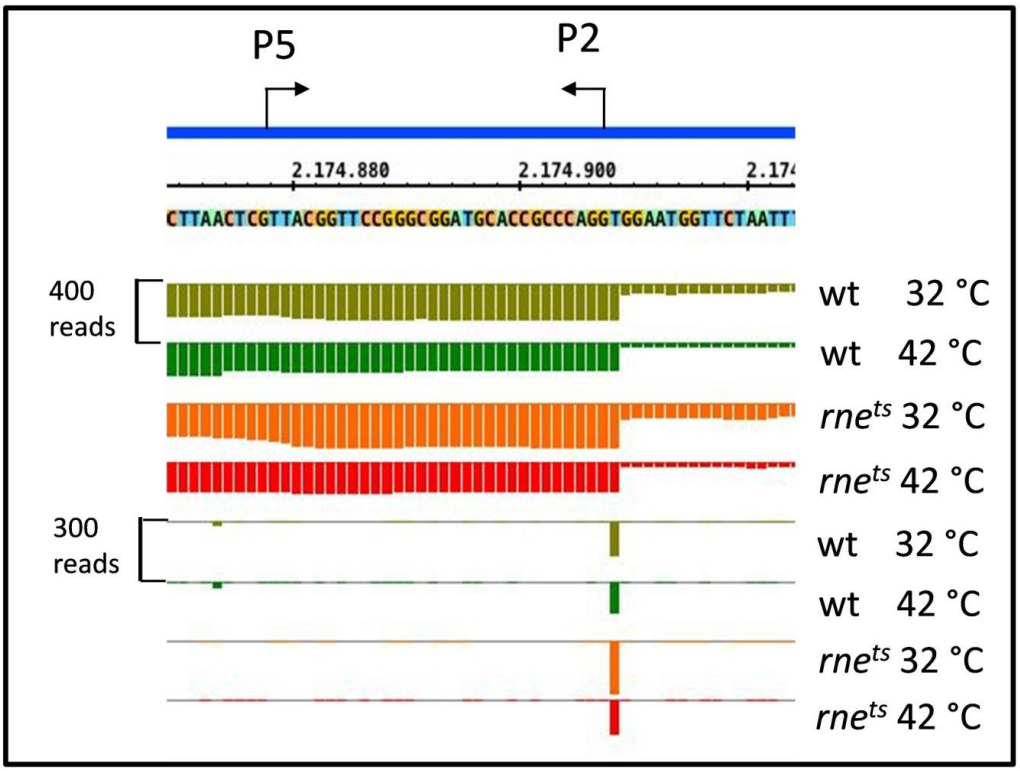

Fig. 5.2: RNA-seq reads as displayed by the Integrated Genome Browser in the P2 promoter region. RNA was isolated from the wild type strain 2.4.1 (wt) or from a derived strain harbouring a temperature-sensitive RNAse E due to a mutation in the *rne* gene. The upper panels show the total RNA reads and the lower panels show 5 ́ends (provided by G. Klug).

However, the increase of the amounts of anti-sense RNA to P2 stemming from another reporter plasmid does not influence the levels of the sense mRNA that is produced by P2 in this study. Based on the above fact, it is conceivable that the stabilization by the anti-sense RNA can only take place, when both sense and anti-sense RNA are produced in close proximity from the same template. It is imaged that the formation of an open complex for the initiation of transcription may also carry out more efficient transcription in the opposite direction. An effect of promoters on superhelicity-dependent processes is well documented (Beaucage *et al.*, 1991).

5.2 The regulation of the *isc-suf* operon by protein regulators

The expression of the *isc-suf* genes in *R. sphaeroides* that are dependent on the availability of iron and the application of hydrogen peroxide was revealed in previous work (Peuser *et al.*, 2011; Peuser *et al.*, 2012; Remes *et al.*, 2014; Remes *et al.*, 2015).

OxyR, Fur/Mur, Irr, and IscR regulators play important roles in the expression of the *isc-suf* operon (Table 5.1).

RSP	+/-H_2O_2 Wt	+/-H_2O_2 Δ*oxyR*	+/- Fe microaerobic wt	+/-Fe Δ*fur/mur*	+/- Fe Δ*irr*	+/- Fe Δ*iscR*	+ Fe Δ*irr*/wt	+ Fe Δ*iscR*/wt	+/- Fe anoxic
0444	- 1.4	- 1.4	1.1	1.5	1.7	- 1.7	1.0	1.1	- 1.7
iscR/0443	11.2	9.2	1.8	3.1	4.7	- 2.2	- 1.6	1.6	- 2.2
iscS/0442	9.4	6.7	1.6	2.7	3.9	- 2.0	?	1.9	- 2.0
sufB/0440	10.0	5.1	1.6	2.1	3.7	1.6	1.7	1.4	1.6
0439	8.1	3.5	1.8	3.3	3.4	1.6	1.5	1.4	1.6
sufC/0437	8.3	1.9	1.9	3.8	4.3	1.6	1.4	1.4	1.6
sufD/0434	3.6	- 1.4	2.5	3.9	4.3	1.5	1.4	1.5	1.5
0433	1.1	- 2.4	2.1	2.9	4.1	1.3	1.0		1.0
0432	- 1.2	- 2.5	1.7	2.2	3.6	1.1	?		1.1
sufS/0431	- 2.1	- 3.2	1.7	2.1	2.9	1.0	?		1.1

Table 5.1: Effect of hydrogen peroxide or iron availability on the expression of genes of the *isc-suf* operon and on RSP_0444. All data are stemmed from previously pubished microarray analysis (Klug *et al.*, 1997; Peuser *et al.*, 2011; Peuser *et al.*, 2012; Remes *et al.*, 2014; Remes *et al.*, 2015; Remes *et al.*, 2017). The fold changes between the two conditions or two strains as indicated by the heading of each column are given (provided by G. Klug).

5.2.1 The regulation of the *isc-suf* operon by Fur/Mur

In *E. coli*, the iron regulator Fur palys an important role of in the expression of the *iscR* and *suf* operon (Roche *et al.*, 2013) (Fig. 1.3). Fur-Fe^{2+} acts as a repressor to bind with the *suf* promoter and represses the transcription of the series of *suf* genes (Lee *et al.*, 2008) . It also can repress the transcription of the sRNA rhyB (Masse *et al.*, 2007), which base pairs with the Shine-Dalgarno (SD) sequence of *iscR* mRNA resulting in the degradation of the 3´ part of the *isc* operon mRNA and the stabilization of the 5´part including the *isc* coding region (Desnoyers *et al.*, 2009). However, in iron limitation condition or other oxidative stresses, Fur repression is released and the sRNA *ryhB* is expressed, which leads to the activation of the *suf*

operon. Meanwhile, the formation of apo-IscR further increased the expression of *suf* genes. Thus the Fur promotes a switch from the Isc to the Suf system.

However, iron-dependent regulation in alpha-proteobacteria mainly occurs by other regulators that are different from Fur (Johnston *et al.*, 2007; Peuser *et al.*, 2011). Many genes that are dependent on iron have a stronger expression in the Fur mutant of *R. sphaeroides* (Peuser *et al.*, 2011), which indicates that Fur/Mur plays a role in the regulation of the iron metabolism and is involved in repressing the related genes under iron depletion. In this study, there was a weak influence (1.8-fold change) on the activity of P3 in iron depletion of the mutant Fur/Mur, indicating that Fur/Mur had an activating function in iron depletion. The analyse of the sequences in the vicinity of P3 of the *isc-suf* operon indicated that there was no similar Fur/Mur box to the *sitA* promoter. The weak effect of Fur/Mur on many genes and P3 related to the iron metabolism indicated that the regulation of Fur/Mur on the P3 of the *isc-suf* operon was indirect.

5.2.2 The regulation of the *isc-suf* operon by IscR

An IscR box was predicted in the P2 promoter region (Rodionov *et al.*, 2006), and the influence of the regulator IscR on the expression of *isc-suf* operon was investigated in previous work (Remes *et al.*, 2015). In this study, the activity of P2 was indeed influenced by IscR. Furthermore, the activity of P2 under iron depletion condition and under the oxidative stress by tBOOH was dependent on IscR. Thus, the regulator IscR in *R. sphaeroides* play a role as the sensor for iron availability and organic peroxide stress. IscR can bind to the *iscR* promoter (P2), which was confirmed in previous study (Remes *et al.*, 2015). In this study, the activity of P1 under iron depletion and the activity of P3 under iron repletion and depletion were also influfenced by IscR and the binding of IscR to P1 and P3 with similarity to the IscR box was also confirmed in the gel mobility shift analysis *in vitro*. However, it was different from P2, because the activities of P1 and P3 were independent of IscR under the oxidative stress by tBOOH, even though IscR can bind to P1 or P3. It is possibly similar to *E. coli* with two types of IscR binding sites, Type 1 and Type 2. In *E. coli*, Holo-IscR (containing the Fe-S cluster)

showed stronger affinity to Type1 sites than apo-IscR (without the Fe-S cluster), while the two forms of IscR possessed similar affinities to bind to Type 2 sites (Giel *et al.*, 2006). This kind of the regulatory mechanism was even present in the Gram-positive *Thermincola potens* (Santos *et al.*, 2014). Holo-IscR strongly repressed the activity of P2 and all the combined promoter with P2 in this study. However, the repressing effect of IscR on the activity of P3 disappeared when all of the upstream promoters were present. The reason may be that the upstream regulatory elements also influenced P3 or the P12543 reporter carring a complete copy of *isc*R produced more IscR to further repress the activity of P12543.

5.2.3 The regulation of the *isc-suf* operon by Irr

An Irr box was also predicted in the P2 promoter region (Rodionov *et al.*, 2006), and the influence of the regulators Irr on the gene expression was investigated in a previous work (Peuser *et al.*, 2012). An Irr box is present around P2 and a minor significant difference of P2 (1.8-fold) was indeed detected in the Irr mutant compared to wild type. However, the binding of Irr to P2 was not detected in the gel mobility shift analysis *in vitro*. A minor significant difference of P1 (1.5-fold) was also detected in the Irr mutant under iron repletion. Meanwhile, it was similar to P2 that the binding of Irr to P1 was not detected in the gel mobility shift analysis *in vitro*. The above results implied that Irr did not play a major role in the regulation of P1 and P2 under the tested conditions and suggested that the influence of Irr on P1 and P2 was indirect. Surprisingly, a more significant influence of Irr on P3 that was detected when all upstream promoters were included under iron depletion. Since the P12543 reporter carries a complete copy of *isc*R, the increase of the activity of P3 in this strain possibly came from the elevated levels of IscR or stronger interaction between Irr and P3 under iron depletion. Higher IscR levels could increase the effect of iron in the Irr mutant. However, the binding of Irr to an Irr box in the P3 region *in vitro* proved that the influence of Irr on the activity of P3 was direct.

5.2.4 The regulation of the *isc-suf* operon by OxyR

The influences of OxyR on iron-dependent and oxidative stress-dependent in the

iron metabolism was demonstrated in previous work (Zeller *et al*. 2005; Zeller *et al*. 2007; Remes *et al*. 2014). The activity of P5 was strongly increased in the OxyR mutant and the binding of both OxyR types to P5 was further confirmed in the gel mobility shift analysis *in vitro*. The activity of P5 with 112 nt of upstream region was dependent on the the repressing effect of OxyR, while the activity of P5 with 88 nt of upstream region was independent of OxyR. But the fragments including 112 nt or 88 nt upstream of P5 could bind to reduced and oxidatived OxyR, indicating that the difference of the activity for P5-88 and P5-112 was not due to the binding of OxyR. However, the effect of P5-88 on P2 (P25-88/P125-88) activity was similar in the wild type and the OxyR mutant. However, the repressing effect of OxyR was only observed for the P5 promoter but was not observed in the P254, P1254 or P12543 fusions. Therefore, the effect of OxyR on the expression of *isc-suf* was not due to the the binding of OxyR to the P5 region. The expression of RSP_0444 could be affected by the binding of OxyR to P5, since P5 is the promoter for initiating RSP_0444. However, previous microarray studies revealed that the expression of RSP_0444 was independent on the hydrogen peroxide and OxyR (Table 5.1) (Zeller *et al.*, 2005; Zeller *et al.*, 2007). In most known cases, OxyR plays a role as activator for gene expression under oxidative stress. However, repressor function of OxyR under non-stress condition was also reported in *R. sphaeroides* (Zeller *et al.*, 2007) .

RirA protein was confirmed to play an important role in the iron regulation in *Rhizobia* (Imam *et al.*, 2014). The genes RSP_2888 and RSP_3341 of *R. sphaeroides* have 59-63% identity to *rirA* from *Rhizobium leguminosarum* or *Agrobacterium tumefaciens* (*Rhizobium radiobacter*). However, the double RirA homologues of *R. sphaeroides* play no major role in the oxidative stress and iron-dependent regulation of the *isc-suf* operon.

These above results are described in a model (Fig. 5.3) that visualizes the complex regulatory network regulating the expression of *isc-suf* in *R. sphaeroides*.

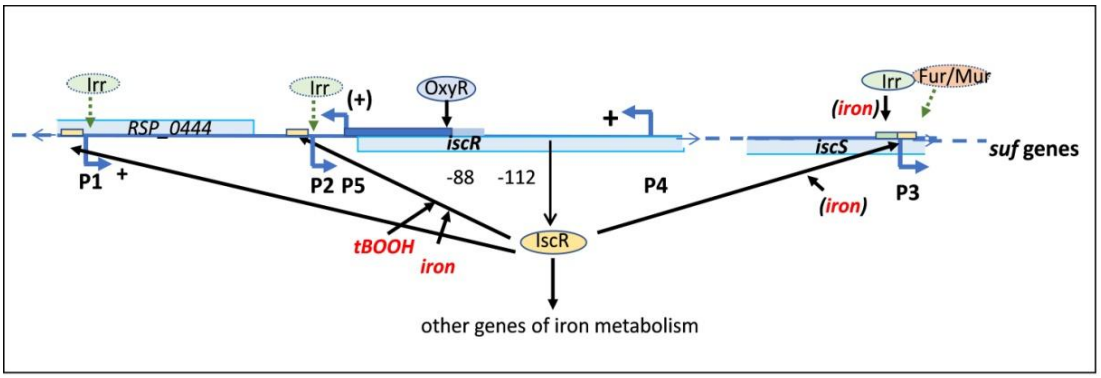

Fig. 5.3: Schematic model combining the influence of other promoters on P2 and the action of different proteins on the activity of the *isc-suf* promoters. + indicates a stimulating effect of P1, P4 and P5 (dependent on length of upstream region) on P2 activity. The IscR protein binds to IscR boxes (yellow bars) in the promoter regions of P1 and P2 and P3, OxyR binds to upstream of the P5 promoter (indicated by solid arrows), and Irr binds to an Irr-box (green bar) in the P3 promoter region. At P2 IscR mediates the response to iron and tBOOH. Iron-dependent actvity of P3 is only observed in absence of IscR or the absence of Irr. Green arrows indicate activation by the protein regulators, black arrows repression. The small effects of Irr on P1 and P2 and of Fur/Mur on P3 are most likely indirect and do not involve direct binding (indicated by dashed arrows) (Nie *et al.*, 2019).

5.3 Interplay between photosynthetic complexes and Fe-S cluster assembly

The formation of photosynthetic complexes in *R. sphaeroides* demands the higher amount of Fe-S cluster under phototrophic conditions and the *isc-suf* operon regulates the assembly of Fe-S cluster. Therefore, there was a hypothesis that the amounts of photosynthetic complexes affect *isc-suf* operon expression or vice versa (Fig. 5.4). It is imaged that the high demand of photosynthetic complexes for Fe-S cluster leads to high expression of *isc-suf* operon for Fe-S cluster synthesis, which results in producing a lower amount of the holo-IscR repressor and subsequently causes less repression of IscR-dependent promoters. However, our results showed that higher amounts of photosynthetic complexes in the wild type under anaerobic dark condition or phototrophy have no effects on the activity of the *isc-suf* promoters except P1 and P2. Only the activity of the weak P1 in low oxygen was higher under anaerobic conditions, while the activity of P2 that was strongly dependent on IscR (Remes *et al.*, 2014; Nie *et al.*, 2019) was reduced under anaerobic dark condition when the production of photosynthetic complexes was highest. Conversely, the activity of P2 in the mutants with reduced amounts of photosynthetic complexes was

elevated. Nevertheless, the activity of P2 in all these mutants was higher in presence of oxygen with less amounts of photosynthetic complexes than that under anaerobic conditions with higher production of photosynthetic complexes. The above results excluded a direct correlation of the amounts of photosynthetic complexes and the activity of the *isc-suf* promoters.

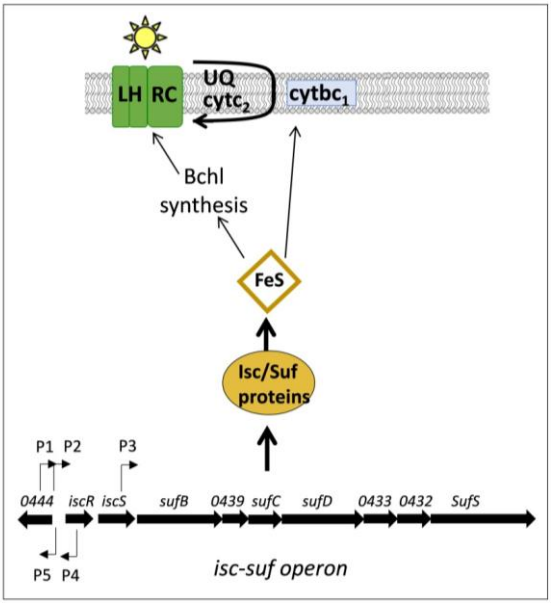

Fig. 5.4: Interplay between the protein products of the *isc-suf* operon of *R. sphaeroides* and the formation of photosynthetic complexes (provided by G. Klug).

In the App11 mutant, the activities of all the promoters were increased by different levels besides P2. However, the amount of photosynthetic complexes was very low. This mutant lacks the anti-repressor AppA, an important redox- and light-dependent regulator that affects all genes of the PpsR regulator including genes for the PpaA and PrrA regulators (Imam *et al.*, 2015). PrrA not only regulates the photosynthesis genes, but also targetes many other genes (Imam *et al.*, 2014). Thus, the deficiency of AppA not only drastically reduces the amounts of photosynthetic complexes, but also may cause the observed effect on *isc-suf* promoters. The Gadc2 mutant lacking cytochrom c2 can not perform photosynthetic electron transport to the photo-oxidized reaction center, but the strongest effect on the activities of *isc-suf* promoter appears under all the conditions in the Gadc2 mutant. The Gadc2 mutant results in the reduction for the activity of all promoters in presence of oxygen and the reduction of the activities for P1, P4, P5 and P12543 under anaerobic dark condition,

in addition to the reduction of the amounts of photosynthetic complexes. Though no photosynthetic electron transport takes place in presence of oxygen and under anaerobic dark condition, Cytc2 can still contribute to the respiratory electron transport. Therefore, the effects of the mutation on the activities *of isc-suf* promoter and the amounts of photosynthetic complexes may be caused by altered respiratory electron transport.

The above results demonstrate that formation of photosynthetic complexes does not result in a significant changes of the activities of the *isc-suf* promoters. The increase of the assembly of Fe-S cluster under low oxygen or anaerobic conditions may be due to post-transcriptional regulatory mechanisms. Although only the weakest P1 has a significant increase under anaerobic conditions, a significant higher amount of *isc-suf* mRNAs synthesized under anaerobic dark condition than that under microaerobic conditions in the presence of iron was detected by RNAseq. This strongly suggested additional regulation maybe at level of RNA stability or at protein level. However, the level of *isc-suf* mRNA was not increased under anaerobic conditions in the absence of iron, and had no effects on oxygen and iron for RSP_0444 downstream genes that are transcribed from P5 (Remes et al., 2014). The reduction of the level of *iscS* mRNA and slightly higher level of suf mRNA were observed in the IscR mutant (Remes *et al.*, 2015) and the reduction of formation of photosynthetic complexes upon a drop of oxygen tension was detected in the IscR mutant in this study. These results indicate a certain relation between the Isc system and formation of photosynthetic complex. However, our data showed that this effect is not due to altered levels of photosynthetic mRNAs. The reduction of formation of photosynthetic complexes in the IscR mutant was possibly affected by the impaired formation of Fe-S cluste leading to the reduced expression of whole *isc-suf* operon.

In conclusion, the coordination of the amounts of photosynthetic complexes and *isc-suf* operon expression may occur at the level of post-transcriptional rather than the transcriptional level.

6 Summary

Fe-S proteins are present in all organisms and play many essential roles, but different kinds of stresses can destroy Fe-S cluster. *R. sphaeroides* is able to form photosynthetic complexes, which need more additional Fe-S cluster for the synthesis of the $Cytbc_1$ complex and of bacteriochlorophyll. So *R. sphaeroides* had to develop some regulatory mechanisms to balance the damage and requirement of the assembly of Fe-S cluster.

The *isc-suf* operon was identified as an important system for the regulation of Fe-S cluster assembly in *R. sphaeroides*. The results of this study show that three sense promoters contributed to the transcription of *isc-suf* (P1 and P2 together allowed higher transcription rates of *isc-suf* than P2 alone) and two anti-sense promoters influenced sense promoters transcription (P4 and P5 stimulated P2 activity). The iron-dependent regulators (Irr, IscR, Fur/Mur, RirA) and oxidative stress-dependent regulator (OxyR) play important roles in the expression of the *isc-suf* operon. The regulator IscR of *R. sphaeroides* plays a role as sensor for iron availability and organic peroxide stress (tBOOH) by bindings to P1, P2 and P3. The influences of Fur/Mur on the *isc-suf* operon were most likely indirect. Similarly, Irr influenced the P1 and P2 activities indirectly. However, direct binding of Irr to P3 was demonstrated. The activity of P5 was strongly increased in the OxyR mutant and the bindings of OxyR to P5 was demonstrated, indicating a repressing function of OxyR on P5 activity in *R. sphaeroides*. However, the two RirA homologues of *R. sphaeroides* play no major role in the oxidative stress and iron-dependent regulation of the *isc-suf* operon. These results demonstrate that a complex regulatory network of iron-sulfur cluster assembly is present in *R. sphaeroides*. The formation of photosynthetic complexes did not result in significant changes in the activities of the *isc-suf* promoters. The increase of the assembly of Fe-S cluster under low oxygen or anaerobic conditions was probably due to post-transcriptional regulatory mechanisms rather than the regulation of transcriptional level.

7 References

Adrait, A., Jacquamet, L., Le Pape, L., Gonzalez de Peredo, A., Aberdam, D., Hazemann, J.L., Latour, J.M. and Michaud-Soret, I. (1999) Spectroscopic and saturation magnetization properties of the manganese- and cobalt-substituted Fur (ferric uptake regulation) protein from *Escherichia coli*. *Biochemistry* **38**: 6248-6260.

Althaus, E.W., Outten, C.E., Olson, K.E., Cao, H. and O'Halloran, T.V. (1999) The ferric uptake regulation (Fur) repressor is a zinc metalloprotein. *Biochemistry* **38**: 6559-6569.

Amarelle, V., Koziol, U. and Fabiano, E. (2019) Highly conserved nucleotide motifs present in the 5'UTR of the heme-receptor gene *shmR* are required for HmuP-dependent expression of *shmR* in *Ensifer meliloti*. *Biometals* **32**: 273-291.

Amarelle, V., Rosconi, F., Lazaro-Martinez, J.M., Buldain, G., Noya, F., O'Brian, M.R. and Fabiano, E. (2016) HmuS and HmuQ of *Ensifer/Sinorhizobium meliloti* degrade heme *in vitro* and participate in heme metabolism *in vivo*. *Biometals* **29**: 333-347.

Andre, G., Haudecoeur, E., Courtois, E., Monot, M., Dupuy, B., Rodionov, D.A. and Martin-Verstraete, I. (2017) Cpe1786/IscR of Clostridium perfringens represses expression of genes involved in Fe-S cluster biogenesis. *Res Microbiol* **168**: 345-355.

Andreini, C., Rosato, A. and Banci, L. (2017) The Relationship between environmental dioxygen and iron-sulfur proteins explored at the genome level. *PLoS One* **12**: e0171279.

Andrews, S.C., Robinson, A.K. and Rodriguez-Quinones, F. (2003) Bacterial iron homeostasis. *FEMS Microbiol Rev* **27**: 215-237.

Angelini, S., Gerez, C., Ollagnier-de Choudens, S., Sanakis, Y., Fontecave, M., Barras, F. and Py, B. (2008) NfuA, a new factor required for maturing Fe/S proteins in *Escherichia coli* under oxidative stress and iron starvation conditions. *J Biol Chem* **283**: 14084-14091.

Aranzaes, J.R., Belin, C. and Astruc, D. (2007) Assembly between gold-thiolate nanoparticles and the organometallic cluster $[Fe(eta_5\text{-}C_5H_5)(mu_3\text{-}CO)]_4$ toward redox sensing of oxo-anions. *Chem Commun (Camb)*: 3456-3458.

Arisaka, S., Sukigara, H. and Osanai, T. (2018) Genetic manipulation to overexpress *rpaA* altered photosynthetic electron transport in *Synechocystis sp*. PCC 6803. *J Biosci Bioeng* **126**: 139-144.

Bagg, A. and Neilands, J.B. (1987) Ferric uptake regulation protein acts as a repressor, employing iron (II) as a cofactor to bind the operator of an iron transport operon in *Escherichia coli*. *Biochemistry* **26**: 5471-5477.

Beaucage, S.L., Miller, C.A. and Cohen, S.N. (1991) Gyrase-dependent stabilization of pSC101 plasmid inheritance by transcriptionally active promoters. *Embo J* **10**: 2583-2588.

Beauchene, N.A., Mettert, E.L., Moore, L.J., Keles, S., Willey, E.R. and Kiley, P.J. (2017) O_2 availability impacts iron homeostasis in *Escherichia coli*. *Proc Natl Acad Sci U S A* **114**: 12261-12266.

Beinert, H., Holm, R.H. and Munck, E. (1997) Iron-sulfur clusters: nature's modular, multipurpose structures. *Science* **277**: 653-659.

Blanc, B., Gerez, C. and Ollagnier de Choudens, S. (2015) Assembly of Fe/S proteins in bacterial systems: Biochemistry of the bacterial ISC system. *Biochim Biophys Acta* **1853**: 1436-1447.

Bordoy, A.E. and Chatterjee, A. (2015) *Cis*-Antisense transcription gives rise to tunable genetic switch behavior: A Mathematical Modeling Approach. *PLoS One* **10**: e0133873.

Borek, A., Ekiert, R. and Osyczka, A. (2018) Functional flexibility of electron flow between quinol oxidation Qo site of cytochrome bc1 and cytochrome c revealed by combinatory effects of mutations in cytochrome b, iron-sulfur protein and cytochrome c1. *Biochim Biophys Acta Bioenerg* **1859**: 754-761.

Braatsch, S., Gomelsky, M., Kuphal, S. and Klug, G. (2002) A single flavoprotein, AppA, integrates both redox and light signals in *Rhodobacter sphaeroides*. *Mol Microbiol* **45**: 827-836.

Braatsch, S. and Klug, G. (2004) Blue light perception in bacteria. *Photosynth Res* **79**: 45-57.

Braun, V., Hantke, K. and Koster, W. (1998) Bacterial iron transport: mechanisms, genetics, and regulation. *Met Ions Biol Syst* **35**: 67-145.

Bryant, D.A. and Frigaard, N.U. (2006) Prokaryotic photosynthesis and phototrophy illuminated. *Trends Microbiol* **14**: 488-496.

Buhning, M., Valleriani, A. and Leimkuhler, S. (2017) The role of SufS is restricted to Fe-S cluster biosynthesis in *Escherichia coli*. *Biochemistry* **56**: 1987-2000.

Cadet, J., Carvalho, V.M., Onuki, J., Douki, T., Medeiros, M.H. and Di Mascio, P.D. (1999) Purine DNA adducts of 4,5-dioxovaleric acid and 2,4-decadienal. *IARC Sci Publ*: 103-113.

Carey, J.N., Mettert, E.L., Roggiani, M., Myers, K.S., Kiley, P.J. and Goulian, M. (2018) Regulated stochasticity in a bacterial signaling network permits tolerance to a rapid environmental change. *Cell* **175**: 1989-1990.

Chao, T.C., Becker, A., Buhrmester, J., Puhler, A. and Weidner, S. (2004) The *Sinorhizobium meliloti* fur gene regulates, with dependence on Mn(II), transcription of the *sitABCD* operon, encoding a metal-type transporter. *J Bacteriol* **186**: 3609-3620.

Chareyre, S., Barras, F. and Mandin, P. (2019) A small RNA controls bacterial sensitivity to gentamicin during iron starvation. *PLoS Genet* **15**: e1008078.

Chiu, S.M., Xue, L.Y., Lam, M., Rodriguez, M.E., Zhang, P., Kenney, M.E., Nieminen, A.L. and Oleinick, N.L. (2010) A requirement for bid for induction of apoptosis by photodynamic therapy with a lysosome- but not a mitochondrion-targeted photosensitizer. *Photochem Photobiol* **86**: 1161-1173.

Choi, J. and Ryu, S. (2019) Regulation of iron uptake by fine-tuning the iron responsiveness of the iron sensor Fur. *Appl Environ Microbiol* **85**. pii: e03026-18. doi: 10.1128/AEM.03026-18.

Choudhary, M., Fu, Y.X., Mackenzie, C. and Kaplan, S. (2004) DNA sequence duplication in *Rhodobacter sphaeroides* 2.4.1: evidence of an ancient partnership between chromosomes I and II. *J Bacteriol* **186**: 2019-2027.

Choudhary, M. and Kaplan, S. (2000) DNA sequence analysis of the photosynthesis region of *Rhodobacter sphaeroides* 2.4.1. *Nucleic Acids Res* **28**: 862-867.

Christman, M.F., Morgan, R.W., Jacobson, F.S. and Ames, B.N. (1985) Positive control of a regulon for defenses against oxidative stress and some heat-shock proteins in *Salmonella typhimurium*. *Cell* **41**: 753-762.

Clayton, R.K. (1966) The bacterial photosynthetic reaction center. *Brookhaven Symp Biol* **19**: 62-70.

Comayras, F., Jungas, C. and Lavergne, J. (2005) Functional consequences of the organization of the photosynthetic apparatus in *Rhodobacter sphaeroides*. I. Quinone domains and excitation transfer in chromatophores and reaction center.antenna complexes. *J Biol Chem* **280**: 11203-11213.

Costa, D., Amarelle, V., Valverde, C., O'Brian, M.R. and Fabiano, E. (2017) The Irr and RirA proteins participate in a complex regulatory circuit and act in concert to modulate bacterioferritin

expression in *Ensifer meliloti* 1021. *Appl Environ Microbiol* **83**. pii: e00895-17. doi: 10.1128/AEM.00895-17.

Coy, M. and Neilands, J.B. (1991) Structural dynamics and functional domains of the fur protein. *Biochemistry* **30**: 8201-8210.

Crack, J.C., Stapleton, M.R., Green, J., Thomson, A.J. and Le Brun, N.E. (2014) Influence of association state and DNA binding on the O(2)-reactivity of [4Fe-4S] fumarate and nitrate reduction (FNR) regulator. *Biochem J* **463**: 83-92.

Crespo-Rivas, J.C., Navarro-Gomez, P., Alias-Villegas, C., Shi, J., Zhen, T., Niu, Y., Cuellar, V., Moreno, J., Cubo, T., Vinardell, J.M., Ruiz-Sainz, J.E., Acosta-Jurado, S. and Soto, M.J. (2019) *Sinorhizobium fredii* HH103 RirA is required for oxidative stress resistance and efficient symbiosis with soybean. *Int J Mol Sci* **20**. pii: E787. doi: 10.3390/ijms20030787

Desnoyers, G., Morissette, A., Prevost, K. and Masse, E. (2009) Small RNA-induced differential degradation of the polycistronic mRNA *iscRSUA*. *EMBO J* **28**: 1551-1561.

Devasagayam, T.P. and Kamat, J.P. (2002) Biological significance of singlet oxygen. *Indian J Exp Biol* **40**: 680-692.

Di Mascio, P., Kaiser, P.S. and Sies, H. (1989) Quenching of singlet molecular-oxygen by carotenoids. *Biological Chemistry Hoppe-Seyler* **370**: 778-778.

Dokpikul, T., Chaoprasid, P., Saninjuk, K., Sirirakphaisarn, S., Johnrod, J., Nookabkaew, S., Sukchawalit, R. and Mongkolsuk, S. (2016) Regulation of the cobalt/nickel efflux operon *dmeRF* in *Agrobacterium tumefaciens* and a link between the iron-sensing regulator RirA and cobalt/nickel resistance. *Appl Environ Microbiol* **82**: 4732-4742.

Dos Santos, P.C. (2017) *B. subtilis* as a model for studying the assembly of Fe-S clusters in Gram-positive bacteria. *Methods Enzymol* **595**: 185-212.

Drews, G. (1985) Structure and functional organization of light-harvesting complexes and photochemical reaction centers in membranes of phototrophic bacteria. *Microbiol Rev* **49**: 59-70.

Drews, G., and Golecki, JR. (1995) In the anoxygenic photosynthetic bacteria. In.: Blankenship, RE, Madigan, MT, and Bauer, CE, eds, pp. 231–257, Kluwer Press.

Eisenhardt, K.M.H., Reuscher, C.M. and Klug, G. (2018) PcrX, an sRNA derived from the 3'- UTR of the *Rhodobacter sphaeroides puf* operon modulates expression of puf genes encoding proteins of the bacterial photosynthetic apparatus. *Mol Microbiol* **110**: 325-334.

Eraso, J.M. and Kaplan, S. (2009) Regulation of gene expression by PrrA in *Rhodobacter sphaeroides* 2.4.1: role of polyamines and DNA topology. *J Bacteriol* **191**: 4341-4352.

Escolar, L., Perez-Martin, J. and de Lorenzo, V. (1999) Opening the iron box: transcriptional metalloregulation by the Fur protein. *J Bacteriol* **181**: 6223-6229.

Espiritu, E., Chamberlain, K.D., Williams, J.C. and Allen, J.P. (2019) Bound manganese oxides capable of reducing the bacteriochlorophyll dimer of modified reaction centers from *Rhodobacter sphaeroides*. *Photosynth Res*. doi: 10.1007/s11120-019-00680-3

Fenton, H. (1894) Oxidation of tartaric acid in presence of iron. *J. Chem. Soc., Trans.* **65(65)**: 899–911.

Fidai, I., Wachnowsky, C. and Cowan, J.A. (2016) Glutathione-complexed [2Fe-2S] clusters function in Fe-S cluster storage and trafficking. *J Biol Inorg Chem* **21**: 887-901.

Fleischhacker, A.S., Stubna, A., Hsueh, K.L., Guo, Y., Teter, S.J., Rose, J.C., Brunold, T.C., Markley, J.L., Munck, E. and Kiley, P.J. (2012) Characterization of the [2Fe-2S] cluster of *Escherichia coli* transcription factor IscR. *Biochemistry* **51**: 4453-4462.

Flint, D.H., Tuminello, J.F. and Emptage, M.H. (1993) The inactivation of Fe-S cluster containing hydro-lyases by superoxide. *J Biol Chem* **268**: 22369-22376.

Foerstner, K.U., Reuscher, C.M., Haberzettl, K., Weber, L. and Klug, G. (2018) RNase E cleavage shapes the transcriptome of *Rhodobacter sphaeroides* and strongly impacts phototrophic growth. *Life Sci Alliance* **1**: e201800080.

Frank, H.A., Christensen, R.L. (1995) Singlet energy transfer from carotenoids to bacteriochlorophylls. . *Anoxygenic Photosynthetic Bacteria.* **Kluwer Academic Publisher**: 373- 384.

Frazzon, J. and Dean, D.R. (2001) Feedback regulation of iron-sulfur cluster biosynthesis. *Proc Natl Acad Sci U S A* **98**: 14751-14753.

Geisselbrecht, Y., Fruhwirth, S., Schroeder, C., Pierik, A.J., Klug, G. and Essen, L.O. (2012) CryB from *Rhodobacter sphaeroides*: a unique class of cryptochromes with new cofactors. *EMBO Rep* **13**: 223-229.

Giel, J.L., Nesbit, A.D., Mettert, E.L., Fleischhacker, A.S., Wanta, B.T. and Kiley, P.J. (2013) Regulation of iron-sulphur cluster homeostasis through transcriptional control of the Isc pathway by [2Fe-2S]-IscR in *Escherichia coli*. *Mol Microbiol* **87**: 478-492.

Giel, J.L., Rodionov, D., Liu, M., Blattner, F.R. and Kiley, P.J. (2006) IscR-dependent gene expression links iron-sulphur cluster assembly to the control of O_2-regulated genes in *Escherichia coli*. *Mol Microbiol* **60**: 1058-1075.

Glaeser, J., Nuss, A.M., Berghoff, B.A. and Klug, G. (2011) Singlet oxygen stress in microorganisms. *Adv Microb Physiol* **58**: 141-173.

Gnandt, E., Dorner, K., Strampraad, M.F.J., de Vries, S. and Friedrich, T. (2016) The multitude of iron-sulfur clusters in respiratory complex I. *Biochim Biophys Acta* **1857**: 1068-1072.

Gomelsky, L., Sram, J., Moskvin, O.V., Horne, I.M., Dodd, H.N., Pemberton, J.M., McEwan, A.G., Kaplan, S. and Gomelsky, M. (2003) Identification and *in vivo* characterization of PpaA, a regulator of photosystem formation in *Rhodobacter sphaeroides*. *Microbiology* **149**: 377-388.

Gomelsky, M., Horne, I.M., Lee, H.J., Pemberton, J.M., McEwan, A.G. and Kaplan, S. (2000) Domain structure, oligomeric state, and mutational analysis of PpsR, the *Rhodobacter sphaeroides* repressor of photosystem gene expression. *J Bacteriol* **182**: 2253-2261.

Gomelsky, M. and Kaplan, S. (1997) Molecular genetic analysis suggesting interactions between AppA and PpsR in regulation of photosynthesis gene expression in *Rhodobacter sphaeroides 2.4.1*. *J Bacteriol* **179**: 128-134.

Gomelsky, M. and Kaplan, S. (1998) AppA, a redox regulator of photosystem formation in *Rhodobacter sphaeroides* 2.4.1, is a flavoprotein. Identification of a novel fad binding domain. *J Biol Chem* **273**: 35319-35325.

Gomelsky, M. and Klug, G. (2002) BLUF: a novel FAD-binding domain involved in sensory transduction in microorganisms. *Trends Biochem Sci* **27**: 497-500.

Gregor, J. and Klug, G. (1999) Regulation of bacterial photosynthesis genes by oxygen and light. *FEMS Microbiol Lett* **179**: 1-9.

Griggs, D.W., Tharp, B.B. and Konisky, J. (1987) Cloning and promoter identification of the iron-regulated cir gene of *Escherichia coli*. *J Bacteriol* **169**: 5343-5352.

Halliwell, B. and Gutteridge, J.M.C. (2007) *Free radicals in biology and medicine,* p. xxxvi, 851 p., 858 p. of plates. Oxford University Press, Oxford ; New York.

Hamza, I., Chauhan, S., Hassett, R. and O'Brian, M.R. (1998) The bacterial irr protein is required for

coordination of heme biosynthesis with iron availability. *J Biol Chem* **273**: 21669-21674.

Han, Y. (2006) Integration of redox and light signals by the regulator protein AppA in *Rhodobacter sphaeroides*. In: Inaugural-Dissertation zur Erlangung des Doktorgrades der Naturwissenschaften. Giessen university, pp.

Han, Y., Meyer, M.H., Keusgen, M. and Klug, G. (2007) A haem cofactor is required for redox and light signalling by the AppA protein of *Rhodobacter sphaeroides*. *Mol Microbiol* **64**: 1090-1104.

Han, Y.C., Braatsch, S., Osterloh, L. and Klug, G. (2004) A eukaryotic BLUF domain mediates light-dependent gene expression in the purple bacterium *Rhodobacter sphaeroides 2.4.1*. *Proceedings of the National Academy of Sciences of the United States of America* **101**: 12306-12311.

Hantke, K. (2001) Iron and metal regulation in bacteria. *Curr Opin Microbiol* **4**: 172-177.

Happ, H.N., Braatsch, S., Broschek, V., Osterloh, L. and Klug, G. (2005) Light-dependent regulation of photosynthesis genes in *Rhodobacter sphaeroides 2.4.1* is coordinately controlled by photosynthetic electron transport via the PrrBA two-component system and the photoreceptor AppA. *Mol Microbiol* **58**: 903-914.

Hubner, P., Willison, J.C., Vignais, P.M. and Bickle, T.A. (1991) Expression of regulatory *Nif* genes in *Rhodobacter capsulatus*. *Journal of Bacteriology* **173**: 2993-2999.

Imam, S., Noguera, D.R. and Donohue, T.J. (2014) Global analysis of photosynthesis transcriptional regulatory networks. *PLoS Genet* **10**: e1004837.

Imam, S., Noguera, D.R. and Donohue, T.J. (2015) An integrated approach to reconstructing genome-scale transcriptional regulatory networks. *PLoS Comput Biol* **11**: e1004103.

Imhoff, J.F. (2001) Transfer of *Rhodopseudomonas acidophila* to the new genus *Rhodoblastus* as *Rhodoblastus acidophilus* gen. nov., comb. nov. *Int J Syst Evol Microbiol* **51**: 1863-1866.

Imlay, J.A. (2003) Pathways of oxidative damage. *Annu Rev Microbiol* **57**: 395-418.

Jacobson, M.R., Brigle, K.E., Bennett, L.T., Setterquist, R.A., Wilson, M.S., Cash, V.L., Beynon, J., Newton, W.E. and Dean, D.R. (1989) Physical and genetic map of the major *nif* gene cluster from *Azotobacter vinelandii*. *J Bacteriol* **171**: 1017-1027.

Jacquamet, L., Aberdam, D., Adrait, A., Hazemann, J.L., Latour, J.M. and Michaud-Soret, I. (1998) X-ray absorption spectroscopy of a new zinc site in the fur protein from *Escherichia coli*. *Biochemistry* **37**: 2564-2571.

Johnson, D.C., Dean, D.R., Smith, A.D. and Johnson, M.K. (2005) Structure, function, and formation of biological iron-sulfur clusters. *Annual Review of Biochemistry* **74**: 247-281.

Johnston, A.W., Todd, J.D., Curson, A.R., Lei, S., Nikolaidou-Katsaridou, N., Gelfand, M.S. and Rodionov, D.A. (2007) Living without Fur: the subtlety and complexity of iron-responsive gene regulation in the symbiotic bacterium *Rhizobium* and other alpha-proteobacteria. *Biometals : an international journal on the role of metal ions in biology, biochemistry, and medicine* **20**: 501-511.

Joshi, H.M. and Tabita, F.R. (1996) A global two component signal transduction system that integrates the control of photosynthesis, carbon dioxide assimilation, and nitrogen fixation. *Proc Natl Acad Sci U S A* **93**: 14515-14520.

Jousset, A.B., Rosinski-Chupin, I., Takissian, J., Glaser, P., Bonnin, R.A. and Naas, T. (2018) Transcriptional landscape of a bla KPC-2 plasmid and response to imipenem exposure in *Escherichia coli* TOP10. *Front Microbiol* **9**: 2929.

Kammler, M., Schon, C. and Hantke, K. (1993) Characterization of the ferrous iron uptake system of *Escherichia coli*. *J Bacteriol* **175**: 6212-6219.

Keen, N.T., Tamaki, S., Kobayashi, D. and Trollinger, D. (1988) Improved broad-host-range plasmids for DNA cloning in Gram-negative bacteria. *Gene* **70**: 191-197.

Kehrer, J.P. (2000) The Haber-Weiss reaction and mechanisms of toxicity. *Toxicology* **149**: 43-50.

Kehres, D.G., Janakiraman, A., Slauch, J.M. and Maguire, M.E. (2002) Regulation of *Salmonella enterica serovar Typhimurium* mntH transcription by H_2O_2, Fe^{2+}, and Mn^{2+}. *J Bacteriol* **184**: 3151-3158.

Keyer, K. and Imlay, J.A. (1996) Superoxide accelerates DNA damage by elevating free-iron levels. *Proc Natl Acad Sci U S A* **93**: 13635-13640.

Kitatsuji, C., Izumi, K., Nambu, S., Kurogochi, M., Uchida, T., Nishimura, S., Iwai, K., O'Brian, M.R., Ikeda-Saito, M. and Ishimori, K. (2016) Protein oxidation mediated by heme-induced active site conversion specific for heme-regulated transcription factor, iron response regulator. *Sci Rep* **6**: 18703.

Klebba, P.E., McIntosh, M.A. and Neilands, J.B. (1982) Kinetics of biosynthesis of iron-regulated membrane proteins in *Escherichia coli*. *J Bacteriol* **149**: 880-888.

Klug, G., Jager, A., Heck, C. and Rauhut, R. (1997) Identification, sequence analysis, and expression of the *lepB* gene for a leader peptidase in *Rhodobacter capsulatus*. *Mol Gen Genet* **253**: 666-673.

Kobayashi, K., Nakagaki, M., Ishikawa, H., Iwai, K., O'Brian, M.R. and Ishimori, K. (2016) Redox-dependent dynamics in heme-bound bacterial iron response regulator (Irr) protein. *Biochemistry* **55**: 4047-4054.

Koster, W. (2001) ABC transporter-mediated uptake of iron, siderophores, heme and vitamin B12. *Res Microbiol* **152**: 291-301.

Kovach, M.E., Elzer, P.H., Hill, D.S., Robertson, G.T., Farris, M.A., Roop, R.M., 2nd and Peterson, K.M. (1995) Four new derivatives of the broad-host-range cloning vector pBBR1MCS, carrying different antibiotic-resistance cassettes. *Gene* **166**: 175-176.

Lane, N. (2002) *Oxygen : the molecule that made the world*, p. x, 374 p. Oxford University Press, Oxford ; New York.

Lee, J.H., Yeo, W.S. and Roe, J.H. (2004) Induction of the *sufA* operon encoding Fe-S assembly proteins by superoxide generators and hydrogen peroxide: involvement of OxyR, IHF and an unidentified oxidant-responsive factor. *Mol Microbiol* **51**: 1745-1755.

Lee, K.C., Yeo, W.S. and Roe, J.H. (2008) Oxidant-responsive induction of the *suf* operon, encoding a Fe-S assembly system, through Fur and IscR in *Escherichia coli*. *J Bacteriol* **190**: 8244-8247.

Lemire, J.A., Harrison, J.J. and Turner, R.J. (2013) Antimicrobial activity of metals: mechanisms, molecular targets and applications. *Nat Rev Microbiol* **11**: 371-384.

Lill, R. (2009) Function and biogenesis of iron-sulphur proteins. *Nature* **460**: 831-838.

Liu, S., Zheng, Z., Tie, J., Kang, J., Zhang, G. and Zhang, J. (2018) Impacts of Fe^{2+} on 5-aminolevulinic acid (ALA) biosynthesis of *Rhodobacter sphaeroides* in wastewater treatment by regulating *nif* gene expression. *J Environ Sci (China)* **70**: 11-19.

Lloyd, D.R., Phillips, D.H. and Carmichael, P.L. (1997) Generation of putative intrastrand cross-links and strand breaks in DNA by transition metal ion-mediated oxygen radical attack. *Chem Res Toxicol* **10**: 393-400.

Loiseau, L., Gerez, C., Bekker, M., Ollagnier-de Choudens, S., Py, B., Sanakis, Y., Teixeira de Mattos, J., Fontecave, M. and Barras, F. (2007) ErpA, an iron sulfur (Fe-S) protein of the A-type essential for respiratory metabolism in *Escherichia coli*. *Proc Natl Acad Sci U S A* **104**: 13626-13631.

Macalady, J.L., Hamilton, T.L., Grettenberger, C.L., Jones, D.S., Tsao, L.E. and Burgos, W.D. (2013) Energy, ecology and the distribution of microbial life. *Philos Trans R Soc Lond B Biol Sci* **368**: 20120383.

Malkin, R. and Rabinowitz, J.C. (1966) The reconstitution of clostridial ferredoxin. *Biochem Biophys Res Commun* **23**: 822-827.

Mank, N.N., Berghoff, B.A., Hermanns, Y.N. and Klug, G. (2012) Regulation of bacterial photosynthesis genes by the small noncoding RNA PcrZ. *Proc Natl Acad Sci U S A* **109**: 16306-16311.

Masse, E., Salvail, H., Desnoyers, G. and Arguin, M. (2007) Small RNAs controlling iron metabolism. *Curr Opin Microbiol* **10**: 140-145.

Masse, E., Vanderpool, C.K. and Gottesman, S. (2005) Effect of RyhB small RNA on global iron use in *Escherichia coli*. *J Bacteriol* **187**: 6962-6971.

Masuda, S. and Bauer, C.E. (2002) AppA is a blue light photoreceptor that antirepresses photosynthesis gene expression in *Rhodobacter sphaeroides*. *Cell* **110**: 613-623.

Matsumoto, K., Saito, J., Yokoo, T., Hori, C., Nagata, A., Kudoh, Y., Ooi, T. and Taguchi, S. (2019) Ribulose-1,5-bisphosphate carboxylase/oxygenase (RuBisCO)-mediated de novo synthesis of glycolate-based polyhydroxyalkanoate in *Escherichia coli*. *J Biosci Bioeng* **128**: 302-306.

McEwan, A.G. (1994) Photosynthetic electron transport and anaerobic metabolism in purple non-sulfur phototrophic bacteria. *Antonie Van Leeuwenhoek* **66**: 151-164.

Metz, S., Haberzettl, K., Fruhwirth, S., Teich, K., Hasewinkel, C. and Klug, G. (2012) Interaction of two photoreceptors in the regulation of bacterial photosynthesis genes. *Nucleic Acids Res* **40**: 5901-5909.

Michaud-Soret, I., Adrait, A., Jaquinod, M., Forest, E., Touati, D. and Latour, J.M. (1997) Electrospray ionization mass spectrometry analysis of the apo- and metal-substituted forms of the Fur protein. *FEBS Lett* **413**: 473-476.

Morgan, J.W. and Anders, E. (1980) Chemical composition of Earth, Venus, and Mercury. *Proc Natl Acad Sci U S A* **77**: 6973-6977.

Nader, S., Perard, J., Carpentier, P., Arnaud, L., Crouzy, S. and Michaud-Soret, I. (2019) New insights into the tetrameric family of the Fur metalloregulators. *Biometals* **32**: 501-519.

Neidle, E.L. and Kaplan, S. (1993) Expression of the *Rhodobacter sphaeroides hemA* and *hemT* genes, encoding two 5-aminolevulinic acid synthase isozymes. *J Bacteriol* **175**: 2292-2303.

Nesbit, A.D., Giel, J.L., Rose, J.C. and Kiley, P.J. (2009) Sequence-specific binding to a subset of IscR-regulated promoters does not require IscR Fe-S cluster ligation. *J Mol Biol* **387**: 28-41.

Nie, X., Remes, B. and Klug, G. (2019) Multiple sense and antisense promoters contribute to the regulated expression of the *isc-suf* operon for iron-sulfur cluster assembly in *Rhodobacter*. *Microorganisms* **7**. pii: E671. doi: 10.3390/microorganisms7120671.

Nishino, K., Takahashi, S. and Nishida, H. (2018) Comparison of gene expression levels of *appA*, *ppsR*, and *EL368* in *Erythrobacter litoralis spheroplasts* under aerobic and anaerobic conditions, and under blue light, red light, and dark conditions. *J Gen Appl Microbiol* **64**: 117-120.

Oh, J.I. and Kaplan, S. (1999) The cbb3 terminal oxidase of *Rhodobacter sphaeroides 2.4.1*: structural and functional implications for the regulation of spectral complex formation. *Biochemistry* **38**: 2688-2696.

Oh, J.I. and Kaplan, S. (2000) Redox signaling: globalization of gene expression. *EMBO J* **19**: 4237-4247.

Outten, F.W., Djaman, O. and Storz, G. (2004) A *suf* operon requirement for Fe-S cluster assembly during iron starvation in *Escherichia coli*. *Mol Microbiol* **52**: 861-872.

Pandey, R., Armitage, J.P. and Wadhams, G.H. (2017) Use of transcriptomic data for extending a model of the AppA/PpsR system in *Rhodobacter sphaeroides*. *BMC Syst Biol* **11**: 146.

Pellicer Martinez, M.T., Crack, J.C., Stewart, M.Y., Bradley, J.M., Svistunenko, D.A., Johnston, A.W., Cheesman, M.R., Todd, J.D. and Le Brun, N.E. (2019) Mechanisms of iron- and O_2-sensing by the [4Fe-4S] cluster of the global iron regulator RirA. *Elife* **8**. pii: e47804. doi: 10.7554/eLife.47804.

Pellicer Martinez, M.T., Martinez, A.B., Crack, J.C., Holmes, J.D., Svistunenko, D.A., Johnston, A.W.B., Cheesman, M.R., Todd, J.D. and Le Brun, N.E. (2017) Sensing iron availability via the fragile [4Fe-4S] cluster of the bacterial transcriptional repressor RirA. *Chem Sci* **8**: 8451-8463.

Penfold, R.J. and Pemberton, J.M. (1994) Sequencing, chromosomal inactivation, and functional expression in *Escherichia coli* of *ppsR*, a gene which represses carotenoid and bacteriochlorophyll synthesis in *Rhodobacter sphaeroides*. *J Bacteriol* **176**: 2869-2876.

Perard, J., Nader, S., Levert, M., Arnaud, L., Carpentier, P., Siebert, C., Blanquet, F., Cavazza, C., Renesto, P., Schneider, D., Maurin, M., Coves, J., Crouzy, S. and Michaud-Soret, I. (2018) Structural and functional studies of the metalloregulator Fur identify a promoter-binding mechanism and its role in *Francisella tularensis* virulence. *Commun Biol* **1**: 93.

Pernitzsch, S.R. and Sharma, C.M. (2012) Transcriptome complexity and riboregulation in the human pathogen *Helicobacter pylori*. *Front Cell Infect Microbiol* **2**: 14.

Peuser, V., Metz, S. and Klug, G. (2011) Response of the photosynthetic bacterium *Rhodobacter sphaeroides* to iron limitation and the role of a Fur orthologue in this response. *Environ Microbiol Rep* **3**: 397-404.

Peuser, V., Remes, B. and Klug, G. (2012) Role of the Irr protein in the regulation of iron metabolism in *Rhodobacter sphaeroides*. *PLoS One* **7**: e42231.

Pinochet-Barros, A. and Helmann, J.D. (2018) Redox Sensing by Fe(2+) in bacterial Fur family metalloregulators. *Antioxid Redox Signal* **29**: 1858-1871.

Prentki, P., Binda, A. and Epstein, A. (1991) Plasmid vectors for selecting IS1-promoted deletions in cloned DNA: sequence analysis of the omega interposon. *Gene* **103**: 17-23.

Purvis, D.J., Theiler, R. and Niederman, R.A. (1990) Chromatographic and protein chemical analysis of the ubiquinol-cytochrome c2 oxidoreductase isolated from *Rhodobacter sphaeroides*. *J Biol Chem* **265**: 1208-1215.

Py, B. and Barras, F. (2010) Building Fe-S proteins: bacterial strategies. *Nature Reviews Microbiology* **8**: 436-446.

Qi, Z. and O'Brian, M.R. (2002) Interaction between the bacterial iron response regulator and ferrochelatase mediates genetic control of heme biosynthesis. *Mol Cell* **9**: 155-162.

Redmond, R.W. and Gamlin, J.N. (1999) A compilation of singlet oxygen yields from biologically relevant molecules. *Photochem Photobiol* **70**: 391-475.

Remes, B., Berghoff, B.A., Forstner, K.U. and Klug, G. (2014) Role of oxygen and the OxyR protein in the response to iron limitation in *Rhodobacter sphaeroides*. *BMC Genomics* **15**: 794.

Remes, B., Eisenhardt, B.D., Srinivasan, V. and Klug, G. (2015) IscR of *Rhodobacter sphaeroides* functions as repressor of genes for iron-sulfur metabolism and represents a new type of iron-sulfur-binding protein. *Microbiologyopen* **4**: 790-802.

Remes, B., Rische-Grahl, T., Muller, K.M.H., Forstner, K.U., Yu, S.H., Weber, L., Jager, A., Peuser, V. and Klug, G. (2017) An RpoHI-dependent response promotes outgrowth after extended stationary phase in the alphaproteobacterium *Rhodobacter sphaeroides*. *J Bacteriol* **199**. pii: e00249-17. doi: 10.1128/JB.00249-17.

Roche, B., Aussel, L., Ezraty, B., Mandin, P., Py, B. and Barras, F. (2013) Iron/sulfur proteins biogenesis in prokaryotes: formation, regulation and diversity. *Biochim Biophys Acta* **1827**: 455-469.

Rodionov, D.A., Gelfand, M.S., Todd, J.D., Curson, A.R. and Johnston, A.W. (2006) Computational reconstruction of iron- and manganese-responsive transcriptional networks in alpha-proteobacteria. *PLoS Comput Biol* **2**: e163.

Roeder, B., Naether, D., Lewald, T., Braune, M., Nowak, C. and Freyer, W. (1990) Photophysical properties and photodynamic activity in *vivo* of some tetrapyrroles. *Biophys Chem* **35**: 303-312.

Romsang, A., Duang-Nkern, J., Saninjuk, K., Vattanaviboon, P. and Mongkolsuk, S. (2018) Pseudomonas aeruginosa nfuA: Gene regulation and its physiological roles in sustaining growth under stress and anaerobic conditions and maintaining bacterial virulence. *PLoS One* **13**: e0202151.

Ryter, S.W. and Tyrrell, R.M. (1998) Singlet molecular oxygen ($^{(1)}O_2$): a possible effector of eukaryotic gene expression. *Free Radic Biol Med* **24**: 1520-1534.

Sangwan, I., Small, S.K. and O'Brian, M.R. (2008) The *Bradyrhizobium japonicum* Irr protein is a transcriptional repressor with high-affinity DNA-binding activity. *J Bacteriol* **190**: 5172-5177.

Saninjuk, K., Romsang, A., Duang-Nkern, J., Vattanaviboon, P. and Mongkolsuk, S. (2019) Transcriptional regulation of the *Pseudomonas aeruginosa* iron-sulfur cluster assembly pathway by binding of IscR to multiple sites. *PLoS One* **14**: e0218385.

Santos, J.A., Alonso-Garcia, N., Macedo-Ribeiro, S. and Pereira, P.J.B. (2014) The unique regulation of iron-sulfur cluster biogenesis in a Gram-positive bacterium. *Proceedings of the National Academy of Sciences of the United States of America* **111**: E2251-E2260.

Sasaki, S., Minamisawa, K. and Mitsui, H. (2016) A *Sinorhizobium meliloti* RpoH-regulated gene is involved in iron-sulfur protein metabolism and effective plant symbiosis under intrinsic iron limitation. *J Bacteriol* **198**: 2297-2306.

Schindel, H.S. and Bauer, C.E. (2016) The RegA regulon exhibits variability in response to altered growth conditions and differs markedly between *Rhodobacter* species. *Microb Genom* **2**: e000081.

Schwartz, C.J., Giel, J.L., Patschkowski, T., Luther, C., Ruzicka, F.J., Beinert, H. and Kiley, P.J. (2001) IscR, an Fe-S cluster-containing transcription factor, represses expression of *Escherichia coli* genes encoding Fe-S cluster assembly proteins. *Proc Natl Acad Sci U S A* **98**: 14895-14900.

Schwiesow, L., Mettert, E., Wei, Y., Miller, H.K., Herrera, N.G., Balderas, D., Kiley, P.J. and Auerbuch, V. (2018) Control of *hmu* Heme Uptake Genes in *Yersinia pseudotuberculosis* in

Response to Iron Sources. *Front Cell Infect Microbiol* **8**: 47.

Seaver, L.C. and Imlay, J.A. (2004) Are respiratory enzymes the primary sources of intracellular hydrogen peroxide? *J Biol Chem* **279**: 48742-48750.

Selvi, M.T. and Sharma, R. (2008) Cell maturity gradient determines light regulated accumulation of proteins in pearl millet leaves. *Physiol Mol Biol Plants* **14**: 1-8.

Sesto, N., Wurtzel, O., Archambaud, C., Sorek, R. and Cossart, P. (2013) The excludon: a new concept in bacterial antisense RNA-mediated gene regulation. *Nat Rev Microbiol* **11**: 75-82.

Sevilla, E., Sarasa-Buisan, C., Gonzalez, A., Cases, R., Kufryk, G., Peleato, M.L. and Fillat, M.F. (2019) Regulation by FurC in Anabaena links the oxidative stress response to photosynthetic metabolism. *Plant Cell Physiol* **60**: 1778-1789.

Sharma, C.M., Hoffmann, S., Darfeuille, F., Reignier, J., Findeiss, S., Sittka, A., Chabas, S., Reiche, K., Hackermuller, J., Reinhardt, R., Stadler, P.F. and Vogel, J. (2010) The primary transcriptome of the major human pathogen *Helicobacter pylori*. *Nature* **464**: 250-255.

Shimada, H., Iba, K. and Takamiya, K. (1992) Blue-light irradiation reduces the expression of *puf* and *puc* operons of *Rhodobacter sphaeroides* under semi-aerobic conditions. *Plant and Cell Physiology* **33**: 471-475.

Simon, R., Oconnell, M., Labes, M. and Puhler, A. (1986) Plasmid vectors for the genetic-analysis and manipulation of *Rhizobia* and other Gram-negative bacteria. *Method Enzymol* **118**: 640-659.

Singleton, C., White, G.F., Todd, J.D., Marritt, S.J., Cheesman, M.R., Johnston, A.W. and Le Brun, N.E. (2010) Heme-responsive DNA binding by the global iron regulator Irr from *Rhizobium leguminosarum*. *J Biol Chem* **285**: 16023-16031.

Sirijovski, N., Mamedov, F., Olsson, U., Styring, S. and Hansson, M. (2007) *Rhodobacter capsulatus* magnesium chelatase subunit BchH contains an oxygen sensitive iron-sulfur cluster. *Arch Microbiol* **188**: 599-608.

Small, S.K., Puri, S., Sangwan, I. and O'Brian, M.R. (2009) Positive control of ferric siderophore receptor gene expression by the Irr protein in *Bradyrhizobium japonicum*. *J Bacteriol* **191**: 1361-1368.

Smith, A.T., Linkous, R.O., Max, N.J., Sestok, A.E., Szalai, V.A. and Chacon, K.N. (2019) The FeoC [4Fe-4S] cluster is redox-active and rapidly oxygen-sensitive. *Biochemistry* **58**:4935-4949.

Stazic, D., Lindell, D. and Steglich, C. (2011) Antisense RNA protects mRNA from RNase E degradation by RNA-RNA duplex formation during phage infection. *Nucleic Acids Res* **39**: 4890-4899.

Stojiljkovic, I. and Hantke, K. (1995) Functional domains of the *Escherichia coli* ferric uptake regulator protein (Fur). *Mol Gen Genet* **247**: 199-205.

Storz, G., Tartaglia, L.A. and Ames, B.N. (1990) Transcriptional regulator of oxidative stress-inducible genes: direct activation by oxidation. *Science* **248**: 189-194.

Sund, C.J., Rocha, E.R., Tzianabos, A.O., Wells, W.G., Gee, J.M., Reott, M.A., O'Rourke, D.P. and Smith, C.J. (2008) The *Bacteroides fragilis* transcriptome response to oxygen and H_2O_2: the role of OxyR and its effect on survival and virulence. *Mol Microbiol* **67**: 129-142.

Suwanto, A. and Kaplan, S. (1989) Physical and genetic mapping of the *Rhodobacter sphaeroides* 2.4.1 genome: presence of two unique circular chromosomes. *J Bacteriol* **171**: 5850-5859.

Sztukowska, M., Bugno, M., Potempa, J., Travis, J. and Kurtz, D.M., Jr. (2002) Role of rubrerythrin in the oxidative stress response of *Porphyromonas gingivalis*. *Mol Microbiol* **44**: 479-488.

Tabita, F.R., Gibson, J.L., Falcone, D.L., Lee, B.G. and Chen, J.H. (1990) Recent studies on the molecular biology and biochemistry of CO_2 fixation in phototrophic bacteria. *FEMS Microbiol Rev* **7**: 437-443.

Takahashi, Y. and Tokumoto, U. (2002) A third bacterial system for the assembly of iron-sulfur clusters with homologs in archaea and plastids. *Journal of Biological Chemistry* **277**: 28380-28383.

Tanaka, N., Yuda, E., Fujishiro, T., Hirabayashi, K., Wada, K. and Takahashi, Y. (2019) Identification of IscU residues critical for de novo iron-sulfur cluster assembly. *Mol Microbiol* **112**:1769-1783

Todd, J.D., Wexler, M., Sawers, G., Yeoman, K.H., Poole, P.S. and Johnston, A.W. (2002) RirA, an iron-responsive regulator in the symbiotic bacterium *Rhizobium leguminosarum*. *Microbiology* **148**: 4059-4071.

van Niel, C.B. (1944) The culture, general physiology, morphology, and classification of the non-sulfur purple and brown bacteria. *Bacteriological reviews* **8**: 1-118.

Vergnes, A., Viala, J.P., Ouadah-Tsabet, R., Pocachard, B., Loiseau, L., Meresse, S., Barras, F. and Aussel, L. (2017) The iron-sulfur cluster sensor IscR is a negative regulator of Spi1 type III secretion system in *Salmonella enterica*. *Cell Microbiol* **19**.

Vermeglio, A. and Joliot, P. (1999) The photosynthetic apparatus of *Rhodobacter sphaeroides*. *Trends Microbiol* **7**: 435-440.

Wan, F., Kong, L. and Gao, H. (2018) Defining the binding determinants of *Shewanella oneidensis* OxyR: Implications for the link between the contracted OxyR regulon and adaptation. *J Biol Chem* **293**: 4085-4096.

Wang, B.Y., Huang, H.Q., Li, S., Tang, P., Dai, H.F., Xian, J.A., Sun, D.M. and Hu, Y.H. (2019) Thioredoxin H (TrxH) contributes to adversity adaptation and pathogenicity of *Edwardsiella piscicida*. *Vet Res* **50**: 26.

Wei, W., Liu, T., Li, X., Wang, R., Zhao, W., Zhao, G., Zhao, S. and Zhou, Z. (2017) Lysine acetylation regulates the function of the global anaerobic transcription factor FnrL in *Rhodobacter sphaeroides*. *Mol Microbiol* **104**: 278-293.

Wexler, M., Todd, J.D., Kolade, O., Bellini, D., Hemmings, A.M., Sawers, G. and Johnston, A.W. (2003) Fur is not the global regulator of iron uptake genes in *Rhizobium leguminosarum*. *Microbiology* **149**: 1357-1365.

Woese, C.R., Stackebrandt, E., Weisburg, W.G., Paster, B.J., Madigan, M.T., Fowler, V.J., Hahn, C.M., Blanz, P., Gupta, R., Nealson, K.H. and Fox, G.E. (1984) The phylogeny of purple bacteria: the alpha subdivision. *Syst Appl Microbiol* **5**: 315-326.

Woodmansee, A.N. and Imlay, J.A. (2003) A mechanism by which nitric oxide accelerates the rate of oxidative DNA damage in *Escherichia coli*. *Mol Microbiol* **49**: 11-22.

Wu, Y. and Outten, F.W. (2009) IscR controls iron-dependent biofilm formation in *Escherichia coli* by regulating type I fimbria expression. *J Bacteriol* **191**: 1248-1257.

Yamamoto, H., Fang, M., Dragnea, V. and Bauer, C.E. (2018) Differing isoforms of the cobalamin binding photoreceptor AerR oppositely regulate photosystem expression. *Elife* **7**. pii: e39028. doi: 10.7554/eLife.39028.

Yang, J., Panek, H.R. and O'Brian, M.R. (2006) Oxidative stress promotes degradation of the Irr protein to regulate haem biosynthesis in *Bradyrhizobium japonicum*. *Mol Microbiol* **60**: 209-218.

Yanischperron, C., Vieira, J. and Messing, J. (1985) Improved M13 Phage Cloning Vectors and Host Strains - Nucleotide-Sequences of the M13mp18 and Puc19 Vectors. *Gene* **33**: 103-119.

Yano, A., Horiya, S., Minami, T., Haneda, E., Ikeda, M. and Harada, K. (2010) Identification of antisense RNA stem-loops that inhibit RNA-protein interactions using a bacterial reporter system. *Nucleic Acids Res* **38**: 3489-3501.

Yeo, W.S., Lee, J.H., Lee, K.C. and Roe, J.H. (2006) IscR acts as an activator in response to oxidative stress for the *suf* operon encoding Fe-S assembly proteins. *Mol Microbiol* **61**: 206-218.

Yin, L., Dragnea, V., Feldman, G., Hammad, L.A., Karty, J.A., Dann, C.E. and Bauer, C.E. (2013) Redox and light control the heme-sensing activity of AppA. *Mbio* **4**:e00563-13.

Yu, J., Tan, L.M., Kawakami, T., Wang, P., Fu, L.M., Wang-Otomo, Z.Y. and Zhang, J.P. (2018) Cooperative photoprotection by multicompositional carotenoids in the LH1 antenna from a mutant strain of *Rhodobacter sphaeroides*. *J Phys Chem B* **122**: 8028-8036.

Zappa, S., Li, K. and Bauer, C.E. (2010) The tetrapyrrole biosynthetic pathway and its regulation in *Rhodobacter capsulatus*. *Adv Exp Med Biol* **675**: 229-250.

Zeilstra-Ryalls, J.H. and Kaplan, S. (1995) Aerobic and anaerobic regulation in *Rhodobacter sphaeroides* 2.4.1: the role of the *fnrL* gene. *J Bacteriol* **177**: 6422-6431.

Zeilstra-Ryalls, J.H. and Kaplan, S. (2004) Oxygen intervention in the regulation of gene expression: the photosynthetic bacterial paradigm. *Cell Mol Life Sci* **61**: 417-436.

Zeller, T. and Klug, G. (2004) Detoxification of hydrogen peroxide and expression of catalase genes in *Rhodobacter*. *Microbiology* **150**: 3451-3462.

Zeller, T., Moskvin, O.V., Li, K.Y., Klug, G. and Gomelsky, M. (2005) Transcriptome and physiological responses to hydrogen peroxide of the facultatively phototrophic bacterium *Rhodobacter sphaeroides*. *Journal of Bacteriology* **187**: 7232-7242.

Zeller, T., Mraheil, M.A., Moskvin, O.V., Li, K., Gomelsky, M. and Klug, G. (2007) Regulation of hydrogen peroxide-dependent gene expression in *Rhodobacter sphaeroides*: regulatory functions of OxyR. *J Bacteriol* **189**: 3784-3792.

Zheng, C. and Dos Santos, P.C. (2018) Metallocluster transactions: dynamic protein interactions guide the biosynthesis of Fe-S clusters in bacteria. *Biochem Soc Trans* **46**: 1593-1603.

Zheng, L., Cash, V.L., Flint, D.H. and Dean, D.R. (1998) Assembly of iron-sulfur clusters. Identification of an *iscSUA-hscBA-fdx* gene cluster from *Azotobacter vinelandii*. *J Biol Chem* **273**: 13264-13272.

Zheng, M. and Storz, G. (2000) Redox sensing by prokaryotic transcription factors. *Biochem Pharmacol* **59**: 1-6.

Ziegelhoffer, E.C. and Donohue, T.J. (2009) Bacterial responses to photo-oxidative stress. *Nat Rev Microbiol* **7**: 856-863.

Acknowledgements

First and formost I would like to thank my supervisor Prof. Dr. Gabriele Klug for her constant support and excellent guidance. It is her encouragement and valuable suggestions that gave me motives and inspiration to make progress in my scientific research. I also thank Apl. Prof. Dr. Elena Evguenieva-Hackenberg, Prof. Dr. Sylvia Schnell and Prof. Dr. Reinhard Dammann for being the examiners on my defence.

Further, I would like to thank all my colleagues for providing tips in my experiments and also for the nice working atmosphere what they create.

I want to thank CSC for the financial support, also I send my thanks to many other people, too numerous to mention, who helped in their own little way throughout this work.

Last, but not least, I would like to take this opportunity to thank my parents. I am forever grateful to my husband Dr. Zhiping Zhao for his help and support. I sincerely appreciate and thank him for sharing my happiness and sorrow. I also sincerely appreciate and thank my litter daughter Jiayi Zhao, who brings me much more happiness. Jiayi stayed with me in Gießen for nearly four years since she was younger than three years old. Her growth in Gießen Regenbogenland Städtische Kindertagesstätte and Friedrich-Wilhelm-Raiffeisen-Schule Wetzlar (FWR Wetzlar) makes me feel happy and motivate me to work hard.

Erklärung

Hiermit Erklärung ich, dass ich die vorliegende Arbeit selbstständig verfasst habe und dabei keine anderen als die angegebenen Quellen und Hilfsmittel verwendet habe. Zitate sind als solche gekennzeichnet.

Giessen, den 19.12.2019

Xin Nie